OPTIMIZATION OF ELECTRICAL DISCHARGE MACHINING PROCESS USING AN ADAPTIVE CONTROLLER BASED ON FUZZY LOGIC

SAMUEL KARANJA KABINI

DOCTOR OF PHILOSOPHY
(Mechatronic Engineering)

JOMO KENYATTA UNIVERSITY OF AGRICULTURE AND TECHNOLOGY

2018

Optimization of Electrical Discharge Machining Process Using an Adaptive Controller Based on Fuzzy Logic

Samuel Karanja Kabini

A thesis submitted in fulfillment for the degree of Doctor of Philosophy in Mechatronic Engineering in the Jomo Kenyatta University of Agriculture and Technology

2018

DECLARATION

This thesis is my original work and has not been presented for a degree in any other university.

Signature..... Date.....

Samuel Karanja Kabini

This thesis has been submitted for examination with our approval as the University supervisors:

Signature..... Date.....

Prof. Eng. Bernard W. Ikua, PhD
JKUAT, Kenya

Signature..... Date.....

Eng. Prof. John M. Kihiu, PhD
JKUAT, Kenya

Signature..... Date.....

Prof. George N. Nyakoe, PhD
JKUAT, Kenya

DEDICATION

I dedicate this work to my entire family. They have always been there to lift me up when I fall, and to celebrate with me when I succeed.

To my wife, Triza: I will not be able to repay your support and sacrifices for me, either on earth or in heaven. But the simple words, Thank You, are the only thing I can say.

ACKNOWLEDGEMENTS

I thank the Almighty God, without whom this work would not have even started. I thank Him for giving me the opportunity to undertake this course to completion. I would also like to express my humble gratitude to my supervisors, Prof. Eng. B.W. Ikua, Eng. Prof. J. M. Kihiu and Prof. G.N. Nyakoe, not only for their invaluable guidance and advice throughout my studies, but also for listening to me when I was excited about a new idea. Thank you for your constructive criticism, and encouragement. You assured me that I could do it.

To Dr.-Ing. H. Zeidler of Professorship of Micromanufacturing Technology, Technische Universität Chemnitz, thank you for all the support and guidance. You are indeed an inspiration. A special mention should be made of all staff members of the Professorship of Micromanufacturing Technology, Technische Universität Chemnitz for their assistance in setting up and carrying out the experiments, and in particular, Dipl.-Ing. Ralf and Mr. Nico Treffkorn who helped me set up my experiments.

Mr. J. Wamai and P. Kipkosgei from the department of Mechatronic Engineering deserve more than a mention for the assistance they accorded me throughout my research. I am happy to acknowledge my debt to Mr. J. K. Matunda, Mr. J. M. Mihari, Mr. J. M. Mwangi and Mr. S. M. Nzioka whose assistance made my research work fun. In addition, I would like to register my appreciation to the Department of Mechatronic Engineering, JKUAT for supporting me throughout my study period. My eternal gratitude goes to Ms. C. W. Nyaga for her encouragement, especially during my travel to TU Chemnitz. Last but not least, I would like to acknowledge DAAD for funding my research and supporting me throughout the entire period of my research.

TABLE OF CONTENTS

LIST OF TABLES

LIST OF FIGURES

LIST OF APPENDICES

LIST OF ABBREVIATIONS

A/D	Analogue to Digital interface
D/A	Digital to Analogue interface
DC	Direct Current
EDM	Electrical Discharge Machining
EWR	Electrode Wear Ratio
FL	Fuzzy Logic
FLC	Fuzzy Logic Controller
FIS	Fuzzy Inference System
GUI	Graphical User Interface
HAZ	Heat Affected Zone
MIMO	Multi-Input Multi-Output
min	Minute
MISO	Multi-Input Single-Output
MOSFET	Metal Oxide Semiconductor Field Effect Transistor
MQL	Minimum Quality Lubrication
MRR	Material Removal Rate (mm^3/min)
SA	Simulated Annealing
SEM	Scanning Electron Microscopy
TWR	Tool Wear Rate (mm^3/min)
UEDM	Ultrasonic-assisted Electrical Discharge Machining
WEDM	Wire Electrical Discharge Machining

NOMENCLATURE

$\boldsymbol{Al}$	Aluminium
$\boldsymbol{C_uZ_n}$	Brass
$\boldsymbol{f}$	Frequency
$\boldsymbol{F_eC}$	Steel
$\boldsymbol{R_a}$	Arithmetic average of absolute roughness values (μm)
$\boldsymbol{R_p}$	Maximum peak height (μm)
$\boldsymbol{R_q}$	Root mean square (μm)
$\boldsymbol{R_v}$	Maximum valley depth (μm)
$\boldsymbol{R_z}$	Average distance between the highest peak and lowest valley in each sampling length (μm)
$\boldsymbol{v}$	Voltage

ABSTRACT

Electrical Discharge Machining (EDM) is a manufacturing process whereby a desired shape is obtained by using electrical discharges. Material is removed from the work piece by a series of rapidly recurring current discharges between two electrodes, separated by a dielectric liquid and subject to an electric voltage. The EDM process has several advantages over conventional machining processes, key among them being the capability to machine very hard materials and cut complex internal profiles. It is also used to machine micro-parts with high dimensional accuracy and surface finish. The EDM mechanism is however very complex mainly due to the many machining parameters involved. The EDM process has some disadvantages such as high rate of electrical energy consumption, low material removal rate, high rate of tool wear and poor surface finish when not properly controlled. These disadvantages have undermined the full potential of EDM. Various researchers have used varied approaches with the aim of optimizing the EDM process for improved efficiency and quality. However, most of these researches have focused on optimization of at most two parameters and have used either predictive neural fuzzy techniques or modeling approaches. These approaches have not addressed the realtime control of the process which could guarantee maximum machining efficiency and high surface quality. In view of this, the main goal of this research was to study the EDM process with a view to designing a fuzzy-based controller that is capable of improving the process' performance by increasing material removal rate, lowering tool wear rate and improving the quality of the surface finish. This would be achieved by optimizing the gap voltage and the duty cycle in realtime.

First, a transistorized pulse generation circuit for an EDM machine at JKUAT was developed. Then extensive experimental work was carried out to determine the effects of gap voltage and duty cycle on material removal rate, tool wear rate and surface quality for machining of aluminium, brass and medium carbon

steel. The data from the experimental results was then used in the creation of data/knowledge base for the fuzzy logic inference system. Based on this data, a Multi-Input Single-Output (MISO) adaptive controller for the optimization of the spark gap voltage/discharge current and duty cycle was developed. The optimization was achieved through the adjustment of the spark gap. The adaptive controller uses realtime monitoring and adjustment modules to detect any changes in the machining parameters and give corresponding voltage control signals to optimize the machining process based on the set parameters and the rule base created for the fuzzy logic controller. Thus the controller continually monitors the actual machining parameters across the electrodes during machining and compares the difference with the optimum values. It also monitors the rate of change of the parameters. The difference between the measured and the optimum values and the rate at which the difference is varying is used to compute the input signals to the machine controllers. To test the performance of the proposed controller, the MRR, TWR and surface finish of the machined part for the controlled process were compared with those of the uncontrolled process. From this study, it was demonstrated that, the fuzzy logic based adaptive controller increased MRR by an average of 36.7%. Surface finish was improved by 54.5% and MRR to TWR ratio was increased by an average of 12.9%.

The increase in MRR and MRR to TWR ratio through the use of the controller makes the EDM process suitable for applications not only in cases where machining of hard materials is needed, but also where faster machining is required. The application of the controller leads to higher productivity, reduced machining costs and wider applicability of the EDM process. Moreover, improved surface quality of the finished products makes the EDM process attractive for machining of dies and molds which require high accuracy and surface quality. Potential beneficiaries of the results obtained in this research include EDM machine manufacturers and specialized machining industries such as mold and die making industries.

CHAPTER ONE

INTRODUCTION

1.1 Background

Electrical discharge machining (EDM) is a specialized thermal machining process capable of accurately machining of materials with different hardness or parts that have complex shapes, which are difficult to machine using conventional mechanical means. It is also a very desirable manufacturing process when machining highly specialized fewer products or where high accuracy is needed and is, especially well-suited for cutting intricate contours or cavities that would be difficult to produce using mechanical means such as grinding or milling. However, the efficiency of the EDM process is low and as such, it is only used when the cost and time of machining are not a major consideration. This is because there is excessive tool wear and the material removal rate in EDM is very low when compared to other machining processes [1]. An example of a case where EDM is applied is when the material being machined is too hard to be machined by other machining processes. Table 1.1 shows comparison of EDM process with other alternative (subtractive) machining processes [2]. It gives the areas of application of each process, its advantages and disadvantages.

Electrical discharge machining has been applied in a wide range of machining processes, ranging from a simple means of making tools and dies to the best alternative of producing micro-scale parts with a relatively high degree of dimensional accuracy and surface quality. Over the years, the EDM process has remained as a competitive and economical machining option fulfilling the demanding machining requirements imposed by the short product development cycles and the growing cost pressures for specialized machining.

Electrical Discharge Machining (EDM) is arguably one of the most accurate manufacturing processes available for machining complex or simple shapes and geome-

Table 1.1: Comparison between EDM and other alternative machining processes

S/No.	Machining process	Areas of application	Advantages	Disadvantages
1.	Milling/ Turning process	• For machining family parts • For machining parts that cannot have a heat affected zone (HAZ) • For machining sculptured surfaces • Machining of relatively non hard material	• Variety of shapes can be obtained through milling/turning • Versatile operation with wide variety of toolings and attachments. • Better dimensional control and surface finish.	• Tooling is quite expensive • It is extremely slow for milling/turning very hard materials • Cannot machine sharp internal corners • Not able to machine very complex shapes
2.	EDM process	• For machining sharp internal corners • For machining the very complex geometry • Where deep cutting is required • For machining high-expertise parts • For machining hard materials	• Machines all hard conductive regardless of hardness • Provides close tolerances on machined parts • Is used for very small work pieces where conventional cutting tools may damage the part from excess cutting tool pressure • There is no direct contact between tool and work piece. Therefore, delicate sections and weak materials can be machined without distortion	• It has low rate of material removal • Produces a heat affected zone on workpiece • Is only used for machining conductive materials • More expensive process than conventional milling or turning

tries. The EDM process is illustrated in Figure 1.1. In the figure, the tool and workpiece form the electrodes, one of which is positive and the other one negative. Across the electrodes, a pulsed DC voltage is applied. The workpiece is submerged in dielectric fluid. The EDM process involves multiple parameters that vary more often during machining. These parameters are; gap voltage, discharge current, spark gap, discharge frequency and, material properties for the electrodes and the dielectric medium. As a result of different combinations of

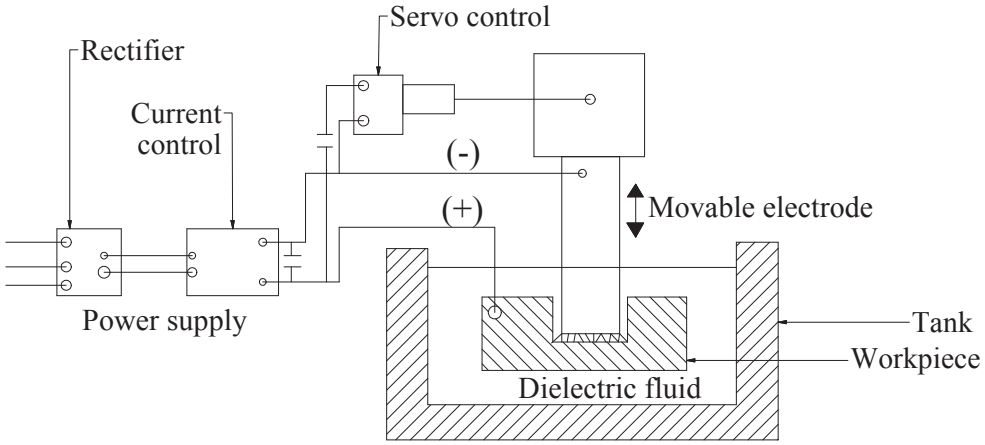

Figure 1.1: Illustration of the EDM process

input/machining parameters, the output parameters namely, electrode wear, material removal rate and quality of the workpiece surface are different for different workpiece and electrode materials. In order to minimize the wear of the electrodes and increase the material removal rate, there is need for careful selection of optimum machining parameters. This can be achieved by development of accurate process model for use in conventional control. However, this is a difficult task due to the presence of many machining parameters that vary rapidly and simultaneously during machining. The problem is also compounded by the fact that, for different materials, the same set of machining parameters may produce different results. The few attempts that have been made to optimize the EDM process include the use of predictive fuzzy logic, artificial neural networks, and

modeling approaches, which have not been very successful [3–6].

This research aimed at developing an adaptive fuzzy logic-based controller, able to continually monitor and alter the machining parameters to achieve optimum values depending on the prevailing machining conditions and the required output. In order to be able to carry out the experimental work on the EDM machine at JKUAT, it was necessary to redesign a pulse generation circuit that would allow for smooth and independent adjustment of machining parameters over a wider range than that provided by the existing Resistor-Capacitor (RC) type pulse generator. The optimization was achieved by online monitoring of the machining process and adjustment of the spark gap and the input machining parameters to the optimum values, hence ensuring that the Material Removal Rate (MRR) was maximized, Tool Wear Rate (TWR) minimized and the quality of the resultant machining surface improved.

1.2 Problem statement

In electrical discharge machining, selection of the appropriate machining parameters has a significant effect on the process performance. This effect is on the quality of the surface finish, material removal rate and electrode/tool wear ratio. Poor combination of the machining parameters results in lower efficiency of the process and vice-versa. The process outputs such as Material Removal Rate (MRR), Electrode/Tool Wear Ratio (E/TWR) and the quality of surface finish of the workpiece can be significantly improved by selecting optimum machining parameters. In many cases, determining the best set of process parameters is difficult and relies heavily on operators experience or reference books values [7]. This not only gives undesirable results, i.e., lower efficiency for the process, but is also tedious. Additionally, this calls for high skills and experience for the operation of the EDM machine.

There is, therefore, need for development of an adaptive controller that monitors

the machining process and adjusts the machining parameters to the optimum values in realtime. This research was aimed at developing such a controller and analyzing its effectiveness in optimizing the EDM process. The controller that was developed was multi-input single-output. This is because there were more than one input parameters and only one control signal was needed to control the piezo for the adjustment of the spark gap.

1.3 Objectives

The main objective was to develop an adaptive fuzzy logic-based controller, for realtime optimization of the machining parameters in electrical discharge machining process. This was achieved by attainment of the following specific objectives:

1. Development of a transistor-based pulse generator for an EDM.
2. Investigation of the effects of gap voltage and duty cycle (machining parameters) on the process outputs (MRR, TWR and surface finish).
3. Design of an adaptive controller for the optimization of the EDM process in real time.
4. Carrying out experiments to test the performance of the adaptive controller.

1.4 Justification of the study

The existing control methods for the EDM process are limited in that, they are unable to monitor and control the process parameters in realtime. This is due to the fact that, the EDM process has multiple and rapidly changing parameters [8].

The Fuzzy Logic (FL) based adaptive controller that was developed boosted the machining efficiency and improved process performance of the electrical discharge machining. More specifically, it maximized material removal rate, reduced the

electrode wear and improved on the quality of the surface for the finished product. It also minimized the need for an experienced machine operator and at the same time reduced the machining time significantly. Further, the research sought to explore the avenue of adaptive control, hence it significantly contributed to development of knowledge in the area of study and research.

1.5 Outline of thesis

This thesis contains five chapters. The first chapter provides an introduction to the research by highlighting the existing problem, the objective and the scope of the research work. Chapter 2 is a literature review on EDM process and the various methods employed in the control of the process. In this chapter, the theory of operation of the EDM process is also explained as well as the details into the operation of fuzzy logic and its applications. In chapter 3, the methodology used in the research is outlined. It details the design process for the transistorized pulse generation circuit and how the experimental work was carried out. The last item in this chapter is on the design of the controller for the EDM process. In chapter 4, the results obtained in the experimental work are discussed at length. The conclusion from the current research is given in chapter 5. In the same chapter, recommendations to be implemented from the current research work and for future research are also made. Finally, the appendix chapter gives the circuit diagram for the initial design for the transistorized pulse generator and the raw data that was obtained from experimental work.

CHAPTER TWO

LITERATURE REVIEW

2.1 Introduction

The first section in this chapter discusses theory of operation of the EDM and explains the parameters that are involved in EDM process. In the section that follows, literature on research that has been done in optimization of the performance of electrical discharge machining, with a view to identifying research gaps is reviewed. Finally, a review of literature on fuzzy logic control is presented. Fuzzy logic is later used in development of the adaptive controller for the control of EDM process.

2.2 Theory of operation of EDM process

The EDM process works by thermally eroding material in the path of electrical discharges that form an arc between a tool electrode and the workpiece. This sparking phenomenon utilizes the widely accepted non-contact technique of material removal [9].

Electrical discharge machining processes can be classified into two types: wire and probe (die sinker). Wire EDM is used primarily for shapes cut through a selected part or assembly. With a wire EDM machine, if a cutout needs to be created, an initial hole must first be drilled in the material, then the wire can be fed through the hole to complete the machining. Sinker (die sinking) EDMs are generally used for complex geometries. In this case, the EDM machine uses a machined electrode, usually, graphite or copper to erode the desired shape into the part or assembly. Sinker EDM can cut a hole into the part without having a hole pre-drilled for the electrode [10].

2.2.1 Components of EDM and mechanism of material removal

The electrical discharge machining system consists of a tool or wire and the workpiece as the electrodes. There exists a potential difference between the workpiece and the tool. The workpiece is immersed in a dielectric (electrically non-conducting) fluid which is circulated to flush away debris emanating from the machining process. Most EDM machine electrodes can rotate about two to three axes allowing for cutting of internal cavities or circular surfaces [11].

The material removal in EDM is by production of a rapid series of repetitive electrical discharges. These electrical discharges are passed between an electrode and the piece of metal being machined. The small amount of material that is removed from the work piece is flushed away with a continuously flowing fluid. The repetitive discharges create a set of successively deeper craters in the workpiece until the final shape is produced. One limitation of EDM is that, the workpiece material must be electrically conductive. Thus, it does not work on materials such as glass or ceramic, or most plastics [11].

In a typical ram/sinker EDM process the tool electrode is made of graphite, copper tungsten or pure copper which is machined into the desired (negative) shape. This specially shaped tool electrode is connected to the power source, attached to a ram, and is slowly fed into the workpiece as was shown in Figure 1.1. In the case of wire-EDM, a very thin wire serves as the electrode. Special brass wires are typically used; the wire is slowly fed through the material and the electrical discharges cut the workpiece. The wire does not touch the workpiece, but the electrical discharges remove small amounts of material along the length of the wire and allow the wire to be moved through the workpiece. The entire machining operation for either sinker or wire EDM is usually performed while submerged in a fluid bath. The fluid serves to flush the machined material away, acts as coolant to minimize the heat affected zone (thereby preventing potential damage to the workpiece) and when it deionizes, it acts as a conductor for the

current to pass between the electrode and the workpiece.

2.2.2 Machining parameters of EDM process

Electrical discharge machining process has many input parameters that include spark gap voltage, discharge current, pulse ON time, servo speed, spark gap and flushing [10, 12].

Spark gap voltage refers to the voltage applied between the electrode and workpiece, while that which can be read across the gap during the spark current discharge is referred as working gap voltage. Discharge current is the current prevailing at the time of material removal, while pulse ON time is the duration time of the EDM spark measured in microseconds.

Servo speed refers to the speed of the device that drives and controls the movement of the quill or ram while spark gap is the distance between the electrode and the workpiece when discharges are occurring. This distance is supposed to be maintained at the required size to avoid short or open circuit. The last parameter in the list, flushing, refers to the removal of machined particles from the machining zone.

The processes that occur during EDM are, sparking, open circuit, short circuit and arcing. Sparking is where electric sparks are generated between two electrodes when a high potential difference is applied across them while they are separated by a narrow gap in a dielectric medium. Localized regions of high temperatures are formed due to the sparks occurring between the two electrode surfaces. Workpiece material in this localized zone melts and vaporizes. Most of the molten and vaporized material is carried away from the inter-electrode gap by the dielectric flow in the form of debris particles [10].

Open circuit refers to a situation where the tool distance of separation between the electrode and the workpiece is more than the maximum gap required for

sparking to occur. There is no potential difference between the tool electrode and the workpiece and as a result, there is no sparking in this case and this should be avoided since it leads to more machining time [13].

Short circuit occurs when the workpiece and tool electrode are in contact or their separation distance is smaller than the minimum separation distance required. This contributes to energy losses with no machining and should be avoided [13].

Arcing is an electric current that is brief, strong and highly luminous. An arc is the luminous current discharge which is produced when strong current leaps across the gap between the tool electrode and the workpiece. In EDM, this is an undesirable process because as it occurs, no machining takes place.

2.2.3 Areas of application

The EDM process is most widely used by the mold-making tool and die industries, but is becoming a common method of making prototype and production parts, especially in the aerospace, automobile and electronics industries in which production quantities are relatively low [14]. The process has also recently been applied even in micro-machining due to its mechanism of material removal, that allows even micro-scale machining. Also, the material removal mechanism provides a host of other advantages over conventional machining processes. One such advantage is that, the process can be used for machining of extremely hard materials.

2.3 Optimization of EDM process

2.3.1 Experimental investigation and modeling approaches

A lot of research has been conducted on electrical discharge machining process. Some researchers have focused on the experimental investigation of the influence of various machining parameters on the process output, while some have gone ahead and developed models for prediction of the optimum input parameters.

Shabgard *et al.* [15] conducted experimental studies to investigate the influence of electrical discharge machining input parameters on the output characteristics of the EDM process. The process characteristics including machining features, i.e., material removal rate, tool wear ratio, arithmetical mean roughness, and surface integrity characteristics comprising of the thickness of white layer and the depth of heat affected zone in machining of AISI H13 tool steel were investigated. The experiments that were performed considered EDM input parameters that included pulse on-time and pulse current. It was found out that, when machining AISI H13 tool steel, increase in pulse on-time led to increase in material removal rate, surface roughness, as well the white layer thickness and depth of heat affected zone. The research also found that increase in pulse current led to sharp increase in the material removal rate and surface roughness. It was thus concluded that maintaining constant level of discharge energy, high pulse current and low pulse on-time led to reduction in the white layer thickness and depth of heat affected zone on the surface of the machined workpiece. These results could be useful in the design of a controller for the EDM process. However, this investigation only focused on one material and may therefore not be sufficient to make a generalized conclusion about the EDM process on all materials.

Carlo *et al.* [16] investigated and analyzed the effects of the electrodes metallic materials (Ag, Ni, Ti, W) on the electrical measurements. Linear mixed-effects models were fitted to the experimental data using the restricted maximum likelihood method. The main conclusion drawn was that the discharge current and voltage as defined and measured in the framework depended on the electrode material even when keeping all the other machining conditions unchanged. This useful data can be used in the design of a controller for the EDM process.

A study on the determination of optimal cutting parameters in wire EDM where a feed-forward neural network was used to associate the cutting parameters with the cutting performance was conducted by Tarng *et al.* [5]. A simulated annealing

(SA) algorithm was then applied to the neural network for solving the optimal cutting parameters based on a performance index within the allowable working conditions. Experimental results showed that the cutting performance of wire-EDM would be greatly enhanced using this approach. The algorithm developed in this study was purely predictive and assumed ideal invariable conditions, i.e., there was no change of parameters once they were set at the beginning of the machining simulation. However, this is normally not the case for the EDM process.

Scott *et al.* [17] investigated the effects of spark on-time duration and spark on-time ratio, on the material removal rate (MRR) and surface integrity of four types of advanced materials: porous metal foams, metal bond diamond grinding wheels, sintered Nd-Fe-B magnets, and carbon-carbon bipolar plates. During the wire EDM process, five types of constraints on the MRR were identified. These were due to short circuit, wire breakage, machine slide speed limit, and spark on-time upper and lower limits. An envelope of feasible EDM process parameters was generated for each work-material. This process envelope was used to select process parameters for maximum MRR and for machining of micro features. Results of Scanning Electron Microscopy (SEM) analysis of surface integrity showed that the envelope was an effective tool in the selection of the EDM machining parameters for maximum MRR and good surface finish in micro-machining. This approach, however, was susceptible to inaccuracy due to the fact that, the process is predictive and requires keying in of the parameters. It cannot also address variations in machining conditions which can only be provided by the incorporating realtime monitoring and control.

Yongshun *et al.* [18] developed a geometric model of the linear motor driven electrical discharge machining (EDM) process based on Z-map method. The model was employed to calculate the minimum gap distance required for sparking to occur and also analyze the possibility of spark generation between the workpiece and electrode surfaces. The model then calculated the crater formed by a sin-

gle spark. The final machined surface topography was then predicted by the model. The influence of peak current and discharge duration on the average surface roughness was also simulated. Experimental work was done to study the effects of machining conditions and verify the effectiveness of the developed geometric model. This research work focused on modeling the sparking phenomenon and the machined surface topography and not on the optimization of the EDM process, which is the subject of current research.

A study was conducted on the influence of silicon powder-mixed dielectric on conventional electrical discharge machining by Pecas and Henriques [19]. The study investigated the performance improvement of conventional EDM when used with a powder-mixed dielectric. A silicon powder was used and the improvement was assessed through quality surface indicators and process time measurements, over a set of different processing areas. The results showed positive influence of the silicon powder in the reduction of the operating time, required to achieve a specific surface quality, and in the decrease of the surface roughness, allowing the generation of mirror-like surfaces. The main challenge of this approach is that it did not address the issue of tool wear and material removal rate.

Zhang *et al.* [8] conducted an investigation on ultrasonic-assisted electrical discharge machining (UEDM) in gas. The study focused on using ultrasonic waves to improve the efficiency of electrical discharge machining in gas medium. In this case, the tool electrode was a thin-walled pipe and the high-pressure gas medium was applied from inside, while the ultrasonic actuation was applied onto the workpiece. The workpiece material used in the experiment was AISI 1045 steel while that of the electrode was copper. The experimental results showed that the MRR increased with increase in open voltage, pulse duration, amplitude of ultrasonic actuation, discharge current. Material removal rate also increased with decrease in wall thickness of electrode pipe. Finally the experimental results showed that the surface roughness increased with increase in open voltage, pulse duration, and

discharge current. Based on experimental results, a theoretical model to estimate the MRR and the surface roughness was developed. This research as mentioned earlier was meant to develop a model to estimate MRR and surface roughness. However, since the EDM parameters are rapidly and randomly varying, without the advantage of realtime control, this approach would not achieve the best achievable results.

The wire electrical discharge machining (EDM) of cross-section with minimum thickness and compliant mechanisms was investigated by Scott *et al.* [20]. The effects of EDM process parameters, particularly the spark cycle time and spark on-time on thin cross-section cutting of NdFeB magnetic material, carbon bipolar plate, and titanium were investigated. An envelope of feasible wire EDM process parameters was generated for the commercially pure titanium. The application of this envelope in selection of suitable EDM process parameters for micro feature generation was demonstrated. Scanning Electron Microscopy (SEM) analysis was done on EDM produced surface and debris. From the observations, a hypothesis based on the thermal and electrostatic stress induced fracture was developed for the explanation of limiting factors for wire EDM cutting of thin-sections. This hypothesis was for cutting of thin sections only.

Bulent *et al.* [21] used a semi-empirical approach to model residual stresses in EDM. Layer removal method was used to measure the residual stress profile as a function of depth beneath the surface caused by die sinking type EDM. Cracking and its consequences on residual stresses were also studied on samples machined at long pulse durations. A modified empirical equation was developed for scaling residual stresses in machined surfaces with respect to operating conditions. In the model, a unit amplitude shape function that represented change in curvature with respect to removal depth was proposed. The proposed form was special form of a Gauss Distribution. It was the sum of two Gaussian peaks, with the same amplitude and pulse width, but opposite center location. The form could also be

represented by three constant coefficients, which depended on the energy released by a power function. This research targeted minimization of stress without any regard to MRR and EWR.

Due to the fact that debris accumulation in the discharge gap cause a poor machining stability and low production efficiency, Jin *et al.* [22] set out to investigate debris and bubble movements during electrical discharge machining. They established a series of experimental devices using transparent materials to observe debris and bubble movements. Based on the observations, the mechanism of debris and bubble exclusion during consecutive pulse discharges was analyzed, and the effects of the electrode jump height and speed on the debris and bubble movements investigated. It was found that during an electrode down time, the bubble expansion was the main factor that excluded the debris from the space/gap between the electrode and the workpiece. At the beginning of consecutive pulse discharges, the bubbles rapidly excluded the debris from the gap. As the discharge continued, the bubbles ability to exclude the debris became weak, resulting in a debris aggregation in the gap and, thus, an unstable machining. Finally, the results showed that, the electrode jump speed affected the mixing degree of the debris and oil. The main challenge in this research was that, it involved investigation of the debris removal without suggesting any improvements.

Nizar *et al.* [23] numerically studied thermal aspects of electric discharge machining process. The numerical results concerning the temperature distribution due to electric discharge machining process were presented. From these thermal results, the material removal rate and the total roughness were deduced and compared with experimental observations. The comparison showed that, taking into account the temperature variation of conductivity was of crucial importance and gave the better correlations with experimental data. Again, this was a fact finding mission without any intentions to optimize the EDM process.

Yih and Zhi [24] investigated electrode wear-compensation in electric discharge

scanning process using a robust gap-control technique. Robust gap-control was applied to compensate for electrode wear in an electric discharge scanning (ED-Scanning) process. This control compensated for the wear, without reference to the wear ratio of the electrodes. A proportional controller for a gap-control system with maximal robustness was designed and robustly analyzed to override the non-linear and time-varying feedback. The simulated and practical responses of that robust gap-control system yielded favorable performances. The controller maintained the location of the discharge on the vertical axis and fixed the depth of the removal to that of a particular layer. The practical scanning process revealed that, the dimension of a hole could be guaranteed only if the data concerning the depth of removal under specific discharge conditions and electrode diameters were applied. This research only focused on the electrode wear compensation without regard to the other machining parameters of EDM process or the impact of the gap compensation on the output parameters.

Seiji *et al.* [25] used a combination of capacitance and conductive working fluid to speed up the fabrication of a narrow, deep hole in metals using electrical discharge machining. This was done by use of a dielectric-encased wire electrode, as opposed to the conventional pipe electrode. The role of the dielectric jacket was to completely suppress unnecessary secondary discharges occurring between the sidewalls of the wire and the fabricated hole. In this study, the effectiveness of the combination of conductive working fluid and a capacitor connected to the work piece and the tool electrode was examined. Although electrode wear was severe, machining speed in this case was twice as fast compared with fabricating a hole (without a capacitor and saline water in a 20 mm thick carbon steel block). The biggest challenge in this research was the severe electrode wear ratio, which is unacceptable.

Muniu *et al.* [26] investigated the applicability of diatomite powder-mixed dielectric fluid in EDM process. In the research, the effect of diatomite powder sus-

pended in distilled water was investigated using graphite as the tool electrode on mild steel workpiece. The process parameters that were used were peak current, pulse-on time and powder concentration. Results showed that the suspension of diatomite powder in dielectric fluid improved the performance characteristics of conventional EDM process. This research improved the EDM process but did not provide the advantage of realtime control. Given that the EDM process has rapidly varying parameters, realtime control would be required to optimize the process regardless of the variation of the machining parameters.

In this section, it can be seen that from the literature that has been reviewed, most researchers have investigated the effects of individual parameters on the EDM process. None of the researchers from reviewed literature has attempted to control the EDM process by online monitoring, or using an adaptive approach.

2.3.2 Parameter control approach

Tarng *et al.* [3] developed a fuzzy pulse discriminating system for electrical discharge machining. The development used fuzzy set theory to construct a new pulse discriminator. The classification of various discharge pulses in EDM was based on the features of the measured gap voltage and gap current. To obtain optimal classification performance, a machine learning method based on a simulated annealing algorithm was adopted to automatically synthesize the membership functions of the fuzzy pulse discriminator. Experimental results showed that, EDM discharge pulses could be correctly and quickly classified under varying cutting conditions using this approach. Notable is that, this research did not investigate other parameters such as duty cycle which are key and need to be optimized for maximum efficiency of the EDM process.

Kun *et al.* [27] conducted a study on improvement of surface finish on SKD steel using electro-discharge machining with aluminum and surfactant added dielectric. In the study, the effect of surfactant and Aluminium powders added in the

dielectric on the surface status of the workpiece after EDM was investigated. It was observed that, the best distribution effect was found when the concentrations of the aluminium powder and surfactant in the dielectric are 0.1 and 0.25 g/L, respectively. An optimal surface roughness (Ra) value of 0.172 μm was achieved with the parameters being, positive polarity, discharge current of 0.3 A, pulse duration time of 1.5 ms, open circuit potential of 140 V, gap voltage of 90 V and surfactant concentration of 0.25 g/L. The surface roughness status of the workpiece was improved up to 60% as compared to that machined under pure dielectric with high surface roughness (Ra) of 0.434 μm. This was a good achievement, but the research only focused on optimization of machining of only one material and hence the results could only be applied for the specific material under investigation.

An investigation on the near dry EDM process was conducted by Kao *et al.* [28]. This process used liquid-gas mixture as a two phase dielectric fluid. This had the benefit that, the concentration of the liquid and properties of the dielectric medium could be tailored to meet desired performance targets. A dispenser for minimum quantity lubrication (MQL) was used to supply a certain amount of liquid droplets at a controlled rate to the gap between the workpiece and the electrode. Wire EDM cutting and EDM drilling were investigated under the wet, dry, and near dry conditions. The mixture of water and air was the dielectric fluid used for near dry EDM. The near dry EDM showed advantages over the dry EDM in higher MRR, sharper cutting edge, and less debris deposition. Compared to wet EDM, near dry EDM had higher material removal rate at low discharge energy. However, the near dry EDM placed a higher thermal load on the electrode, which led to wire breakage in wire EDM and increased electrode wear in EDM drilling. From this research, a mathematical model was also developed to quantitatively correlate the water-air mixture's dielectric strength and viscosity to the gap distance. In the model, it was assumed that the gap distance consisted of the

discharge distance and material removal depth. The model was able to predict the dielectric strengths of various water-air mixtures. This research focussed on the dielectric fluid whereas the effects of variation of machining parameters were not taken into account. Further, since the research was aimed at developing a model, the end result would need further work to cater for the random nature of the EDM process.

More recently, Byiringiro *et al.* [4, 6], developed a tunable fuzzy logic controller (FLC) for monitoring and control of micro-electro discharge machining process which used the behavior of discharge pulses. The control parameters included gap voltage and gap current pulses. Experiments were carried out in order to distinguish and classify the pulses through measurement and analysis of the gap pulses' characteristics. The pulses were then classified into open, sparking, arcing, off and short circuit. The classified pulses were input into the FLC which drove the servo-system maintaining the desired gap width. The simulated results showed that the FLC was able to provide stable machining and improve the micro-EDM process. On this research, and as recommended by the researchers, further work needed to be done to test the FLC on the EDM process and also take into account the rate at which the EDM process parameters change.

2.3.3 Summary of the gaps identified in the review

As seen from the literature, the negative effects of the rapid and random variation of the machining parameters from the set optimum values on the quality of the machined product, MRR and TWR have necessitated research work in this area over the years. However;

(i) most of the previous approaches have only investigated the effects of various parameters on the quality of the machining process, without suggesting any remedy.

(ii) other approaches have only tried to optimize certain or some of the parameters and for certain materials only, and,

(iii) some of the approaches have used predictive techniques that only give values to be used later in the processes, thereby, failing to give an opportunity for real time control.

In view of the literature that has been reviewed, it can be concluded that the process of optimization of the EDM process requires an approach that is capable of dealing with rapidly and randomly varying parameters that are simultaneously and continuously varying. So far, no such approach has been presented. One such approach is the design of a multi-input single-output adaptive controller that is able to monitor the machining process parameters and adjust them to the desired values in real time. Depending on the measured machining parameters, the controller is able to predict a likely occurrence of undesirable machining condition such as short or open circuit and adjust the machining parameters in such a way that it avoids the occurrence of the undesirable machining condition. This research work was aimed at developing such a controller. A fuzzy logic control approach whose literature is presented in section 2.4 was used for the development of the controller.

2.4 Control problem

2.4.1 Background

The design of modern control systems is characterized by stringent performance and robustness requirements and therefore, relies on model-based design methods. This raises a strong need for effective modeling techniques. Many systems are not amenable to conventional modeling approaches due to strongly nonlinear behaviour and lack of precise knowledge of the process under study. Nonlinear identification and control is therefore becoming an important tool which can lead

to improved control systems along with considerable savings of time and cost. Among the different nonlinear control techniques, methods based on fuzzy sets are gradually becoming established [29].

Adaptive control is a method of designing a controller with some adjustable parameters and an embedded mechanism for adjusting these parameters [30]. Adaptive methods have been used mainly to improve online controller's performance [31]. For each control cycle, the adaptive algorithm is normally implemented in three basic steps, namely,

1. Observable data is collected to calculate the controller's performance.
2. The controller's performance is used to calculate the adjustment to a set of controller parameters.
3. The controller's parameters are then adjusted to improve the performance of the controller in the next cycle.

Normally, adaptive controllers are designed based on non or semi modeling approaches such as hybrid fuzzy logic approaches. The hybrid fuzzy logic approach uses the heuristic nature of fuzzy based systems to build adaptive controllers [30]. Figure 2.1 shows block diagram representation of an adaptive controller.

2.4.2 Fuzzy logic

Fuzzy logic has two different meanings. In a narrow sense, fuzzy logic is a logical system, which is an extension of multi-valued logic. However, in a wider sense, fuzzy logic is almost synonymous with the theory of fuzzy sets, a theory which relates to classes of objects with un-sharp boundaries in which, membership is a matter of degree [32].

The word *fuzzy* is used to describe terms that, are not well-known, or are not

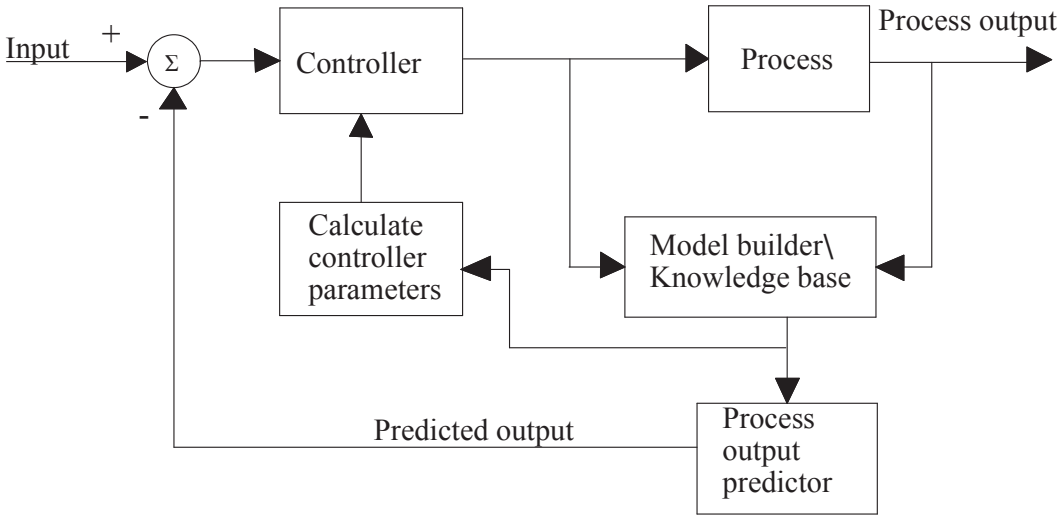

Figure 2.1: Block diagram representation of an adaptive controller

clear enough, or whose closer specification depends on subjectivity, estimation, and even the intuition of the person who is describing them. In everyday life, there are many situations characterized by a certain degree of ambiguity whose description includes terms and expressions such as *majority*, *many*, *several*, *not exactly*, or *quite possible*, all of which can be qualified as fuzzy terms. On the other hand, terms like *false*, *true*, *possible*, *necessary*, *none*, or *all* reflect crisp meanings, and in such a context, represent exact terms [33].

The mathematics of fuzzy set theory, and by extension fuzzy logic were developed in 1965 by Zadeh [34]. New operations for the calculus of logic were proposed, and were in principle, a generalization of classical logic [35]. This theory proposed making the membership function (or the values False and True) operate over the range of real numbers [0.0, 1.0]. The notion central to fuzzy systems is that truth values in fuzzy logic or membership values in fuzzy sets are indicated by a value in this range, with 0.0 representing absolute Falseness and 1.0 representing absolute Truth [36].

There is a distinction between fuzzy systems and probability [37]. Although

both operate over the same numeric range, and at first glance, both have similar values: 0.0 representing False (or non- membership), and 1.0 representing True (or membership), there is a difference between the two theories in that the probability theory indicates the chances of an event happening, while the fuzzy set theory indicates the extent to which the event will occur.

Fuzzy logic control refers to a technique of embodying human thinking into a control system. Fuzzy logic controllers are designed to emulate human deductive thinking, that is, the process people use to infer conclusions from what they know [32].

Fuzzy logic systems are rule-based systems in which an input is first fuzzified, that is, converted from a crisp number to a fuzzy set, and subsequently processed by an inference engine that retrieves knowledge in the form of fuzzy rules contained in a rule-base. The fuzzy sets that are computed by the fuzzy inference as the output of each rule are then combined and defuzzified, that is, converted from a fuzzy set to a crisp number. A fuzzy logic system is a nonlinear mapping from the input to the output space [38].

2.4.3 Fuzzy IF-THEN rules and fuzzy inference systems

Fuzzy IF-THEN rules or fuzzy conditional statements are expressions of the form "IF A, THEN B", where A and B are labels of fuzzy sets that are characterized by appropriate membership functions [34]. Due to their concise form, fuzzy IF-THEN rules are often employed to capture the imprecise modes of reasoning that play an essential role in the human ability to make decisions in an environment of uncertainty and imprecision [39]. An example that describes a simple fact is *IF pressure is high, THEN volume is small*, where *pressure* and *volume* are *linguistic variables*, *high* and *small* are *linguistic values* or *labels* that are characterized by membership functions. Another form of fuzzy IF-THEN rule, proposed by Takagi and Sugeno [40], has fuzzy sets involved only in the premise part. By using Takagi

and Sugeno's fuzzy IF-THEN rule for example, the resistant force on a moving object can be described as:

IF velocity is high, THEN force $= k(velocity)^2$

where, again, *high* in the premise part is a linguistic label characterized by an appropriate membership function. However, the consequent part is described by a nonfuzzy equation of the input variable, velocity. Both types of fuzzy IF-THEN rules have been used extensively in both modeling and control.

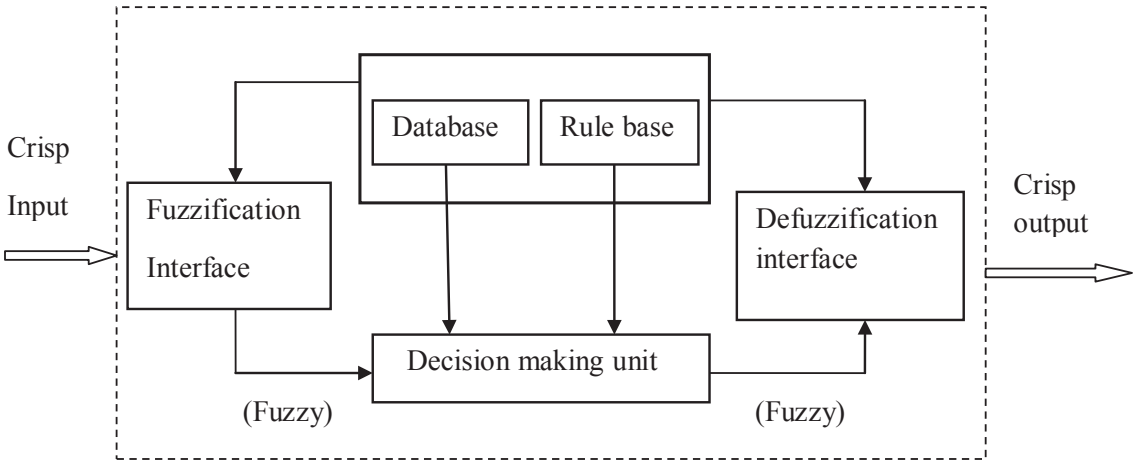

Figure 2.2: Fuzzy inference system (FIS)

Through the use of linguistic labels and membership functions, a fuzzy IF-THEN rule can easily capture decision making capability of humans [30]. Also, due to the qualifiers on the premise parts, each fuzzy IF-THEN rule can be viewed as a local description of the system under consideration. Fuzzy IF-THEN rules form a core part of a fuzzy inference system.

Fuzzy inference systems are also known as fuzzy-rule-based systems, fuzzy models, fuzzy associative memories (FAM), or fuzzy controllers when used as controllers. A fuzzy inference system is composed of five functional blocks as shown in Figure 2.2 [30]. The functional blocks are as follows:

1. A *rule base* containing a number of fuzzy IF-THEN rules.

2. A *database* which defines the membership functions of the fuzzy sets used in the fuzzy rules.

3. A *decision-making unit* which performs the inference operations on the rules.

4. A *fuzzification interface* which transforms the crisp inputs into degrees of match with linguistic values.

5. A *defuzzification interface* which transforms the fuzzy results of the inference into a crisp output.

Usually, the rule base and the database are jointly referred to as the knowledge base. The steps of fuzzy reasoning (inference operations upon fuzzy IF-THEN rules) performed by fuzzy inference systems are [40]:

1. Compare the input variables with the membership functions on the premise part to obtain the membership values of each linguistic label. This process is often called *fuzzification*.

2. Combine the membership values on the premise part to get *firing strength* or *weight* of each rule through a specific T-norm operator.

3. Generate the qualified consequent of each rule depending on the firing strength.

4. Aggregate the qualified consequents to produce a crisp output.

Several types of fuzzy reasoning have been proposed in the past [41]. Depending on the types of fuzzy reasoning and fuzzy IF-THEN rules employed, most fuzzy inference systems (FIS) can be classified into three types as shown in figures 2.3 through 2.5. In these figures a two-rule two-input fuzzy inference system is utilized to show the different types of fuzzy rules and fuzzy reasoning. In figures, μ is the degree of membership and $U(A, B, C)$ is the universe of discourse, while

A, B and C represent the membership functions. Also, w_i represents the i^{th} rule's firing strength.

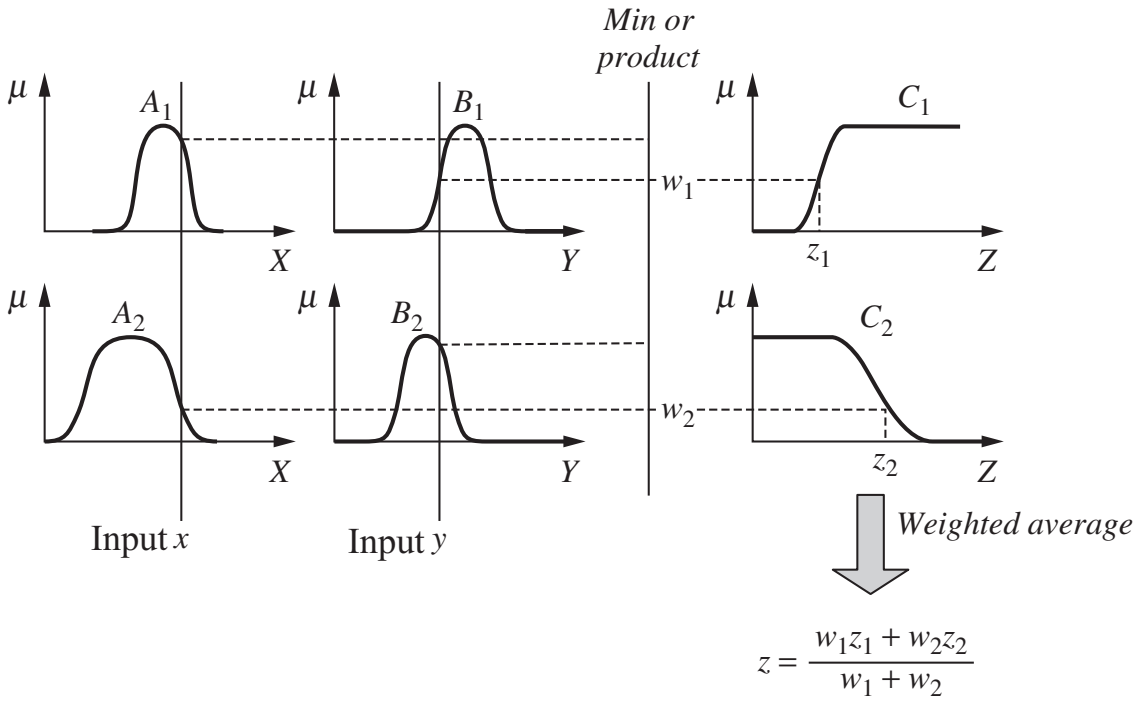

Figure 2.3: Type 1 FIS

1. **Type 1 FIS:** The overall output is the weighted average of each rules crisp output induced by the rule's firing strength. It is obtained as the product or minimum of the degrees of match between the premise part and the output membership functions. The output membership functions used in this scheme must be monotonic functions [41]. This type of FIS is illustrated in Figure 2.3. In this figure, the output is given by z.

2. **Type 2 FIS:** The overall fuzzy output is derived by applying 'max' operation to the qualified fuzzy outputs. Various schemes have been proposed to choose the final crisp output based on the overall fuzzy output; some of them are centroid of area, bisector of area, mean of maxima, maximum criterion, etc [41]. This type of FIS is illustrated in Figure 2.4, in which y* represents the crisp output.

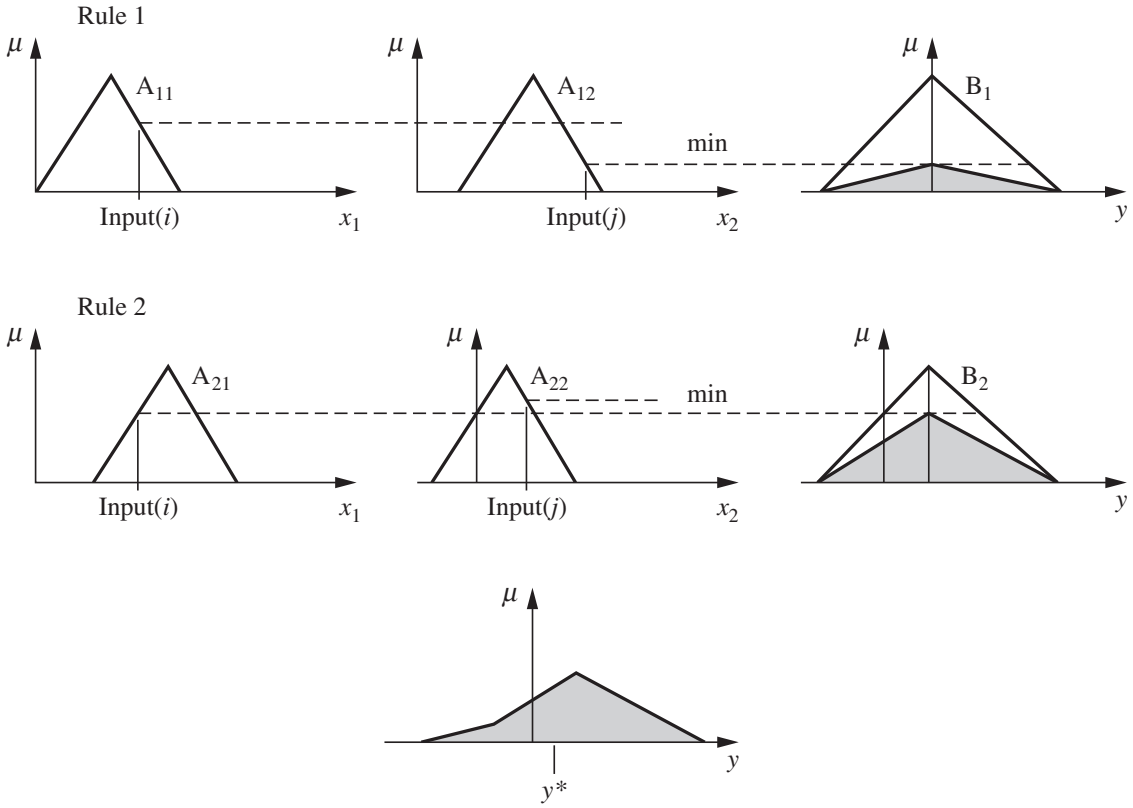

Figure 2.4: Type 2/Mamdani FIS

3. **Type 3 FIS:** In this type, Takagi and Sugeno's fuzzy IF-THEN rules are used. The output of each rule is a linear combination of input variables plus a constant term, and the final output is the weighted average of the rules' outputs [42]. Figure 2.5 illustrates this type of FIS, in which p, q and r are constants, and the output is given by z.

   From the information given, it can be noted that most of the differences in the fuzzy inference systems are in the specification of the consequent part, which may be monotonically non-decreasing, bell-shaped, trapezoidal or triangular membership functions, or crisp function and thus the defuzzification schemes are also different. However, the inference systems' outputs are defuzzified into crisp outputs and the output is always crisp, no matter the inference system used.

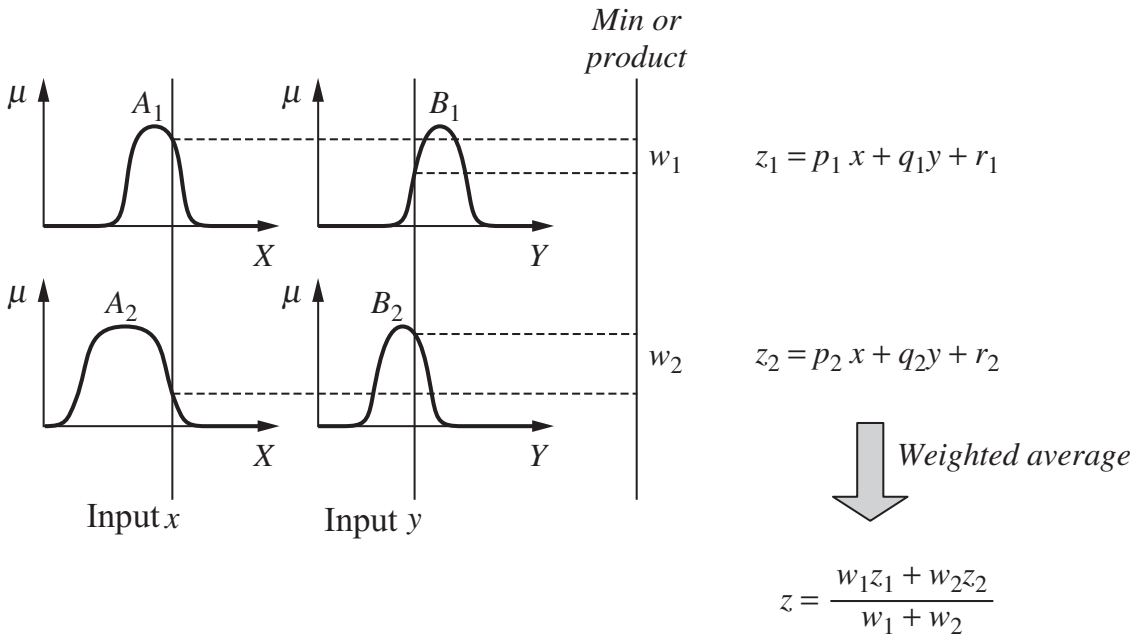

Figure 2.5: Type 3/Takagi-Sugeno FIS

The most widely used inference mechanisms are the Mamdani and Takagi-Sugeno inference mechanisms. The Mamdani inference mechanism is used where there is need to capture human knowledge, while Takagi-Sugeno is used in nonlinear control due to its ability to model nonlinear processes [43].

In the current research, Mamdani FIS is employed to model the EDM control problem. This is because most of the data that is available for the control of the EDM process could easily be expressed in statements form. Also, implementation of this type of control in LabVIEW is possible without need for additional softwares toolkits as compared to Sugeno FIS.

CHAPTER THREE

METHODOLOGY

3.1 Introduction

This chapter outlines the procedure that was followed to effectively achieve the design testing and implementation of the fuzzy logic (FL) based adaptive controller for the EDM process. The first section describes the initial approach aimed at designing a transistorized pulse generation circuit for an EDM machine at JKUAT Engineering workshops for use together with the FL based adaptive controller. The machine at JKUAT had been designed with a Resistor-Capacitor (RC) circuit for pulse generation, but required modification to use transistorized pulse generation circuit which provides the advantage of increased flexibility, thus allowing a wide range of machining parameters and a smoother operation. In this approach there were a few challenges that resulted from limited time and resources such as test equipment that were to be used together with the EDM machine. Due to these challenges, a second approach was adopted. This involved the use of the FL based adaptive controller to control an EDM machine at Technical University of Chemnitz (TU Chemnitz), Germany. The test equipment that were needed for this research work were readily available in TU Chemnitz laboratories.

3.2 Design of transistorized pulse generation circuit for EDM

This section details the process of development of the transistorized pulse generation circuit that was designed for use with EDM machine at JKUAT engineering workshops. The machine had been designed with a Resistor-Capacitor (RC) circuit for pulse generation. The RC type of pulse generator does not allow for a wide range of operating parameters and flexibility in adjustment. Therefore, a transistorised pulse generation circuit that would allow for a wide range of

operating parameters, flexibility and smooth operation was designed [44]. The performance of the transistorised pulse generation circuit on the EDM was also tested. The EDM machine is shown in Figure 3.1.

Figure 3.1: EDM machine based on RC pulse generation

3.2.1 Design considerations for the transistorized pulse generation circuit

The design process for the pulse generation circuit was guided by the requirements of the machining process. The main parameters that needed to be variable were:

- the frequency of the pulses during machining,
- the gap voltage, that is, the DC voltage that is applied between the tool electrode and the workpiece for machining needed to be adjustable,
- the duty cycle. For the pulse signal, there was need for design of controls that would enable the duty cycle to be adjusted.

There were two designs for the transistorized pulse generation circuit. The first one was based on a 555 timer, where the timer generated square wave signals (square pulses) that were needed for switching on and off the power transistors. It also included provisions for adjustments of both the duty cycle and frequency of the pulses.

Metal Oxide Semiconductor Field Effect Transistors (MOSFETs) which are semiconductor devices with three terminals (Emitter, Collector and Gate) were chosen for use in this circuit because they can handle high amounts of power and have high switching speeds. The MOSFETs are voltage controlled and can handle high current and wide load variations, allowing very fast switching with ease of control. A photograph of the 555 timer based circuit is shown in Figure A.1 and its schematic is shown in Figure A.2 in Appendix A. This circuit generated pulses with a frequency of up to 1 kHz, and was simple.

The 555 timer based circuit performed fairly well, but it presented challenges in that, when frequency was adjusted the duty cycle was also altered. Similarly, when the duty cycle was adjusted, the frequency was altered. Thus, it was not possible to independently adjust the frequency without altering the duty cycle and vice versa.

These shortcomings of the 555 timer based circuit brought the need for another approach in the design of the pulse generation circuit whose duty cycle and frequency could be independently adjusted. Thus, a second circuit was designed based on an Arduino® Atmega 328P microprocessor. This microprocessor was chosen because it is easy to program and provides more versatility. The microprocessor also provides higher accuracy and independent control of the necessary parameters as compared to 555 timer [45]. The Arduino® microprocessor was used to generate the required pulse signal from its in-built oscillator. Figure 3.2 shows a photograph of the pulse generation circuit that was fabricated. It has five sub-circuits which are all connected and communicate with each other. The

circuits in the figure are; stepper motor driver circuit for control of the stepper motor, graphical user interface circuit for human interaction, gap control circuit for the control of the spark gap and DC power supply circuit for supply of the machining pulsed DC voltage.

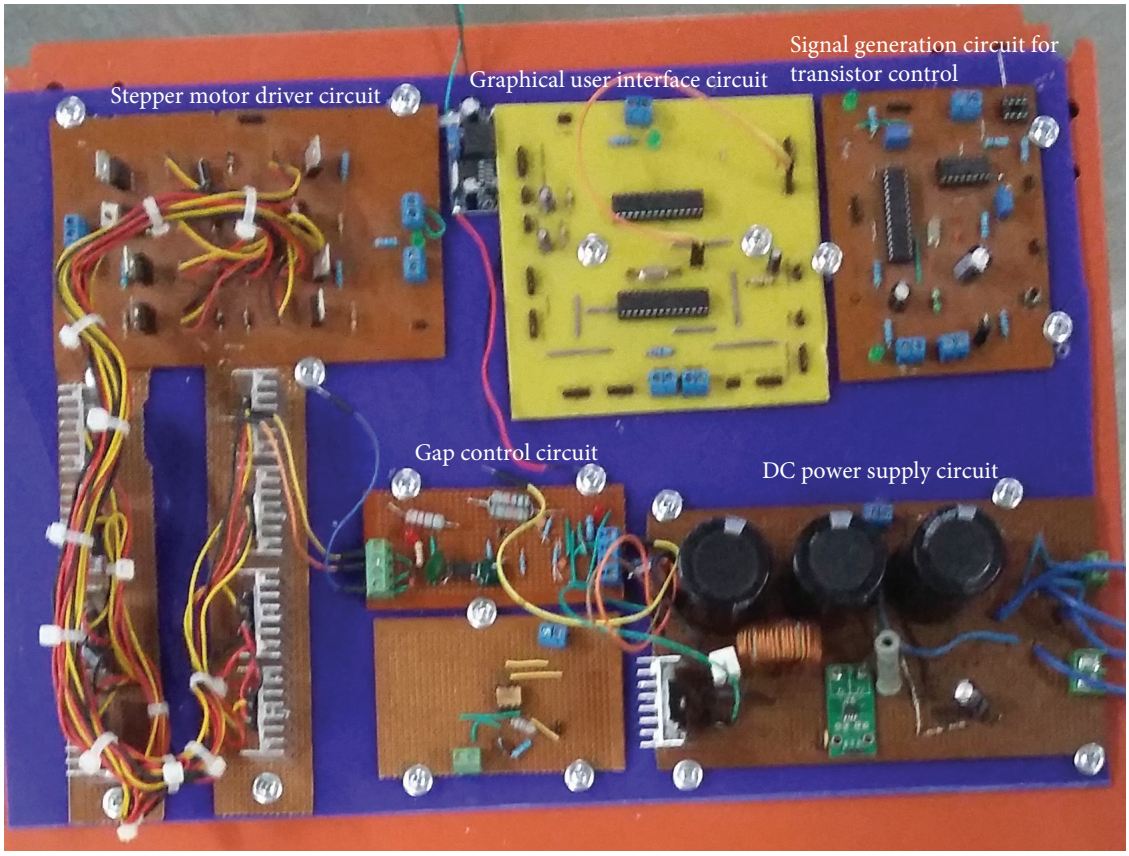

Figure 3.2: EDM control and pulse generation circuit based on Arduino Atmega 328P microprocessor

1. **Graphical user interface circuit**

   To be able to input data for the control of the sparking process of the EDM and view the machining parameters, a graphical user interface (GUI) circuit was developed. This circuit is shown in Figure 3.3. The adjustment of the machining parameters for the EDM process such as frequency, duty cycle, machining voltage is done through the GUI.

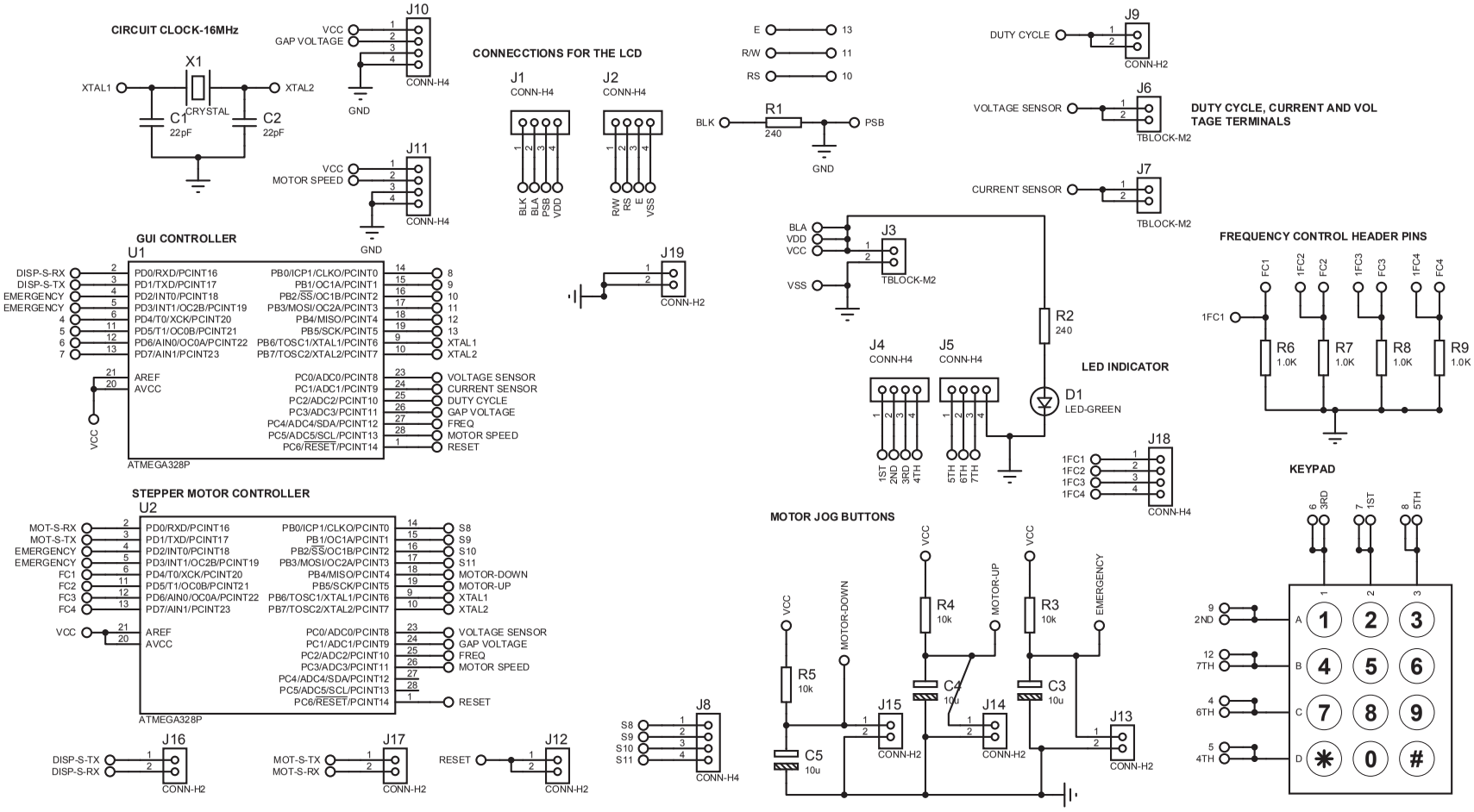

Figure 3.3: Layout of the Arduino Atmega based pulse generation circuit graphic user interface (GUI)

2. **Pulse generation and gap control circuits**

   A pulse generation and gap control circuit for control of firing of the transistors was developed. The schematic diagram of this circuit is shown in Figure 3.4. The pulse generation circuit generates a frequency of between 0 Hz and 10 kHz which controls the firing of the MOSFET. The circuit uses an Arduino Atmega 328P microprocessor for pulse generation. It generates square pulses with independently controllable frequency and duty cycle by use of potentiometers.

   The microprocessor reads frequency and duty cycle values that are input from either the keypad or potentiometers and generates the necessary pulse signals to drive the MOSFET. The potentiometers override frequency and duty cycle values input through the keypad.

   On the other hand, the gap control section of this circuit measures the gap voltage, compares it with some preset threshold and determines if a short or open circuit is likely to occur or has occurred. Preliminary experimental work was done and it was found that, short circuit occurred if the measured voltage is below 5% of the applied machining, hence the motor direction is reversed so that the tool can retract until the value of the measured voltage is above 5% of the applied voltage.

   In the same preliminary experimental work, it was also found that an open circuit occurs for gap voltage above 95% of the applied voltage. Therefore, when this percentage voltage is attained, the motor moves the tool downwards until the value of the measured voltage is below 95% of the applied DC voltage.

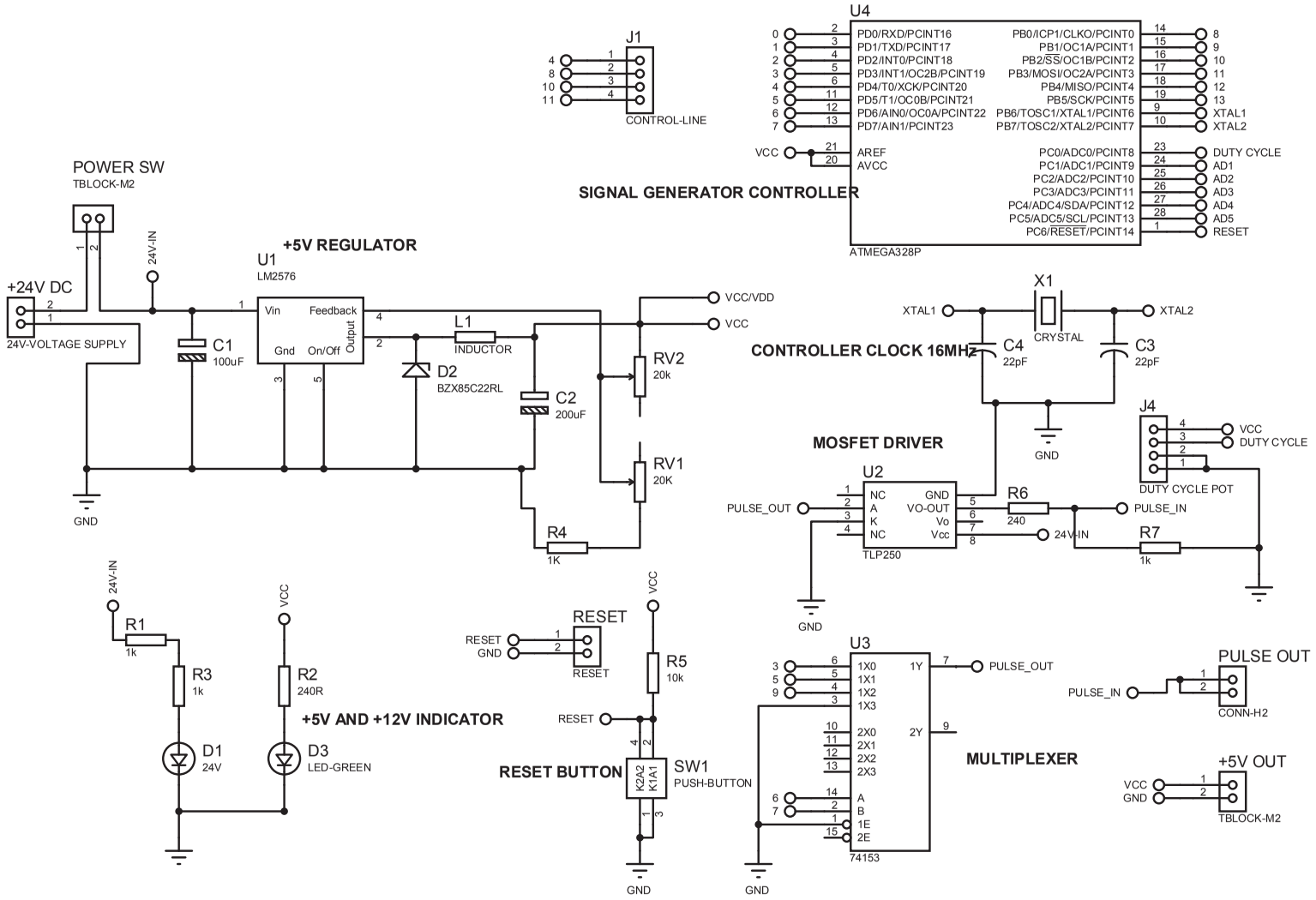

Figure 3.4: Arduino Atmega based pulse generation circuit for the control of transistor switching

3. **DC power supply circuit**

   The circuit shown in Figure 3.5 rectifies the mains supply of 240 V AC and provides a DC output voltage that is required for the material removal process. The DC voltage has range of between 0 V and 100 V. This range was chosen because it reflects the normal operating range of macro EDM machines and also due to limitations of the electronics that were available in processing higher voltages. The adjustment of the open circuit gap voltage is done by a knob on a variable transformer (Variac) that is used to supply AC voltage to the power circuit. When the MOSFET is powered, it provides a square wave signal. The parameters of this square wave signal, i.e., frequency and duty cycle are controlled by the rate and sequence of firing of the MOSFET which is in turn controlled by the pulse generation circuit.

4. **Stepper motor driver circuit**

   The stepper motor driver circuit powers the stepper motor based on the set speed and the input from the gap control circuit. Depending on the nature of signals from the gap control circuit, the motor will move either in the forward or reverse direction and at the commanded speed. The stepper motor speed can also be manually adjusted for rapid movements. The manual override is done by means of a potentiometer. The circuit is shown in Figure 3.6. It consists of bridge circuit for rectification and a main circuit which has a set of transistors that are used for switching to supply the stepper motor with commands for stepwise motion.

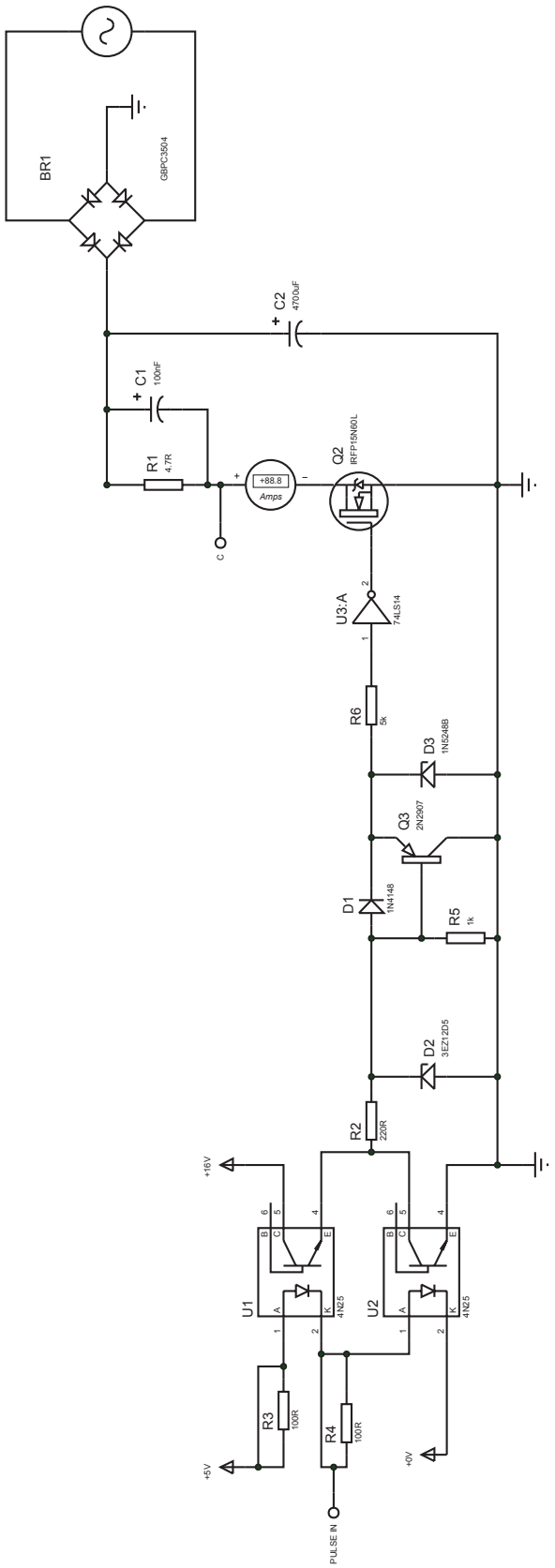

Figure 3.5: DC power supply and regulation unit

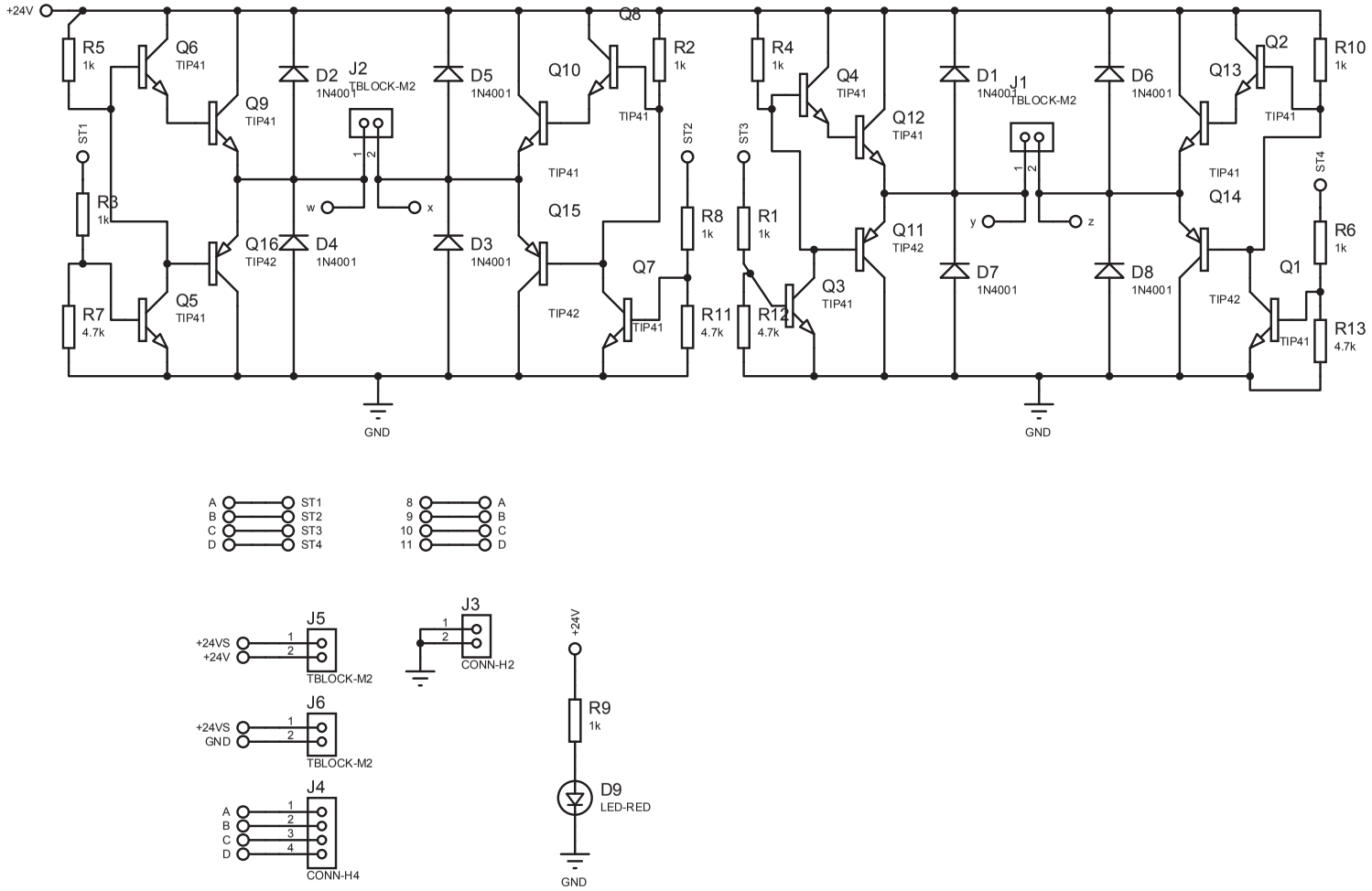

Figure 3.6: Stepper motor driver circuit

3.3 Experimental setup and preliminary experiments

In order to test the functionality of the transistorized pulse generation circuit, preliminary experiments were carried out using the EDM machine shown in Figure 3.7 at JKUAT. The electrical signals were captured using a Hentek DSO5102B digital oscilloscope and recorded into a personal computer. These signals are the pulsed DC voltage and the machining discharges.

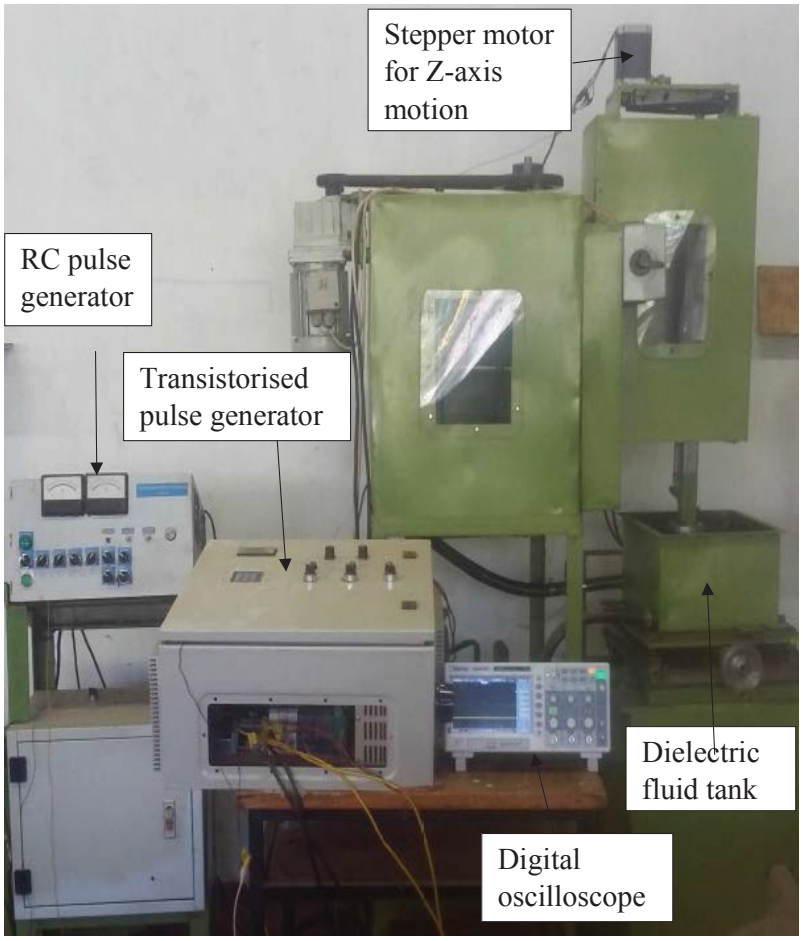

Figure 3.7: EDM machine developed at JKUAT

Since the common range of open circuit voltages for EDM is between 50 V and 300 V [46], an open circuit voltage range of between 50 V and 100 V was chosen for the current design of the transistorized pulse generator. The reason for this is

that the experiments that were to be done were designed for that voltage range. Further, it was due to limitations of the electronics available for manufacture of the circuit. The duty cycle range is between 0% and 100% and the choice of a 20% increment was made on the basis of the number of experiments that needed to be done. Each of the experiments was timed and material removal rate was calculated from the volume of the material removed and the time taken to machine it. In the preliminary experiments, ten identical workpieces (all of them made from mild steel (0.25% C)) were machined. In the first group of five experiments, gap voltage was varied between 50 V and 90 V while the duty cycle was kept constant at 50%. In the other group of five experiments, the duty cycle was varied in steps of 20 while the gap voltage was maintained at 80 V.

The resulting performance parameters i.e., MRR and surface roughness were used to test the performance of the transistorized pulse generator. The surface roughness of the machined workpieces was measured using Mitutoyo SJ301 surface roughness tester shown in Figure 3.8. The workpiece material for all experiments

Figure 3.8: Surface roughness tester

at this stage was low carbon steel (also known as mild steel). Mild steel was chosen because it is a very widely used material and was readily available in the laboratory. The workpieces were machined for a 30 minutes period at a frequency of 1 kHz for each set of experiments. A graphite tool electrode was used for machining with kerosene as the dielectric fluid. The fact that kerosene

is a non conductor that has a boiling point of between 150°C and 300°C, and a flash point of between 35°C and 60°C make it suitable as a dielectric fluid. It is worth noting that the experiments were conducted with both the workpiece and the tool electrode immersed in the dielectric fluid.

3.4 Investigation of influence of EDM process parameters on its outputs

3.4.1 Overview

This section describes the experiments that were carried out to investigate the effect of machining parameters on the EDM process. The machining parameters of interest were duty cycle, gap voltage and discharge current. To determine the effect of each of the parameters under investigation, the results of the machining process were classified based on three parameters which were surface roughness of the machined surface, material removal rate and the tool wear rate.

3.4.2 Machining experiments

Due to the challenges of lack of measurement, test and control equipment at JKUAT, the electrical discharge machining experiments were carried out on a Sarix SX100 micro electrical discharge machine at Technical University of Chemnitz, Germany. The experimental setup was such that data was recorded via a high resolution (with sampling frequency of 1 GHz and sample rates of 5 GS/s) DPO4104 Tektronix oscilloscope shown in Figure 3.9, into a personal computer and the National Instruments PXI system.

The diagram shown in Figure 3.10 illustrates the setup that was used for the machining experiments and data acquisition. Three different materials namely aluminium (Al), brass (C_uZ_n) with 65% C_u and 35% Z_n and medium carbon steel (F_eC) with 0.47% carbon content (AISI 1040 steel) that were readily available in

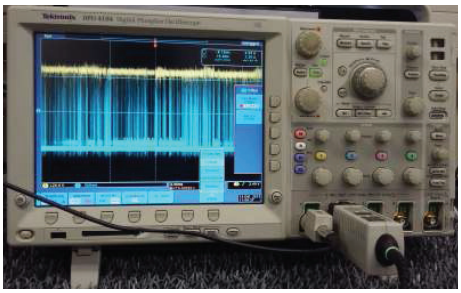

Figure 3.9: High resolution DPO4104 Tektronix oscilloscope

the laboratory were used for the machining experiments.

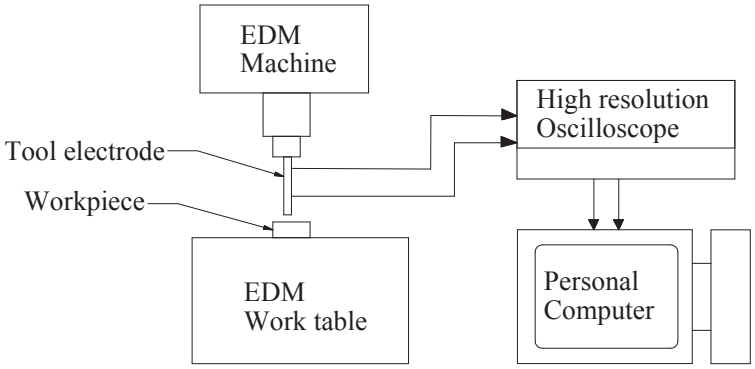

Figure 3.10: Illustration of experimental setup

In each set of experiments, three identical sets of machining experiments were carried out with a specific set of machining parameters as is shown in Table 3.1 and 3.2. The three sets of experiments involved machining three pieces of workpieces under identical conditions, one from each of the materials.

From the results obtained, comparison was done and generalized conclusions drawn on the effects of each of the machining parameters on the EDM process outputs. The findings from the analysis of the experimental results were used as a guide in the design of the adaptive controller for the EDM process.

The machining data was sampled at a sampling rate of 100 Kilo samples per second by the Tektronix DPO4104 oscilloscope. This sampling rate was chosen to coincide with the machining frequency. The signals that were recorded were

Table 3.1: Design of experiments for investigating gap voltage in EDM process

S/No. of experiment	Constant Variable	Adjustable variable	Set of experiments		
			Set 1	Set 2	Set 3
	Duty cycle (%)	Gap voltage (V)	Al	CuZn	FeC
1	50	50	3	3	3
2	50	70	3	3	3
3	50	90	3	3	3
4	50	110	3	3	3
5	50	130	3	3	3
6	50	150	3	3	3

Table 3.2: Design of experiments for investigating duty cycle in EDM process

S/No. of experiment	Constant Variable	Adjustable variable	Set of experiments		
			Set 1	Set 2	Set 3
	Gap voltage (V)	Duty cycle (%)	Al	CuZn	FeC
1	100	10	3	3	3
2	100	30	3	3	3
3	100	50	3	3	3
4	100	70	3	3	3
5	100	90	3	3	3

the spark voltage, corresponding discharge current and the tool wear for each of the machining cycles at the selected sample rate. The EDM machine recorded the tool wear for each machining cycle.

The TWR was calculated from the total amount of tool wear that was recorded by the EDM during machining (in terms of length) and the time taken for machining each of the profiles. Likewise, material removal rate (MRR) was calculated from timed machining cycle for each profile for all experiments. The volume of the machined profile was used to calculate the total amount of material removed during machining.

The quality of the surface finish was analyzed using a Nikon MM-400 measurements microscope shown in Figure 3.11 (a) and Keyence VK-9700 3-D laser scanning microscope shown in the Figure 3.11 (b) at TU Chemnitz.

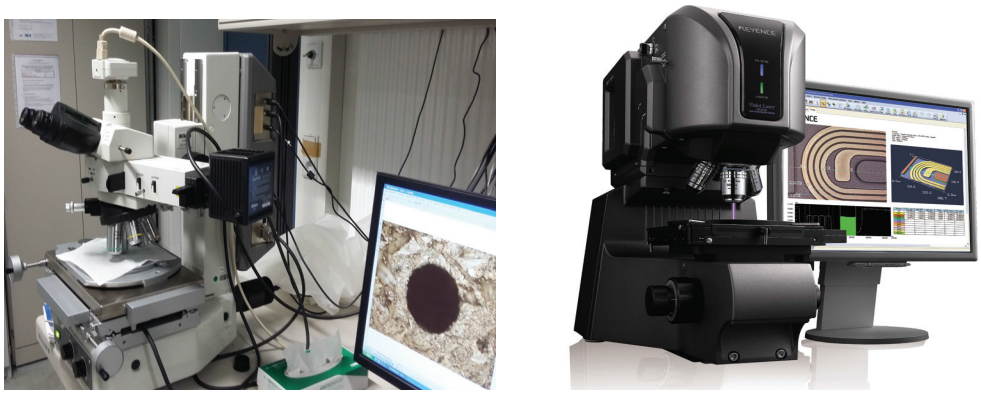

(a) Surface measurement microscope (b) Laser scanning microscope

Figure 3.11: Surface quality measurement microscopes

A tungsten carbide tool electrode of diameter 80 μm and a dielectric oil (HEDMA111) were used for all the machining experiments since they were readily available and suitable for the machining experiments. The tool material characteristics are shown in Table 3.3 and dielectric oil characteristics are as shown in Table 3.4.

Table 3.3: Tungsten carbide properties

Property	**Value/State**
Density	15.8 g/cm^3
Solubility in water	Insoluble
Melting point	2870°C
Boiling point	6000°C
Thermal conductivity	84.02W/mK
Tensile strength	0.3448GPa
Mohs hardness	9

Several sets of electrical discharge machining experiments were conducted on each of the materials. In order to investigate the effects of the individual machining

Table 3.4: Dielectric oil properties

Property	Value/State
Viscosity at 20°C	2.4cSt
Density at 15°C	0.781 Kg/l
Flash point	101°C
Original smell	Neutral

parameters on the EDM process, for each experiment, some of the parameters were held constant and only one parameter, the one under investigation, was varied. The parameters under investigation included gap voltage, discharge current and duty cycle.

3.5 Development of the adaptive controller for the optimization of the EDM process

3.5.1 Overview

A fuzzy logic based adaptive controller that was designed for the optimization of the EDM process has the ability to improve both the system performance and adaptability. The data that had been obtained from experimental work on investigation of the effects of machining parameters on EDM process output parameters was used to design the rules and membership functions for the fuzzy logic controller. The number of rules were minimized by incorporating a monitoring unit in the controller, which ensures that there is realtime monitoring of the machining parameters. The inclusion of the monitoring aspect in the controller helps to limit the deviation of the machining parameters from the intended ones. The monitoring unit also enhances control of the EDM process by monitoring the trend of machining parameters, thus indicating the likelihood of occurrence of an undesirable machining condition such as short or open circuit and, therefore, ensuring correction of parameters before the undesirable machining condition oc-

curs.

The fuzzy logic based adaptive controller works in a closed loop so as to optimize the machining process by selecting the appropriate machining parameters based on the input from the feedback obtained from measurements on the actual machining process. A block diagram showing the layout of the adaptive controller is shown in Figure 3.12. The main controller interface constitutes the main

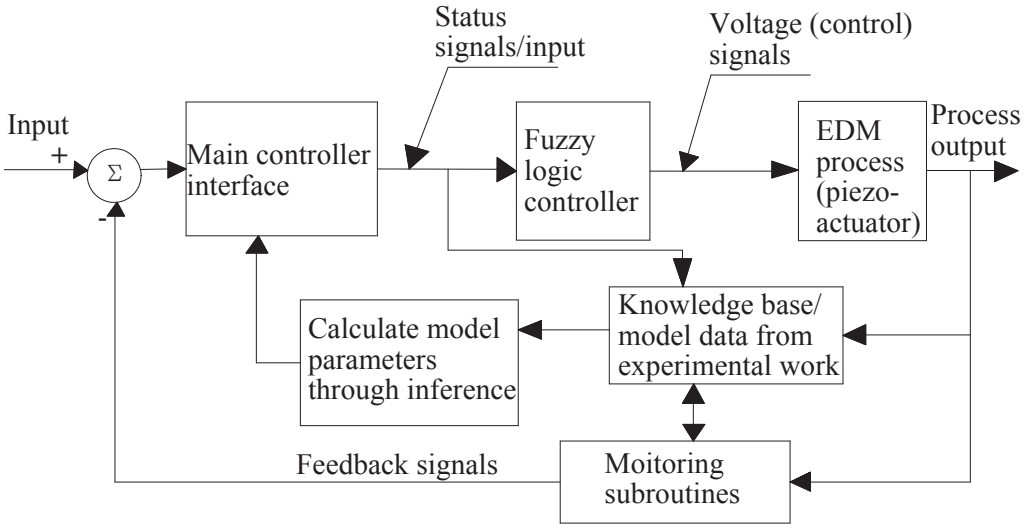

Figure 3.12: Block diagram of the FLC based adaptive controller

subroutine. Its function is to call all the other subroutines and check status data on the monitoring subroutines. The fuzzy logic controller uses the knowledge base to evaluate the status signals and control the machining process by feeding voltage control signals to the piezo-actuator via a driver circuit. The monitoring subroutines check the machining condition indicators and compare them to ideal machining signals. This status data is fed to the FLC. The machining process is then controlled by adjusting the spark gap which is achieved by means of an ultra fast response frequency piezo-actuator (P-611Z Piezo).

In order to effectively control the EDM process, the adaptive controller is designed to have the main control routine/unit, two monitoring subroutines; one

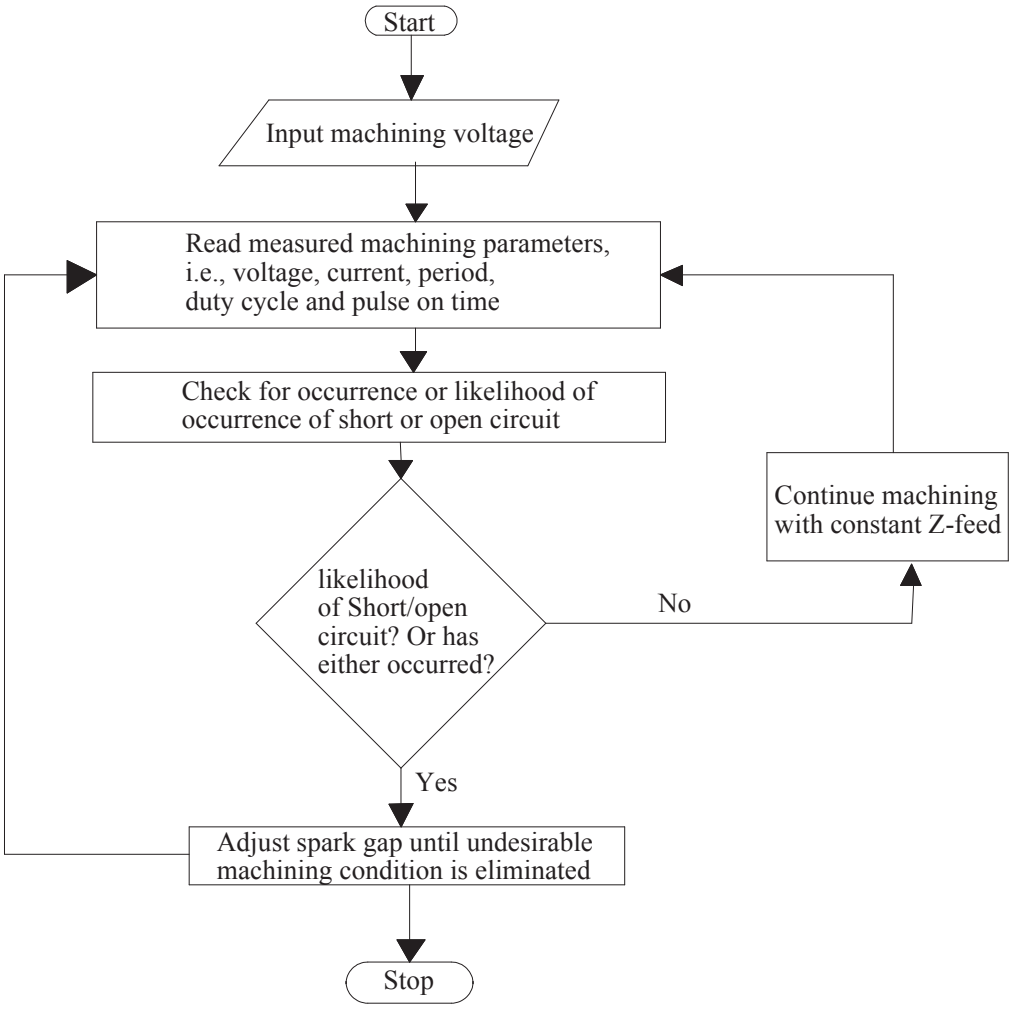

Figure 3.13: Flow chart for the control of EDM

for the duty cycle and the other one for the voltage/current, and, the FL subroutine which is the one that executes the control action. The main control unit communicates with monitoring and control subroutines to achieve the overall objective of optimization of the EDM process. A flow chart for the control action is shown in Figure 3.13.

3.5.2 Main control subroutine

This is the main interface subroutine block of the controller for the EDM process and functions as shown in the flow chart in Figure 3.14. It calls the two monitoring

subroutines, i.e., the timer based current discharge monitoring subroutine and the gap voltage monitoring subroutine. The monitoring subroutines are used to provide feedback to the FLC and therefore enable realtime control.

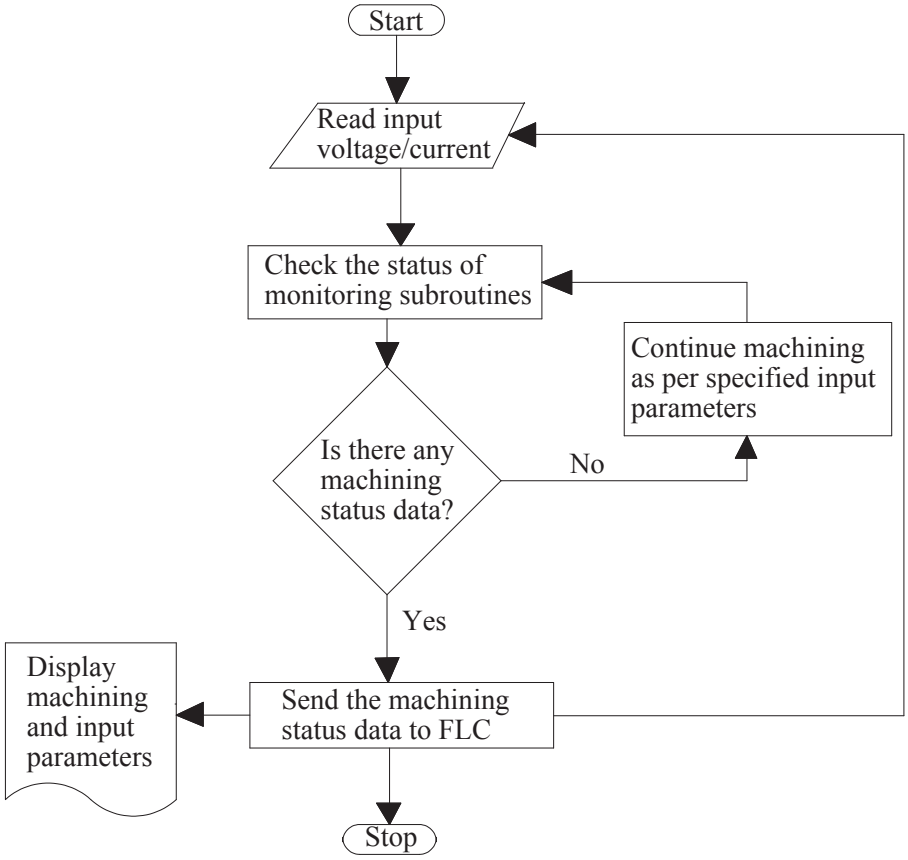

Figure 3.14: Flow chart for the main control subroutine

The main controller checks the status of the monitoring subroutines and feeds their status data into the FLC based subroutine which in turn evaluates the status of the machining process and provides relevant control signals for spark gap control. The control signals are then output to the piezo actuator so as to adjust the spark gap accordingly. Six status parameters, namely: short and open circuits, discharge time, short and open circuit voltages, and measured spark gap voltage, are fed into the FLC as inputs.

The front panel or Graphical User Interface of the controller (GUI) displays the

machining conditions such as detection of short or open circuit and the FLC execution parameters, and shows the measured gap voltage/current. It contains a stop button for stopping the execution of the controller. The GUI also allows for input of machining gap voltage which is set by use of a slider scale. The block diagram for the main subroutine of the adaptive controller is shown in Figure 3.15 and its front panel is shown in Figure 3.16.

The section labelled **A** on the block diagram is where the input gap voltage and current are defined. In this section, the measurement of gap voltage, discharge frequency and duty cycle is also done and the measured signals recorded. Further, the machining status parameters are analyzed here and then sent to the FLC in section **B**. At the FLC execution section (**B**), the status signals are built into an array that is fed into the FLC. The FLC evaluates the signals based on the rule base and gives out an output that is the control signal. The control signal is fed to the section labelled **C** from where it is converted to a voltage signal and output through the DAQ for the control of the piezo actuator.

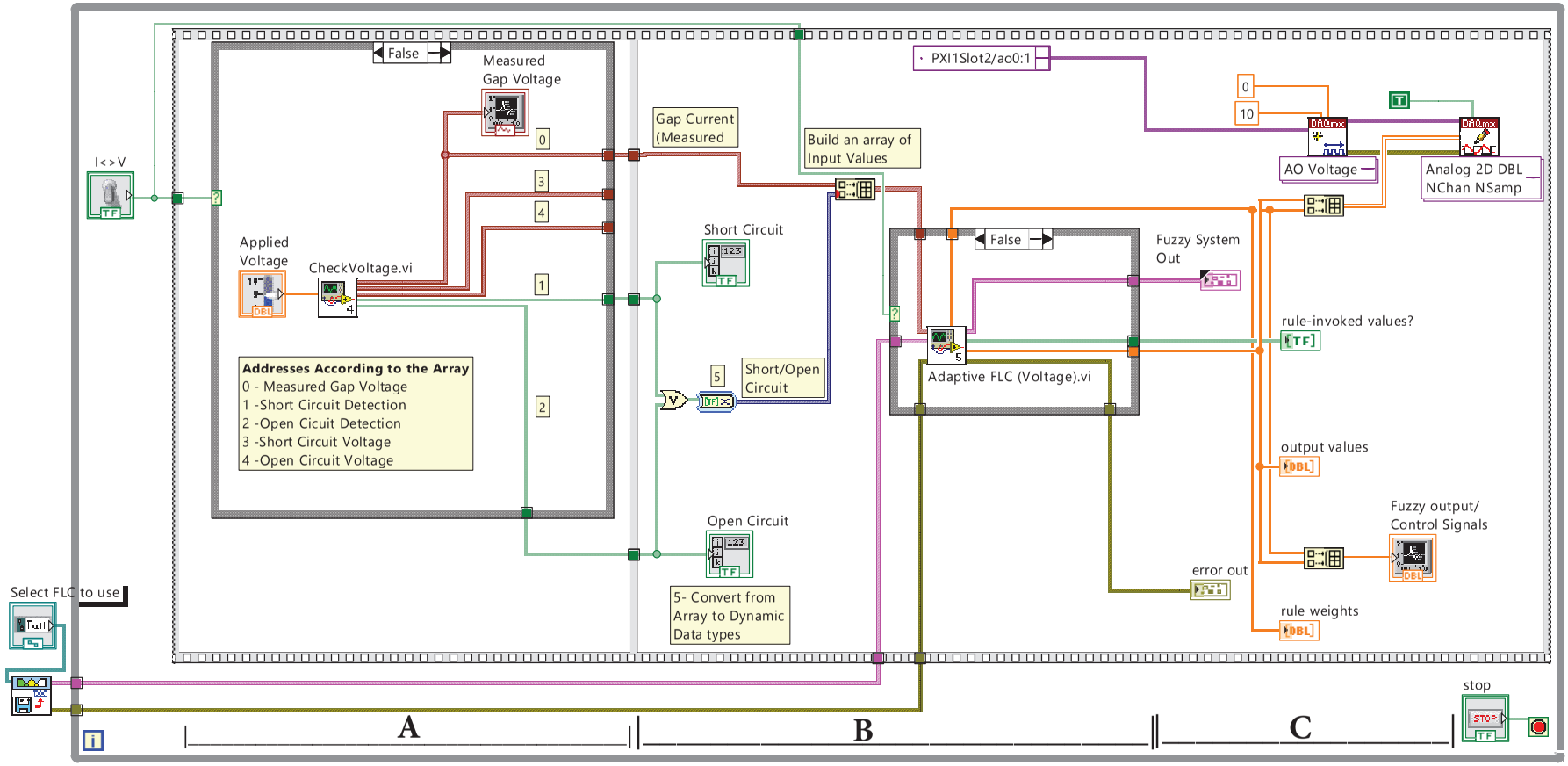

Figure 3.15: Block diagram of the main subroutine of the FLC based adaptive controller

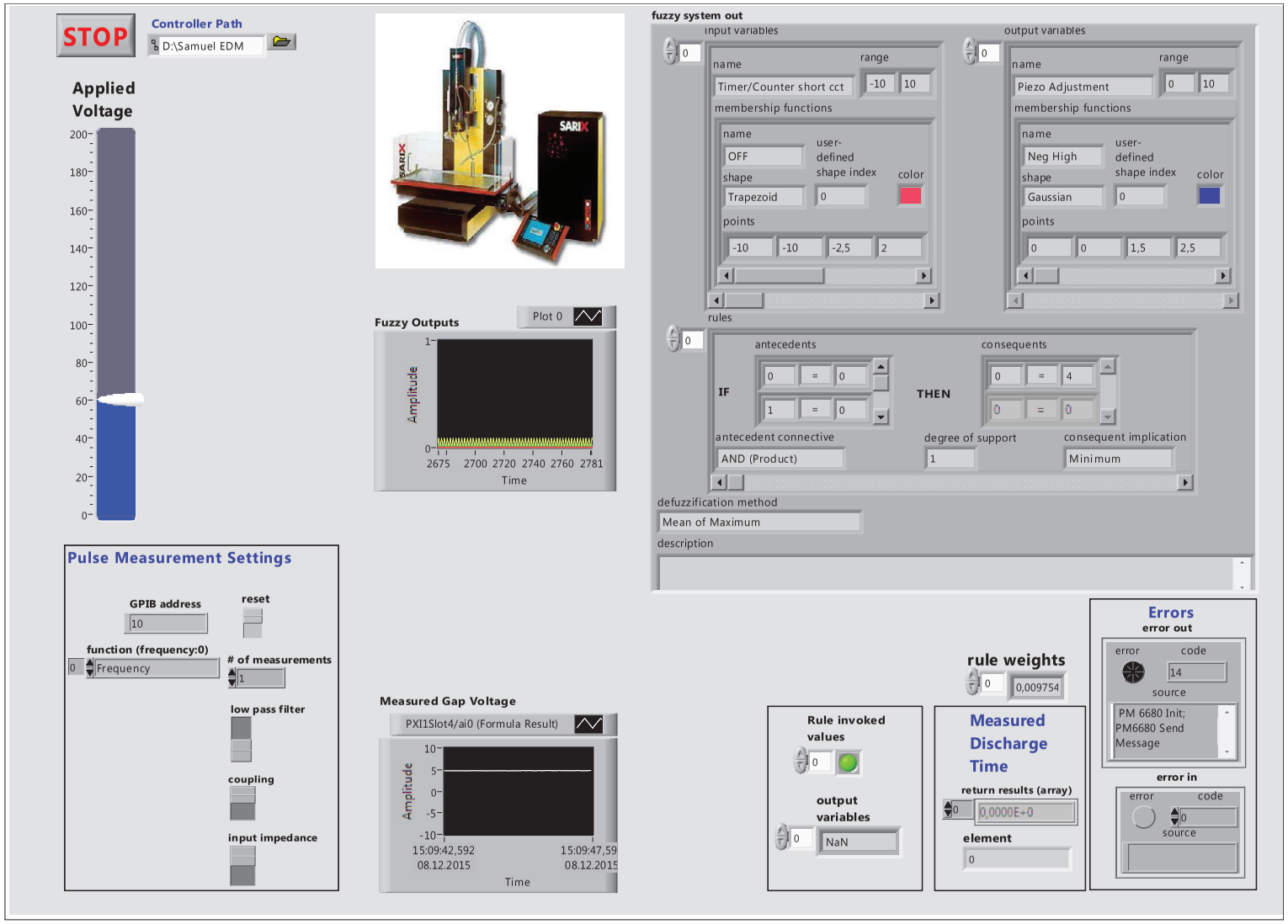

Figure 3.16: Front panel of the FL based adaptive controller

3.5.3 Timer based current discharge monitoring subroutine

From previous researches by Schubert *et al.* [47] on the current discharge characteristics during the EDM process, it was found that, the average period for each effective discharge is about 100 ns. The current research was carried out using the same equipment at TU Chemnitz. Using the results obtained from the research done by Schubert *et al.*, the upper and lower limits for current discharge time were set at 95 ns and 105 ns respectively. The researchers also found out that, if the periodic time for each current discharge increases (frequency of the discharges decreases), there is a likelihood of occurrence of a short circuit. Conversely, if the periodic time decreases (frequency of the discharges increases), there is a likelihood of occurrence of an open circuit. These observations together with the data on the effect of variation of gap voltage and duty cycle on EDM process were used in the design of the controller for the EDM process. The controller is designed to monitor the discharge time for each spark and the periodic time for consecutive current discharges and adjust the gap depending on the behaviour of the discharges so as to minimize chances of occurrence of either short circuit or open circuit as shown in the flow chart in Figure 3.17. Figure 3.18 shows the block diagram that is used to implement this monitoring subroutine of the adaptive controller. The section of the controller shown in Figure 3.18 uses the high resolution programmable timer to check time taken for each discharge signal and if the time is above 105 ns, then a signal is sent to the FLC indicating that a short circuit is likely to occur. However, if the time for current discharge is below 95 ns, then a signal indicating that an open circuit is likely to occur is sent to the FLC. The FLC uses a rule base designed to adjust the gap voltage so as to avoid the occurrence of either short or open circuits. The block diagram shown in Figure 3.20 checks the frequency of the current discharge signals. Increase or decrease in frequency of the current discharges is detected in this section of the controller. A signal is then sent to the FLC indicating whether a short or open

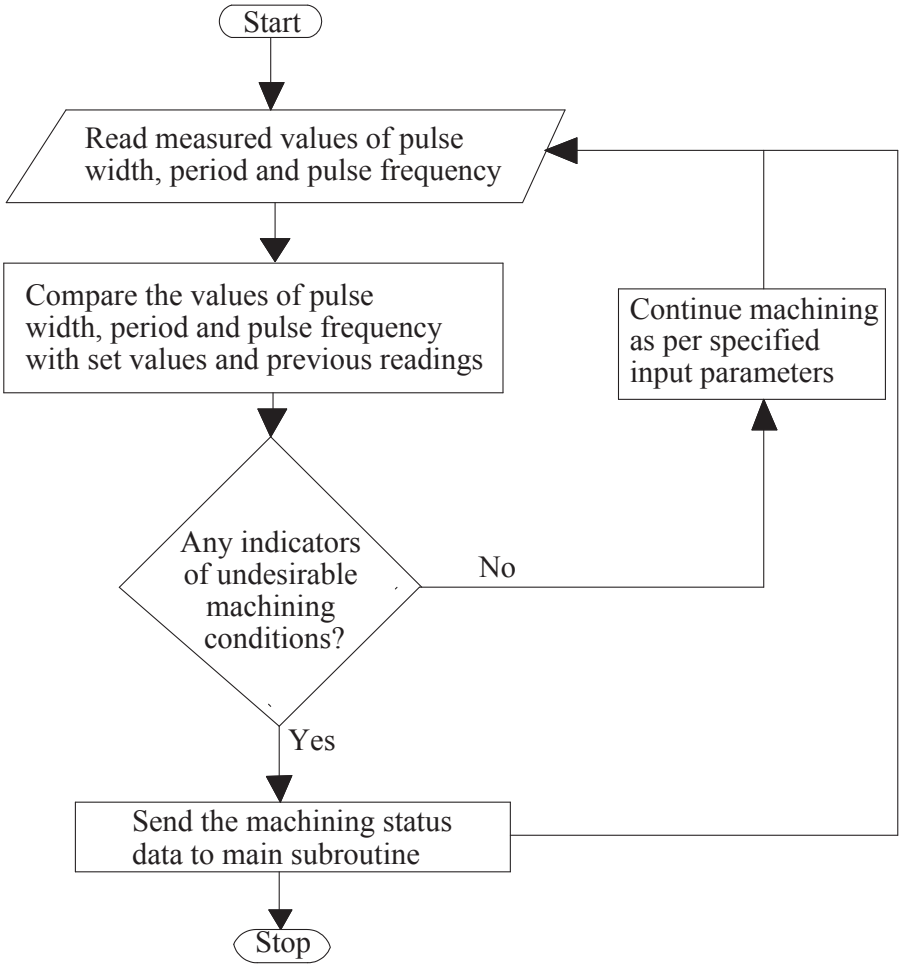

Figure 3.17: Flow chart for the timer based monitoring subroutine

circuit is likely to occur (based on the discharge frequency). In this subroutine, the feedback function of LabVIEW software compares a retained value of the previous frequency with the current one at a frequency of 200 MHz and if a change is detected, it is sent to the main controller. The outputs from this subroutine and from the one shown in Figure 3.18 are compared and if in any of, or in both cases there is an indication of undesirable machining condition, then, the FLC checks the value of the gap voltage and, consequently, outputs a signal to adjust the spark gap so as to avoid occurrence of the undesirable conditions. The timer acquires and monitors signals in this subroutine. It detects a rising edge of a current discharge (when the value of a current signal starts to rise).

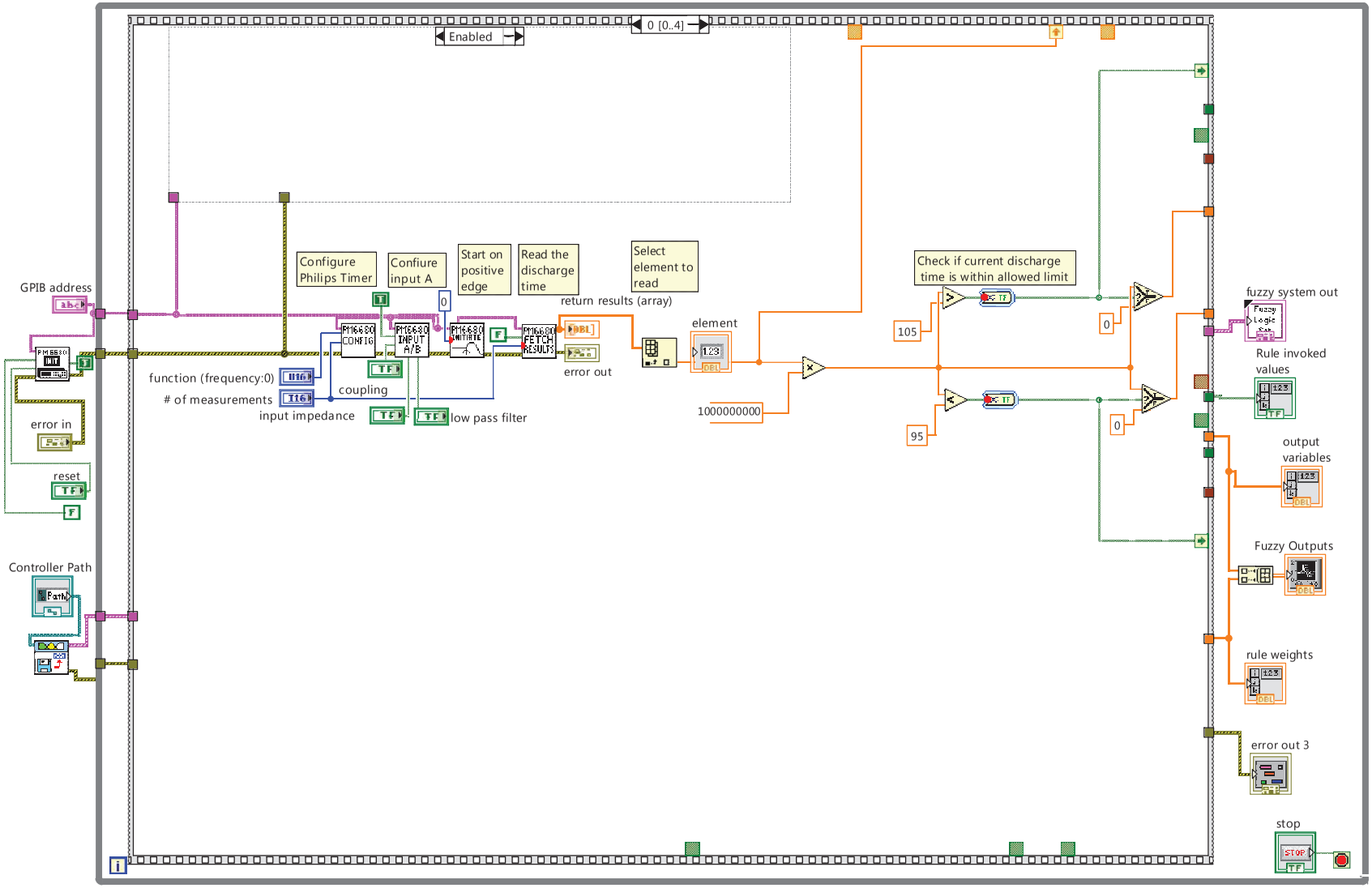

Figure 3.18: Block diagram for monitoring the time of current discharges

The time between two consecutive rising edge detections indicates the period of the current discharges. The software based timer who's flowchart is shown in Figure 3.19 counts ten cycles after which it resets and starts counting again.The time taken to record ten consecutive cycles is compared with that of the immediate previous equal number cycles to check if the trend is towards an increasing or decreasing frequency, or the same as earlier one.A decreasing frequency is an indicator of likelihood of occurrence of short circuit. However, if the frequency of the discharges increases, it is an indicator that an open circuit is likely to occur. On the other hand, if the frequency remains the same, its an indicator of stable machining process. This ability to detect undesirable behaviour in the discharges without the behaviour being explicitly defined makes the controller able to deal with uncertain machining conditions.

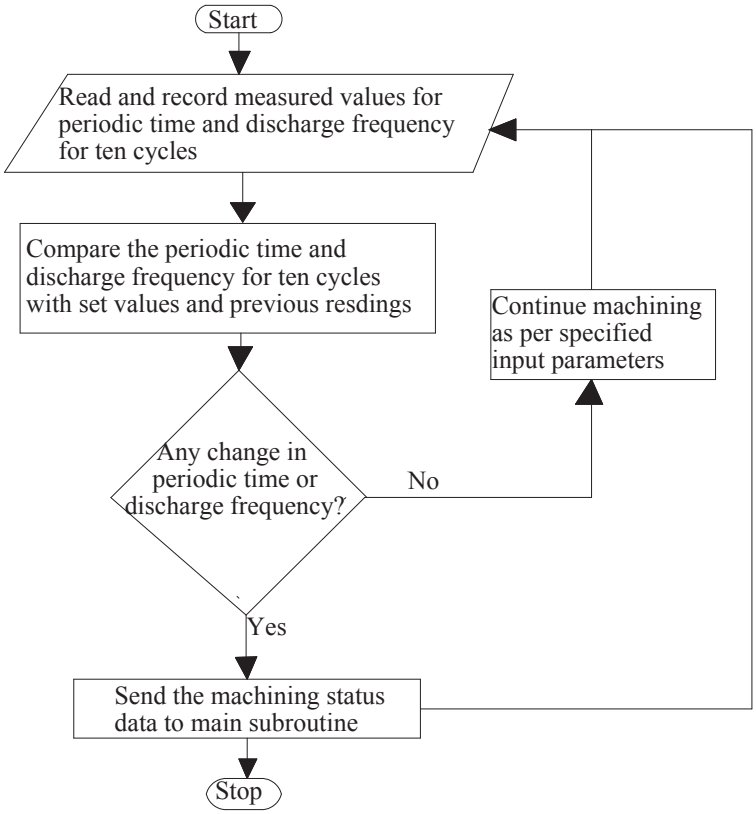

Figure 3.19: Flow chart for software based timer monitoring subroutine

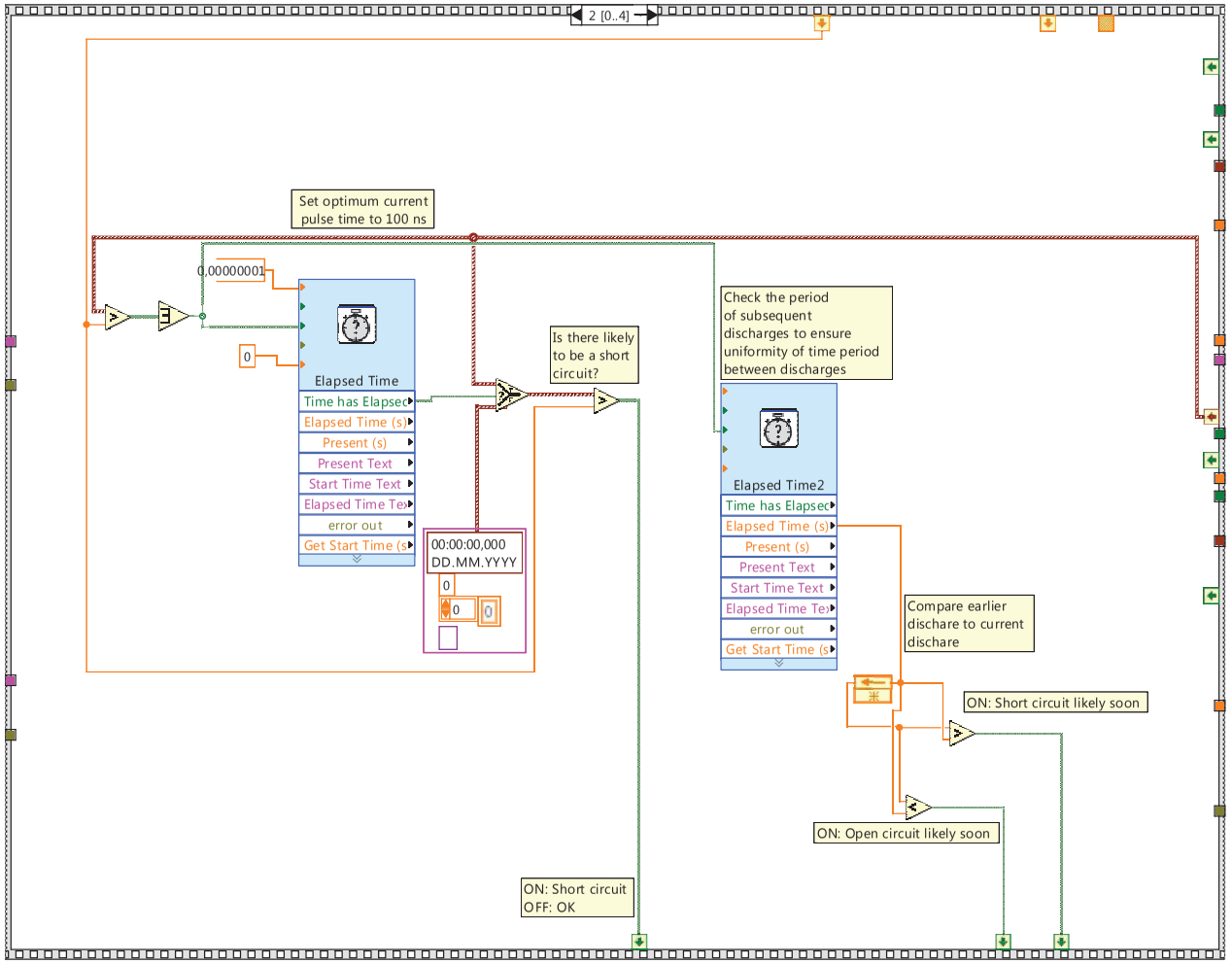

Figure 3.20: Block diagram for monitoring frequency of current discharges

3.5.4 Gap voltage monitoring unit

Another monitoring subroutine of the adaptive controller, the gap voltage monitoring unit is shown in the block diagram in Figure 3.21. This block diagram monitors the gap voltage and compares it with the applied machining voltage. Monitoring is achieved by setting the minimum allowable gap voltage and the maximum allowable gap voltage. The maximum allowable gap voltage is set at 95% of the applied gap voltage and the minimum allowed gap voltage is set at 5% of the applied gap voltage. These are the values above and below which open and short circuits are considered to occur [47]. If the measured gap voltage is below the minimum allowed value, then this subroutine sends a signal to the FLC indicating that a short circuit is likely to occur. On receiving a signal about the occurrence or likelihood of occurrence of short circuit, the FLC sends a voltage control signal to increase the spark gap via the piezo actuator. On the other hand, if the measured gap voltage value is higher than the maximum allowed percentage of the applied voltage, then a signal is sent to the FLC indicating that an open circuit is likely to occur and the FLC in turn sends a control signal to reduce the spark gap via the piezo actuator.

The acquisition of voltage signals is done via NI PXIe-6259 M series and NI PXI-7851 R series National Instruments' data acquisition cards, both integral parts of the NI PXI system. The output signals from this subroutine together with other machining status data from other monitoring subroutines are fed in to the FLC as the inputs. The FLC evaluates all the input machining status data and gives control signals to either increase or reduce the spark gap, or to maintain it the same. The control signals from the FLC are in form of voltage signals which are used to drive the piezo actuator to adjust spark gap. The voltage signals are output via a National Instruments NI PXI-6723 data acquisition card. The reasoning behind the inclusion of the monitoring subroutines is so that they can detect the possibility of occurrence of an undesirable machining condition, and at

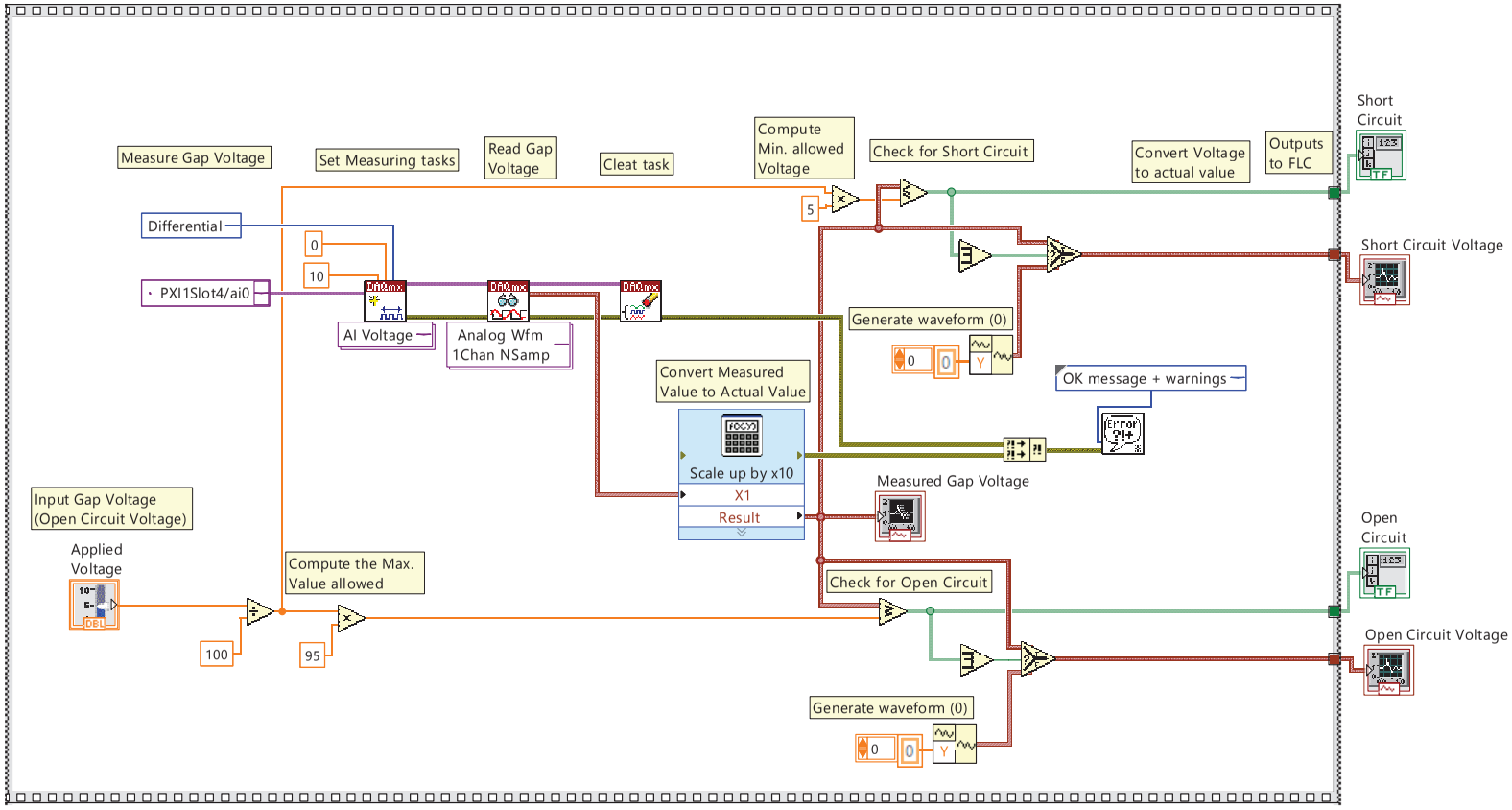

Figure 3.21: Block diagram of gap voltage monitoring subroutine

the same time, make the controller's response faster, hence minimizing the actual occurrence of the undesirable machining conditions. Further, with the monitoring subroutine, if any disturbance is introduced into the machining process, it will be detected from the behaviour of the discharges and a corresponding signal is sent to the FLC for corrective action to be taken. This helps in minimizing the number of membership functions and rules for the FLC because the input and output ranges are narrowed. The result is faster response because of reduced execution time of the FLC and hence more enhanced realtime control.

3.5.5 Fuzzy logic controller

The block diagram for the fuzzy logic controller that was developed for the optimization of the EDM process is shown in Figure 3.22. The FLC has six input parameters namely;

a) short circuit detection (from discharge monitoring subroutine)

b) open circuit detection (from discharge monitoring subroutine)

c) discharge time (from discharge monitoring subroutine)

d) short circuit voltage (from gap voltage monitoring subroutine)

e) open circuit voltage (from gap voltage monitoring subroutine) and

f) gap voltage (from gap voltage monitoring subroutine)

The input signals indicating short or open circuit have only two states, that is, true or false, while the other two signals (discharge time and gap voltage) are analog signals. The input analog signals were mapped into fuzzy sets with seven Gaussian type of membership functions. Also, the output of the FLC has seven Gaussian fuzzy membership functions. The fuzzy rules were generated based on these membership functions. The data on effects of machining parameters on the output parameters was used to determine the relationship between the antecedent and the consequent, and hence develop the rules base. The rule base gives the optimum machining parameters for the EDM process.

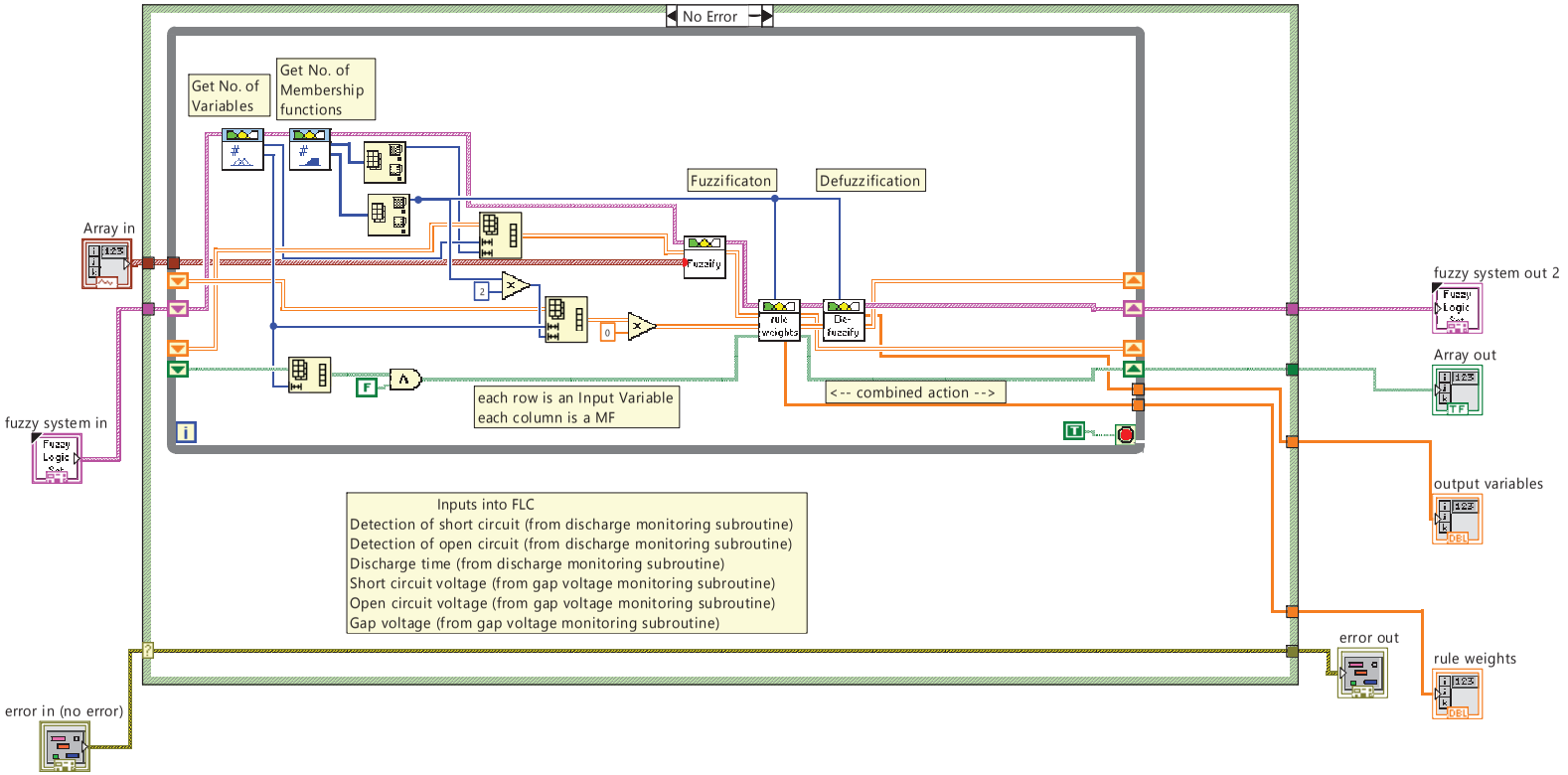

Figure 3.22: Block diagram of the FLC developed for optimization of EDM process

In the FLC, Gaussian membership functions are used to represent input and output variables because this type of membership functions are the best suited to model situations or applications that are non linear in nature [48]. The two analog inputs have 7 membership functions each as shown in Table 3.5. These membership functions are used to map the input parameters from linguistic form into fuzzy form, ranging from extremely low to extremely high.

Table 3.5: Analog input membership functions

Membership function	**Shape**	**Points**
Neg Large	Gaussian	0 ; 0 ; 1.5 ; 2.5
Neg Small	Gaussian	1.5 ; 2.25 ; 2.75 ; 3.5
Neg Very Small	Gaussian	2.5 ; 3.25 ; 3.75 ; 4.5
OK	Gaussian	3.5 ; 4.5 ; 5.5 ; 6.5
Pos Very Small	Gaussian	5.5 ; 6.25 ; 6.75 ; 7.5
Pos Small	Gaussian	6.5 ; 7.25 ; 7.75 ; 8.5
Pos Large	Gaussian	7.5 ; 8.5 ; 10 ; 10

On the other hand, for the inputs that have only two states i.e., digital inputs, the membership functions are shown in Table 3.6. The inputs indicate either true or false states. These inputs show when there is detection of either short or open circuit, or, the likelihood of occurrence of either.

Table 3.6: Digital input membership functions

Membership function	**Shape**	**Points**
OFF	User-Defined	0 ; 0 ; 5 ; 5
ON	User-Defined	5 ; 5 ; 10 ; 10

The output of the FLC is analog and has membership functions in the form shown in Table 3.7. The membership functions for the output of the FLC map the fuzzy output of the FLC into linguistic terms which are instructions for gap adjustment by the piezo actuator which is the actuator.

The structure of the FLC rules is such that there is antecedent, inference and the consequent ('IF then ELSE' format). In total, there are 36 rules which are scaled

Table 3.7: Output membership functions

Membership function	Shape	Points
Extremely Low	Gaussian	0 ; 0 ; 1.5 ; 2.5
Very Low	Gaussian	1.5 ; 2.25 ; 2.75 ; 3.5
Low	Gaussian	2.5 ; 3.25 ; 3.75 ; 4.5
OK	Gaussian	3.5 ; 4.5 ; 5.5 ; 6.5
High	Gaussian	5.5 ; 6.25 ; 6.75 ; 7.5
Very High	Gaussian	6.5 ; 7.25 ; 7.75 ; 8.5
Extremely High	Gaussian	7.5 ; 8.5 ; 10 ; 10

down to 14 in order to minimize the execution time for the FLC by elimination of redundant or closely related rules. The fuzzy logic controller, shown in Figure 3.22, has a fuzzifier, inference mechanism and a defuzzifier. First, the inputs are fuzzified by the fuzzifier from crisp data sets into fuzzy data. Secondly, they are evaluated and a decision given by the inference mechanism based on the rules of the FLC. Thirdly, the consequent given by fuzzy inference mechanism in fuzzy form is defuzzified by the defuzzifier and lastly, the FLC output is given as crisp voltage output values for the control of the piezo actuator.

In the LabVIEW software environment, an analog output channel that was created relays the FLC's output to the data acquisition card, from which it is then fed in to the piezo actuator. The main aim of developing this FL based controller was to ensure that, the maximum MRR is achieved without compromising on the quality of the surface achievable for a given set of machining parameters. To ensure that this objective is achieved, the controller is tested and tuned. Machining experiments for testing the effectiveness of the controller in achieving the set objective are discussed in the next sections.

3.5.6 Implementation of the adaptive controller

The FLC based controller for the EDM process is implemented using a National Instruments PXI system (NI PXIe-1062Q) shown in Figure 3.23 (a), which is a dedicated computer for control fitted with several interface cards for connecting

to measurement devices and actuators.

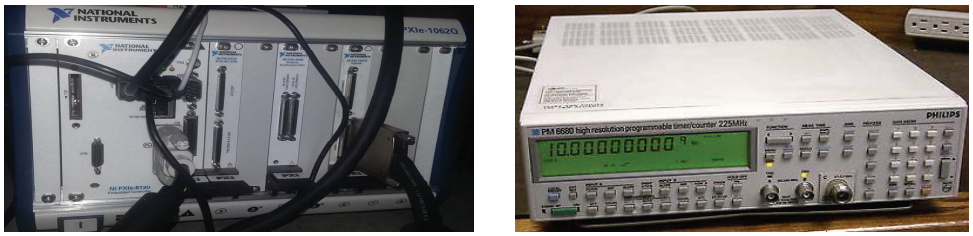

(a) NI PXIe-1062Q PXI system (b) Philips PM6680B timer

Figure 3.23: Data acquisition and control equipment

The EDM controller incorporates a gap votage/current measurement system, in which the measurement of voltage/current is done using a Tektronix DPO4104 oscilloscope. A Philips PM6680B high resolution programmable timer shown in Figure 3.23 (b) measures pulse discharge time and is connected to the National Instruments PXI system using a General Purpose Interface Bus (GPIB) port. The timer has a sample acquisition frequency of 225 MHz, which means that it

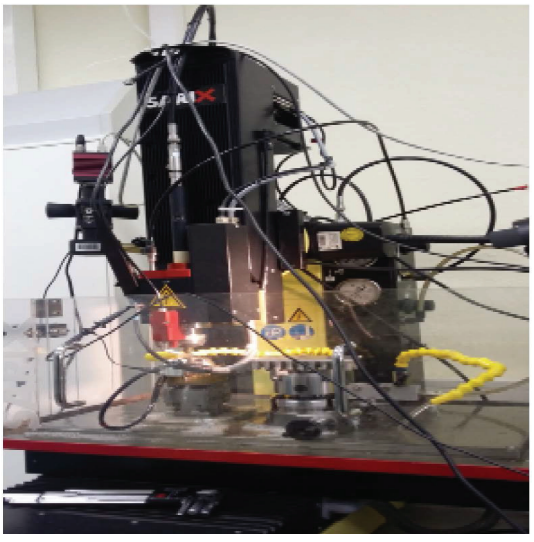

Figure 3.24: Sarix SX100 electrical discharge machine

acquires samples at time intervals of about 4.44 ns. For testing the effectiveness

of the FLC based controller in optimizing the EDM process, controlled machining experiments were conducted on a Sarix SX100 electrical discharge machine shown in Figure 3.24. The control signals from the controller are fed into a piezo

Figure 3.25: Linear piezo actuator

actuator shown in Figure 3.25. The piezo actuator is used to adjust the spark gap, hence effectively varying the gap voltage and current. The piezo actuator has a linear travel range of up to 100 μm, which is enough for the required spark gap adjustments and a high response frequency of 100 MHz which enables very fast gap adjustments.

The block diagram in Figure 3.26 represents the experimental setup that was used for testing the controller. The measured time/period and frequency of the discharges are fed into the timer via the oscilloscope while voltage/current values are directly read by the PXI system via a NI RIO multifunction data acquisition card (NI PXIe-6259) across the two electrodes. The control signals generated by the controller are fed into the piezo-driver circuit from the PXI system. The piezo-driver circuit then generates the necessary voltage control signals to drive the piezo actuator to achieve the desired gap control.

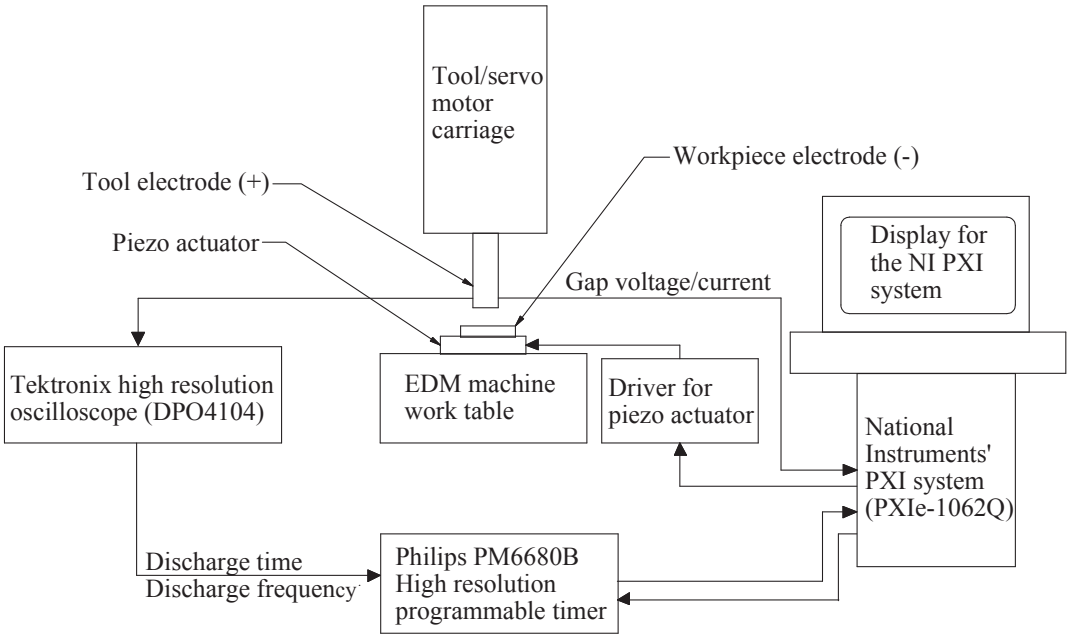

Figure 3.26: Block diagram representation of the experimental setup

CHAPTER FOUR

RESULTS AND DISCUSSION

In this chapter, results from testing of the newly developed transistorised pulse generation circuit for the EDM at JKUAT Engineering workshops are presented in the first section. In the section that follows, results on the investigation of the effects of machining parameters on the EDM process output parameters are presented. The last section of the chapter analyzes the effectiveness of the FLC based controller in optimizing the EDM process. Waveforms were sampled from the transistorized pulse generation circuit. Also, machining experiments were done to test the functionality of the pulse generator and its flexibility. The results from the machining experiments are presented in this section.

4.1 Evaluation of the performance of the pulse generator

The pulse generator has the capability to produce square waves of between 0 Hz and 10 kHz at different DC voltages between 0 V and 100 V. Sample waveforms of the machining pulsed voltage signals at different voltages and frequencies are shown in Figure 4.1.

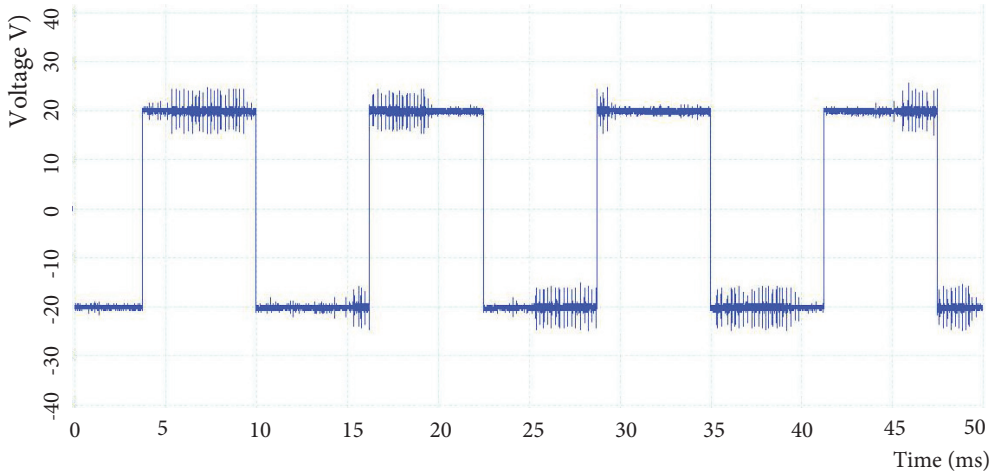

(a) f = 80 Hz, v = 20 V

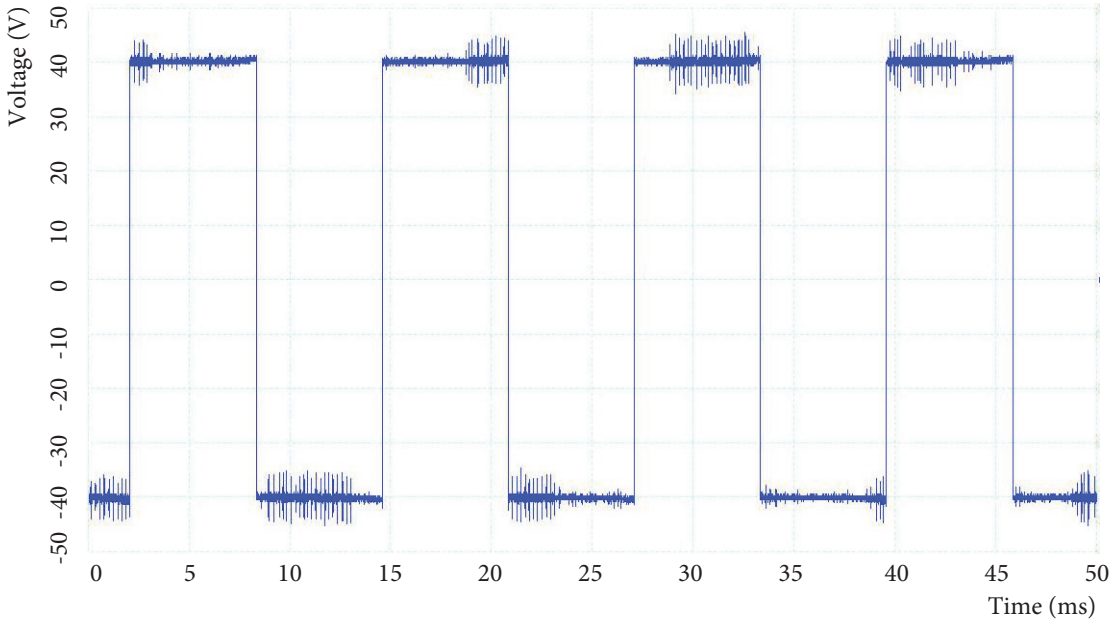

(b) f = 80 Hz, v = 40 V

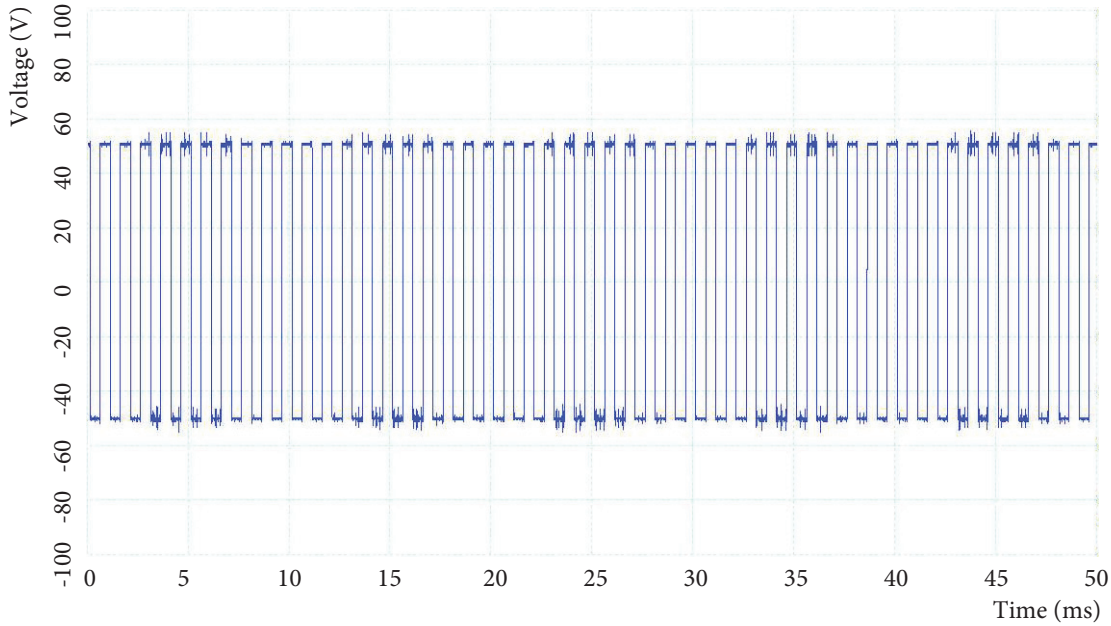

(c) f = 1 kHz, v = 50 V

Figure 4.1: Sample waveforms

The signals were captured at two different frequencies from the controller, that is, at 80 Hz and 1 kHz using a National Instruments card NI USB 6008, in a

LabVIEW® environment as analog signals. The voltage values were adjusted

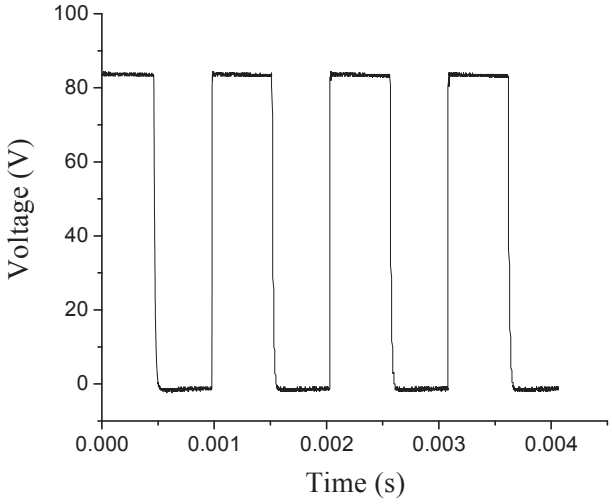

Figure 4.2: Sample voltage pulsed signal acquired at 50% duty cycle, 84 V applied gap voltage and 1 kHz frequency

using a variable transformer (variac) which has a power rating of 2500 W and a voltage range of 0 - 240 V. The frequency was varied using a potentiometer that had been set as the input device for the frequency.

The transistorized pulse generation circuit can generate the required pulsed DC voltage signal while at the same time providing smooth control of machining parameters. A sample waveform of a signal data that was acquired at 1 kHz and 84 V is shown in Figure 4.2.

Figure 4.3 shows discharge voltage signals that were acquired with the magnitude of gap voltage being 74 V (lower than the applied gap voltage of 90 V). These discharges indicate a healthy EDM process, without short or open circuit. When a short circuit occurs, the voltage signal goes to zero, and if open circuit condition occurs, the voltage signal goes to maximum value that is input. It was also found out that significant machining (or MRR) occurred at voltages above 50 V. The upper limit of gap voltage was set at 100 V partly due to the fact that this is the norm, and also due to the limitations of the electronics that were available at the

time of development of the pulse generation circuitry.

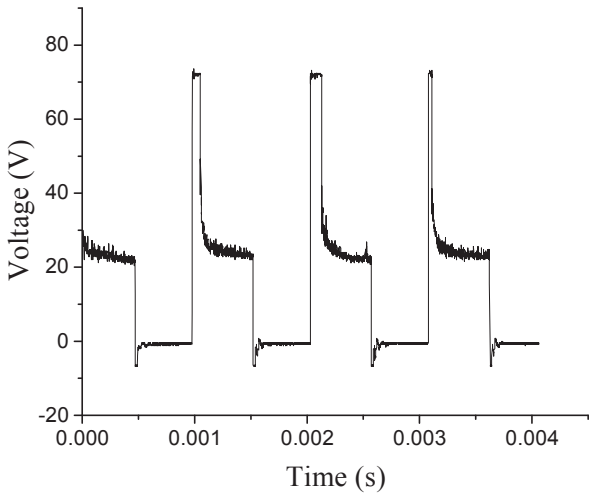

Figure 4.3: Sample discharge voltage signal captured while machining at 50% duty cycle, applied gap voltage of 90 V and a frequency of 1 kHz

In order to evaluate the performance of the transistorized pulse generation circuit, two performance parameters of EDM process were investigated [49] and, the results indicate that the performance of the pulse generator was similar in principle to earlier researches conducted by Subrat *et al.* [50] and Kabini *et al.* [51]. The performance parameters under investigation were MRR and surface roughness of the machined workpieces and the variables were gap voltage and duty cycle. For each data point, three experiments were conducted to avoid any possible error and the mean value used in as the data point. From the graph in Figure 4.4, the material removal rate increases when the gap voltage is increased. At voltages between 50 V and 60 V, the increase in MRR is gradual but becomes more steep as the gap voltage is increased to higher values above 60 V. Consequently, the highest MRR was achieved at gap voltage of 90 V and the least MRR was achieved at gap voltage of 50 V. This is because in electrical discharge machining process, material is removed by a thermal process and the amount of heat energy that is generated for material removal between the tool electrode and the workpiece is directly proportional to the gap voltage. Power is given by the relationship

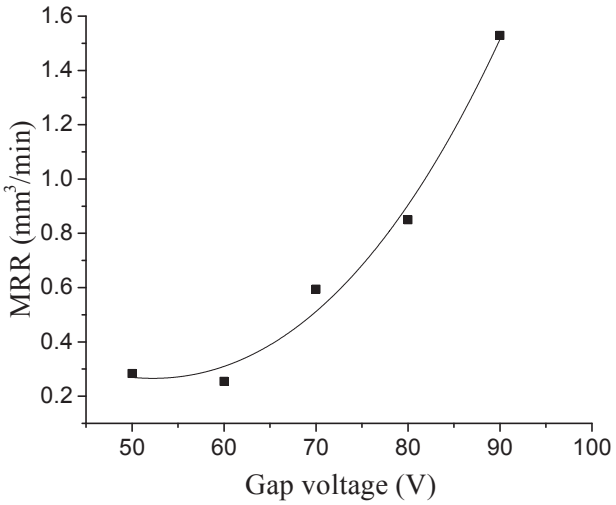

Figure 4.4: Effect of gap voltage on MRR (mild steel)

$P = VI$. Precise adjustments of gap voltage on the pulse generator was attained by adjusting a variable transformer (variac) that was incorporated in the power supply circuit.

Figure 4.5 shows the relationship between gap voltage and surface roughness. The values of surface roughness (Ra) indicate that the roughness of the machined surface increases as the gap voltage is increased. Between voltages of 50 V and 70 V, the surface roughness increases gradually with increase in gap voltage. As seen on the graph, when gap voltage is increased above 70 V, the surface roughness values increase more sharply indicating that the poorest surface finish is achieved at 90 V, and the best surface finish is achieved at 50 V. This is explained by the fact that, when gap voltage is high, the heat energy generated for erosion of material is high causing more erosion of workpiece material [27]. This rapid and high erosion of material results in deeper and uneven profiles on the workpiece surface which in turn translates to poor surface finish.

The performance of the transistorised pulse generator was further evaluated with the duty cycle being the only variable. Figure 4.6 shows a graph indicating the effect of varying duty cycle on material removal rate. It can be seen that, MRR

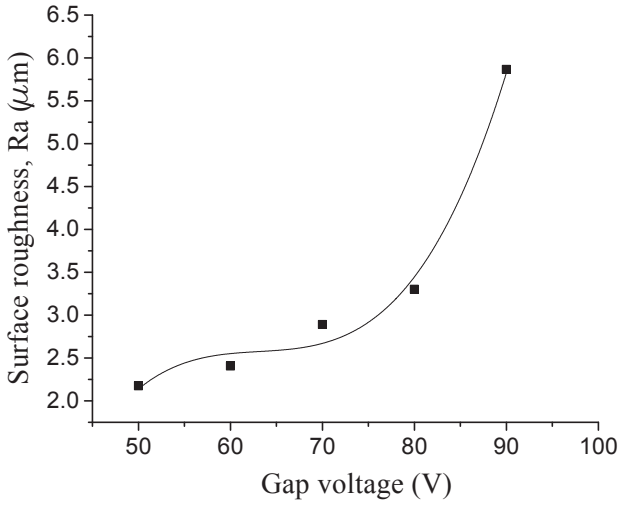

Figure 4.5: Effect of gap voltage on surface roughness (mild steel)

increases from when duty cycle is 10% up to a maximum value when the duty cycle is 50%, after which it decreases. Electrical discharge machining being a thermal process which removes material by thermal erosion [52], lower MRR at low duty cycle is attributed to the fact that, the sparking cycle is not sufficiently long enough to allow enough time for the heating needed to achieve high material removal. Also, lower duty cycle causes more prolonged and frequent open circuit conditions which contribute to lower machining rate. The erosion energy increases as duty cycle is increased and therefore the heat generated at the sparking zone is increased and this results in erosion of a larger zone of the workpiece. This is because when the ON time of the voltage signal is longer, more heat energy is generated at the machining area. This is because the heat energy generated is a function of time. This leads to higher rate of machining. However, the maximum MRR is achieved when the duty cycle is around 50% and for duty cycle above 50%, the sparking energy causes the machined particles to weld on the surface of the machined profile [53]. This is because there are short cooling cycles (pulse OFF time). To mitigate this phenomenon, faster methods of cooling and removal of debris may need to be adopted.

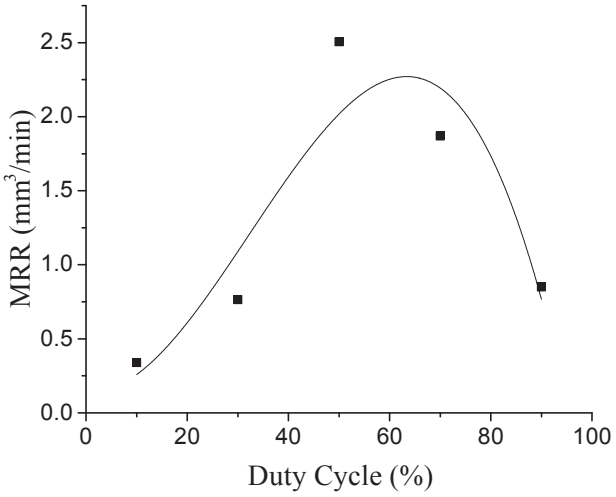

Figure 4.6: Effect of duty cycle on MRR (mild steel)

Finally, the effect of varying duty cycle on surface finish of the machined surface, measured by *Ra* roughness parameter was investigated. The results that were obtained are shown in Figure 4.7. From this figure, it can be seen that the surface roughness increases with increase in duty cycle. This behaviour could be attributed to the fact that, higher duty cycle leads to prolonged heating of the material being machined which in turn leads to over-burnt surfaces and welding of machined particles on the surface [54].

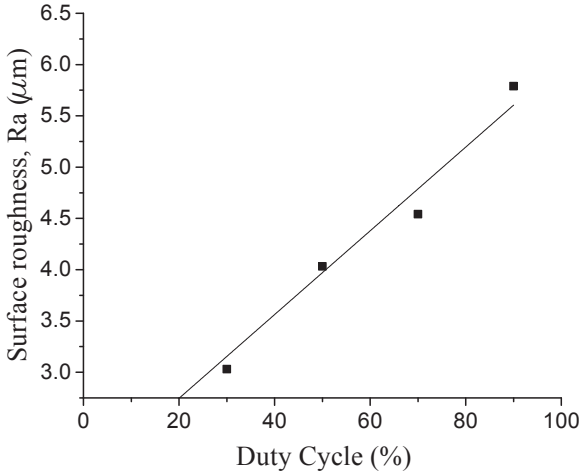

Figure 4.7: Effect of duty cycle on surface roughness (mild steel)

4.2 Investigation of the effect of machining parameters on EDM process output parameters for medium carbon steel, aluminium and brass

Several sets of electrical discharge machining experiments were conducted on each of the three materials namely, aluminium, brass and medium carbon steel (0.47% C). The data obtained in the experiments is shown in tables B.1 through B.12. In order to investigate the effects of the individual machining parameters on the

Table 4.1: Properties of aluminium, brass and steel samples under investigation

Property	**Aluminium alloy 2011**	**Brass (65% Cu, 35% Zn)**	**Medium carbon steel (0.47% C)**
Melting point (°C)	660	900	1400
Electrical conductivity (Siemens/m($\times 10^6$))	36.7	15.9	5.9
Density (g/cm^3)	2.7	8.5	7.7
Thermal conductivity (W/m.K)	237	150	90

EDM process output parameters. For each experiment, some of the machining parameters were held constant and only one parameter, the one under investigation, was varied. The parameters under investigation included gap voltage/current and duty cycle. Table 4.1 shows the physical properties for the three materials under investigation, which include melting point, density, and, thermal and electrical conductivity.

4.2.1 Effect of gap voltage on the surface finish

The machining experiments were carried out for voltages ranging from the minimum possible machining voltage of 50 V to the maximum machining voltage of 150 V on the EDM machine with increments of 20 V. The choice of this range of machining voltage is because significant MRR occurs at voltages above 50 V and the maximum machining voltage as per Sarix SX100 machine is 150 V. The surface roughness was analysed using the 3D laser scanning microscope. The microscope gave 5 measurement values indicative of surface roughness, namely, R_p, R_a, R_q, R_z and R_v. In this analysis, the surface roughness parameter R_a, which is the arithmetic mean of absolute values of peak depths and valley heights on the machined surface was used to express surface roughness. This parameter was chosen solely because it is the most commonly used method of expressing surface roughness [55]. An example of results obtained from measurement of sur-

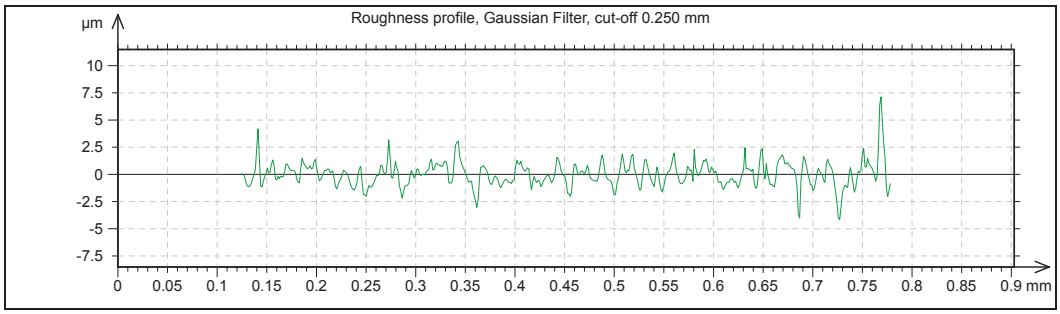

ISO 4287			
Amplitude parameters - Roughness profile			
Rp	3.23	µm	*Gaussian filter, 0.25 mm*
Rv	2.54	µm	*Gaussian filter, 0.25 mm*
Rz	5.77	µm	*Gaussian filter, 0.25 mm*
Ra	0.745	µm	*Gaussian filter, 0.25 mm*
Rq	0.948	µm	*Gaussian filter, 0.25 mm*

Figure 4.8: Sample result data of surface roughness given by the 3D laser scanning microscope for aluminium surface

face roughness of aluminium profile is shown in Figure 4.8. The Gaussian filter for the microscope was set at 0.25 mm to eliminate overshoot and fasten the rise and fall time for the instrument. Figure 4.9 shows the relationship between the

applied gap voltage and the surface roughness of the machined surface for the three materials tested.

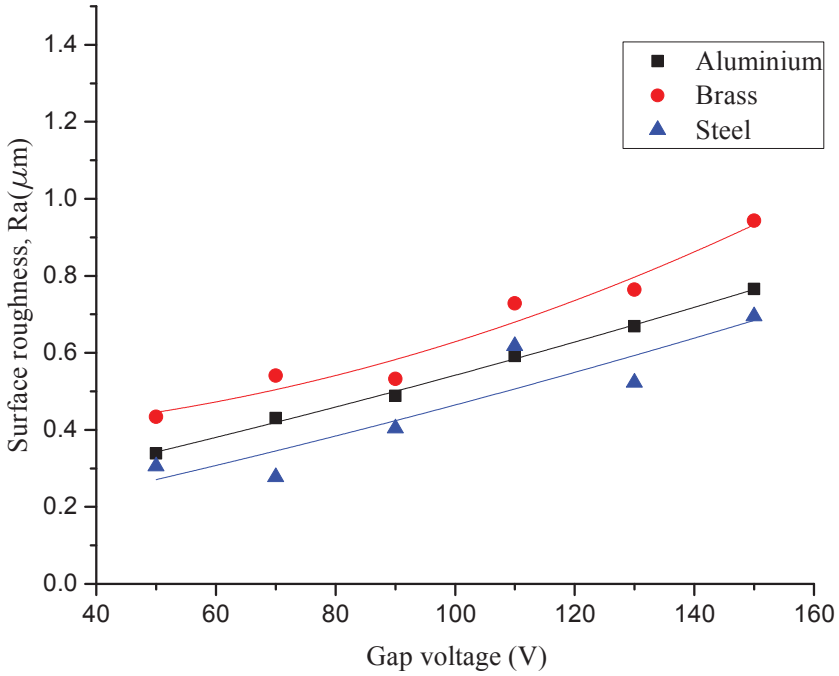

Figure 4.9: Influence of gap voltage on surface roughness

From the graph, it is seen that, as the applied gap voltage is increased, the surface roughness increases for all materials. The explanation for this trend is that, during electrical discharge machining, the power generated at the machining area is directly proportional to the voltage, that is $P = VI$. This power at the machining zone causes material removal by a thermal process and therefore, the higher the power the more the material removal rate, and, the larger the heat affected zone and hence the distortion of the microstructure of the material [21]. It was also observed that, for the same machining conditions, steel had the least values of surface roughness indicating the best surface finish while brass had the highest values of surface roughness indicating poorest surface finish. It was also observed that, while machining brass, machined particles welded onto the surface. These particles could be the ones contributing to higher roughness for the brass. Further, the surface finish for aluminium was better than that of brass

but poorer than that of steel. This difference in surface roughness is attributed to the different melting points, and, thermal and electrical conductivities that contribute to different machinability of different materials as was explained by Scott *et al.* [20] and Ravindranadh *et al.* [56].

4.2.2 Effect of gap voltage on the MRR

In order to determine the effect of gap voltage on material removal rate, timed machining experiments were conducted at different gap voltages and constant duty cycle. For calculation of volume of the material that was removed, the dimensions of the machined profiles were used. The MRR was calculated by dividing the volume of the material that was removed with the machining time for each profile.

The experiments were carried out at a frequency of 100 kHz and a duty cycle of 50 percent using a tool electrode of diameter 80 μm for all machining experiments. The diameters of the machined holes were measured using the surface measurement microscope and the measured diameters are shown on Figure 4.10. The machined workpieces were then cleaned in an ultrasonic bath to remove all the loose particles that had not been washed away during machining. Finally, the machined volume was calculated from the dimensions of the machined cavity. The depths of the machined holes were taken as the heights of the cylinders.

The results of MRR for the three materials were plotted in the graph shown in Figure 4.11. The lines in the graphs represent the best fits for each data sample. From the graph, it is seen that, machining of aluminium recorded the highest MRR. The MRR in machining of brass was second highest and the least MRR occurred in the machining of steel. Since EDM process removes material by electrothermal process, this difference in MRR is as a result of the difference in electrical and thermal conductivity for the three materials as was demonstrated by Chang [57]. In machining aluminium which the highest electrical and ther-

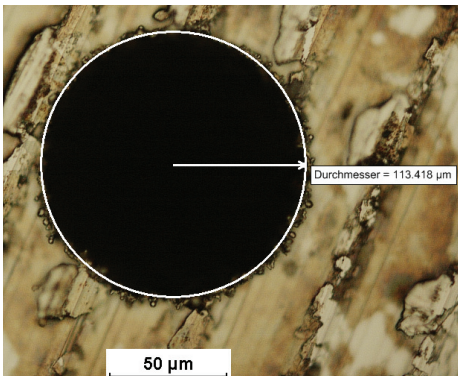

(a) Aluminium

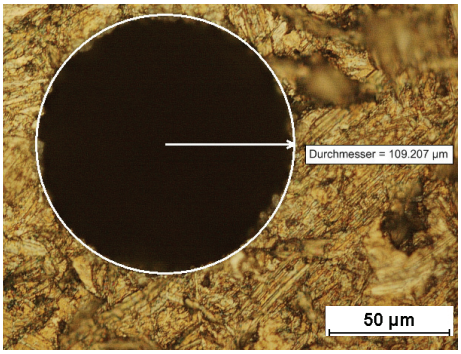

(b) Brass

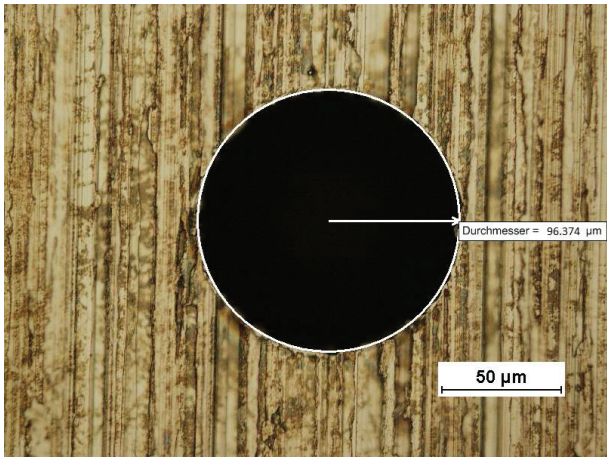

(c) Medium carbon steel (0.47% C)

Figure 4.10: Measured diameters (indicated as *Durchmesser*) obtained on surface measurement microscope at 50 V and 50% duty cycle

mal conductivity and the lowest melting point the highest MRR was achieved. In the machining of brass which had the second highest electrical and thermal conductivity and also second lowest melting point the second highest MRR was achieved. Lastly, machining of steel which had the lowest thermal and electrical conductivity and the highest melting point least MRR was attained. It is also observed that the MRR in machining of the three materials rapidly increases with increase in applied gap voltage especially for values of gap voltage above 90 V.

In all the cases of machining, it can be seen that, MRR increases with increase in applied gap voltage. Comparing the results of surface roughness from Figure 4.9

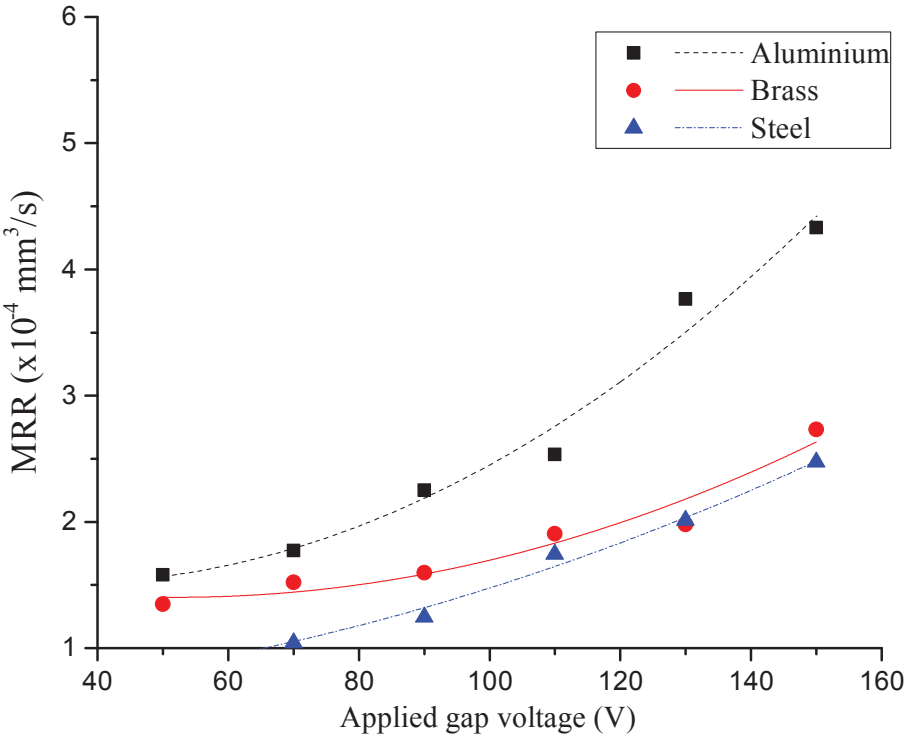

Figure 4.11: Effect of gap voltage on MRR (for Al, CuZn and FeC)

and MRR in Figure 4.11, it can be seen that, the highest MRR was achieved in machining aluminium, followed by brass and lastly steel. However, in regards to quality of the machined surface, the poorest quality was achieved in machining of brass, followed by aluminium and then steel. These two observations could be attributed to two things; first is the fact that in machining brass, machined particles welded onto the machined surface thus reducing MRR, and second, the resulting large region of heat affected zone seen as black region around the machined hole in Figure 4.12 could contribute to higher surface roughness in brass.

Ravindranadh *et al.* [56] reported that different tool electrode and workpiece material combination result in different machinability in EDM and recommended that the machining parameters should be selected based on the properties for the

workpiece and tool electrode materials combination. From further experiments it was found out that machining of brass at lower voltages reduced the heat affected zone and eliminated welding of machined particles on the surface of the workpiece.

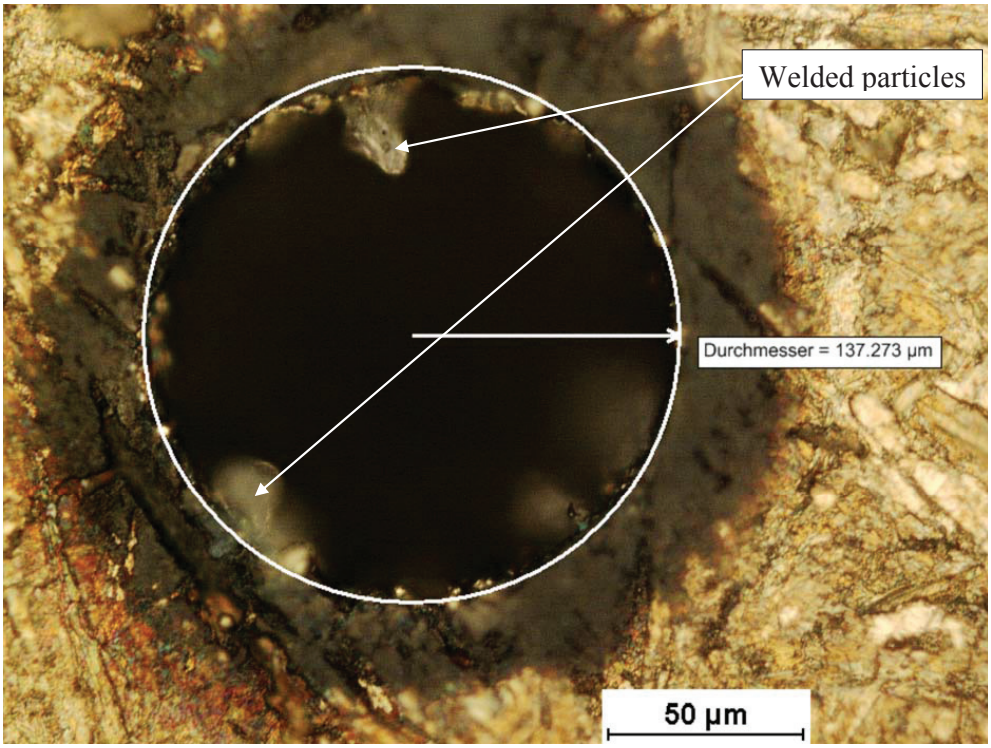

Figure 4.12: Profile of a hole machined on brass at 150 V and 50% duty cycle

4.2.3 Effect of gap voltage on the tool wear rate (TWR)

The Sarix SX100 EDM machine records the tool wear for each machined profile in terms of the length of the worn out tool electrode (h). This recorded tool wear was used to calculate the tool wear rate as,

$$TWR = \frac{\pi r^2 h}{t} \tag{4.1}$$

where r is the radius of the tool in millimetres, h is the worn out length of the tool in millimetres as well, and t is the machining time in seconds. For each value of gap voltage, three experiments were carried out and the average tool worn out

height was used to compute the tool wear rate.

To illustrate the effect of the applied gap voltage on the tool wear rate (TWR), the tool wear rate was plotted against the applied gap voltage on the graph shown in Figure 4.13. From this graph, the tool wear rate was observed to increase with increase in the value of applied gap voltage for machining of the three materials. For the lower values of machining voltage below 80 V, the TWR was highest for machining of brass and lowest for machining of steel. However, for higher values of machining voltage above 90 V, it was observed that the TWR was highest for machining of aluminium followed by steel and least for the machining of brass. According to Mona *et al.* [58] who investigated factors that contribute to tool wear rate, the combined material properties for the workpiece and tool electrode, such as electrical and thermal conductivity, electrical resistivity as well as the melting points influence the tool wear rate. As noted in this research these material properties change as the machining occurs, and thus, the TWR also changes. However, the TWR in brass does not follow the same trend as for steel and aluminium. It was noted that while machining brass at high gap voltage, there was welding of machined brass particles on the surface of the workpiece. The reduced TWR could also be as a result of the same brass particles welding onto the tip of the tool electrode hence reducing the TWR as was noted by Banker *et al.* [59], but is a subject that can be further investigated.

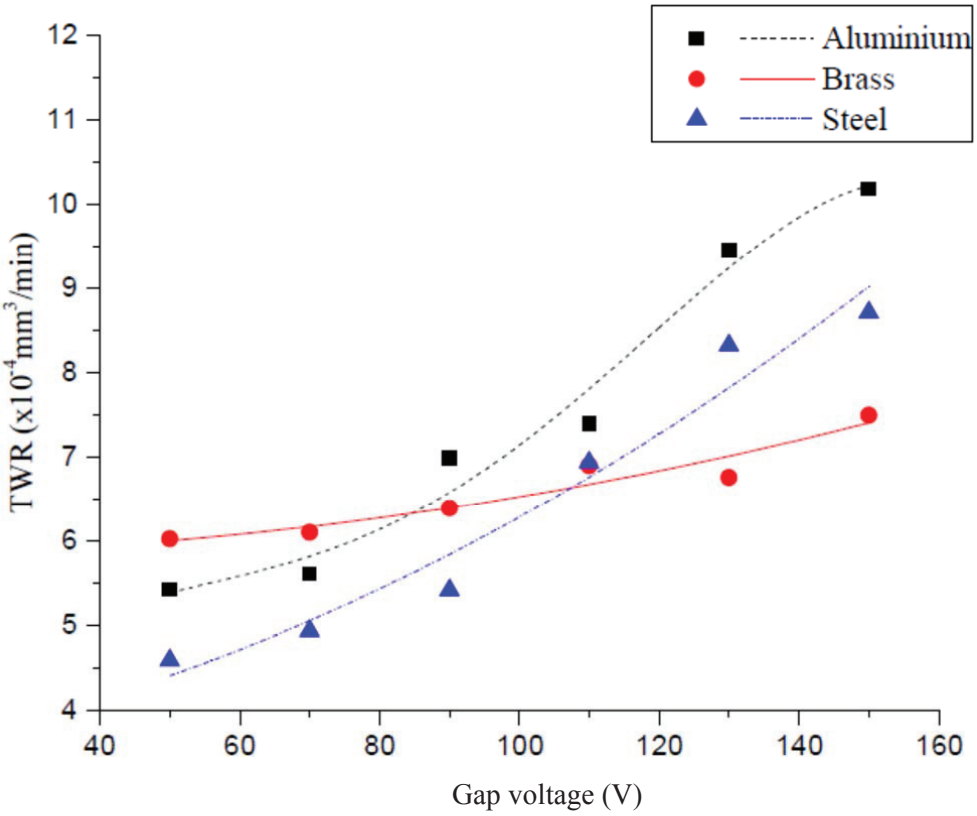

Figure 4.13: Effect of gap voltage on TWR (for Al, CuZn and FeC)

4.2.4 Effect of duty cycle on surface finish

In order to determine the relationship between pulse ON time (T_{ON}) and quality of the machined surface, five sets of experiments were conducted. Each set of experiments involved machining three workpieces, one from each material under identical machining conditions. The duty cycle was varied between the values of 10% T_{ON} and 90% T_{ON} at increments of 20%. The applied gap voltage and machining frequency were held constant at values of 100 V and 100 kHz respectively. Figure 4.14 shows the relationship between the duty cycle and the quality of the surface obtained in terms of surface roughness parameter, R_a.

From Figure 4.14, it is seen that increasing the duty cycle leads to poorer surface finish as indicated by high values of surface roughness, Ra. This trend is observed for all the three materials that were machined. This behaviour could

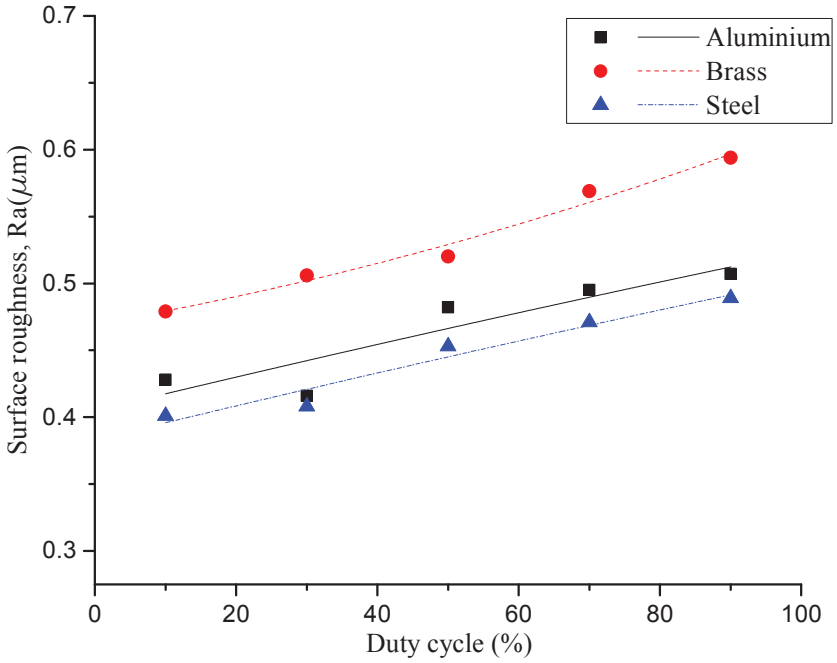

Figure 4.14: Influence of duty cycle on surface finish (for Al, CuZn and FeC)

be attributed to the fact that, higher duty cycle leads to more heating of the material being machined and hence leading to over-burnt surfaces and welding of machined particles on the surface as Sameh [54] noted. This could also be as a result of less cooling time of the surface and hence the overheating since the sparking time is lengthened [60]. One way of overcoming this is to use a hollow electrode with the dielectric fluid pumped through it to act as a coolant, as was demonstrated by Suleiman *et al.* [61]. However, this can only be implemented at the design stage for an EDM and is a challenge for small tool electrodes.

4.2.5 Effect of duty cycle on MRR

In order to investigate the relationship between duty cycle and MRR, fifteen sets of electrical discharge machining experiments were conducted, five sets for each material. Each set of machining experiments involved machining three identical features under the same machining conditions on the same workpiece. The average values of dimensions for the three machined holes were used to calculate the

volume of the material that was removed for each value of duty cycle.

The influence of duty cycle on material removal rate for the three materials that were machined is shown in Figure 4.15. The dashed lines show the best fits for the data sets.

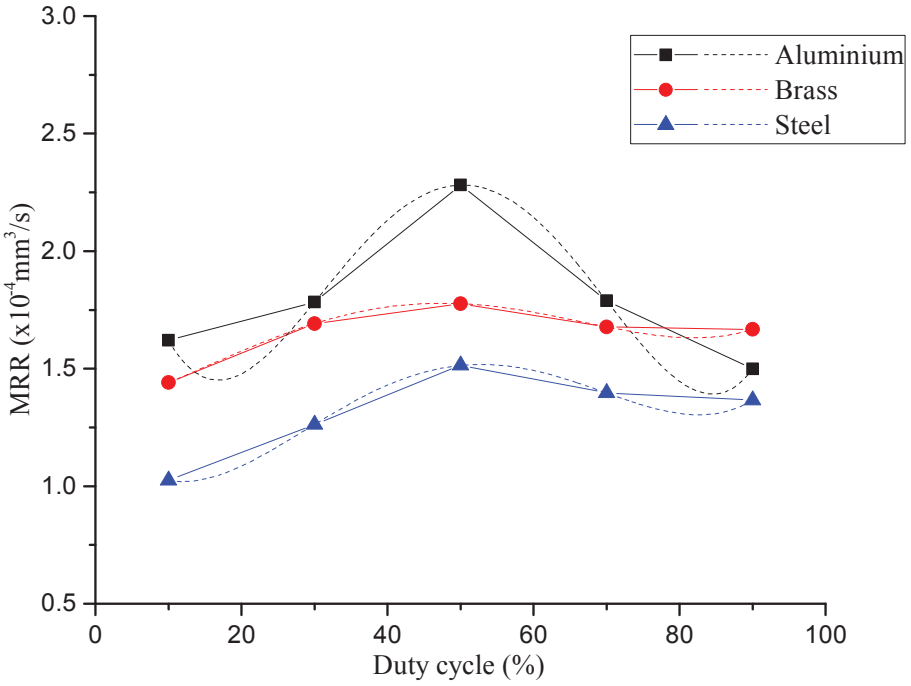

Figure 4.15: Effect of duty cycle on MRR (for Al, CuZn and FeC)

It is seen that, the MRR for the three materials increases gradually from minimum values of between 1.02×10^{-2} mm^3/min and 1.62×10^{-2} mm^3/min to maximum values of between 1.78×10^{-2} mm^3/min and 2.28×10^{-2} mm^3/min at a duty cycle of about 50% and then starts decreasing to lower values of up to between 1.37×10^{-2} mm^3/min and 1.67×10^{-2} mm^3/min at 90% duty cycle. From this observation, it could be said that, in order to achieve the highest MRR for any of the three materials, the best machining duty cycle would be around 50%. For duty cycles below 50%, the MRR is low, and decreases as the duty cycle reduces.

Because EDM is a thermal process which removes material by thermal erosion

[52], lower MRR at low duty cycle is due to the fact that, the sparking cycle is not sufficiently long enough to allow enough time for the heating needed to achieve high material removal. The lower duty cycle also leads to frequent occurrence of open circuit, thus causing lower machining rate. The sparking energy increases as duty cycle is increased and more heat is generated at the sparking zone. This leads to higher rate of machining up to when the duty cycle reaches 50%. However, for duty cycle above 50%, the sparking energy is again high enough to cause welding of machined particles on the surface of the machined profile [53] leading to reduced MRR. This effectively lowers MRR. It is also observed that, for higher duty cycles, there is higher frequency of occurrence of short circuits which is undesirable and reduces the machining rate.

4.2.6 Effect of duty cycle on TWR

For the determination of the effect of varying duty cycle on the TWR, fifteen sets of experiments were carried out. Each set of experiments involved conducting three machining experiments on the same workpiece under identical machining conditions. The average recorded values of the tool wear were used in the computation of the tool wear rate.

During the experiments, tool wear for each hole that was machined was recorded. These values were used to calculate the tool wear rate. The duty cycle was varied from 10% to 90% at intervals of 20%. The gap voltage and frequency of the pulses were maintained at 100 V and 100 kHz respectively. This is because Jaganathan *et al.* [62] conducted research on the optimization of machining parameters in EDM and found out that the optimum MRR is achieved at a voltage between 90 V and 110 V and a machining frequency of about 100 kHz.

The relationship between duty cycle and tool wear rate is shown in Figure 4.16. From the graph, it can be seen that, the tool wear rate is not significantly affected by value of duty cycle for all the three materials. However, the tool wear rate

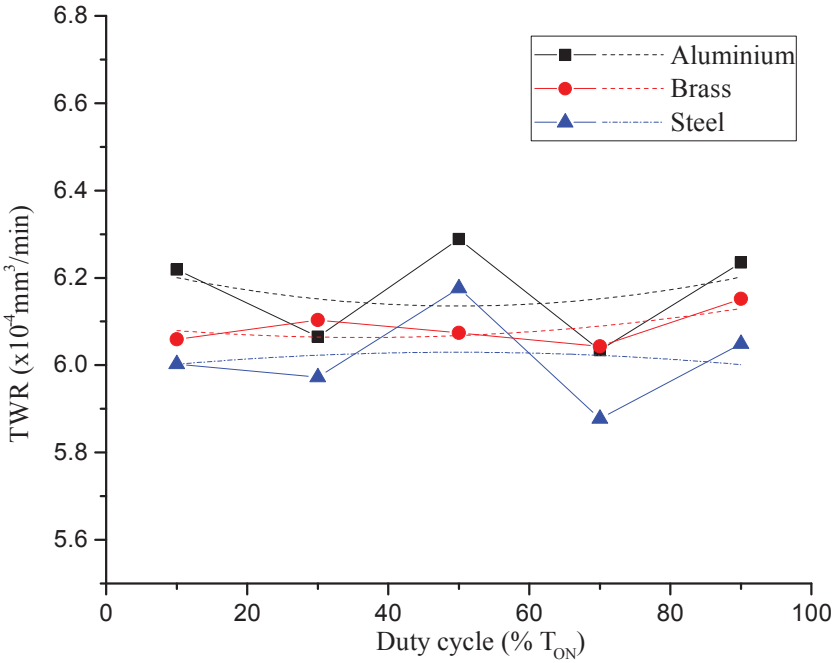

Figure 4.16: Effect of duty cycle on TWR (for Al, CuZn and FeC)

was highest for aluminium and least for steel. This is because the higher the difference between thermal and electrical conductivity between tool electrode and workpiece, the lower the tool wear rate and vice versa as was demonstrated by Suleiman [61]. It can thus be concluded that as per the data that was obtained, the effect of duty cycle on TWR has no significant consequence. This can further be explained by the fact that the standard deviation from the average TWR for each of the three cases of machining remains almost constant regardless of change in the duty cycle.

4.2.7 Summary of the effects of machining parameters on performance parameters

The machining experiments that were conducted to investigate the effect of variation of gap voltage and duty cycle provided insight into the EDM process. The knowledge that was acquired was used in the design of an adaptive controller for the EDM process. These results can be summarised as follows;

i. Surface roughness of the machined surface increases with increase in gap voltage. This observation relates to earlier conclusions in researches by Sameh *et al.* [54] and Mona *et al.* [58].

ii. Material removal rate increases with increase in the gap voltage. Similar observations were made in researches conducted by Ravindranadh *et al.* [56] and Teepu *et al.* [63].

iii. Tool wear rate increases with increase in gap voltage as was demonstrated by Teepu *et al.* [63].

iv. Surface roughness increases with increase in duty cycle as shown in researches by Teepu *et al.* [63] and Dasa *et al.* [64].

v. Material removal rate increases with increase in duty cycle up to about 50% duty cycle and thereafter it decreases [51].

vi. Tool wear rate showed no significant change with either increase or decrease of duty cycle This is shown in researches dony by Rajesha *et al.* [52], Sameh [54] and Shahul *et al.* [65].

From the results that were obtained from the experimental work and as concluded in the cited researches, it is evident that to achieve the best results in the EDM process, a good balance between the machining parameters has to be struck. This knowledge was key in the design of the adaptive controller.

4.3 Investigation of the performance of the adaptive controller in optimizing the EDM process

In order to test the performance of the FLC based controller in optimizing the EDM process, machining experiments were conducted under the control of the adaptive controller. The results were compared with those obtained without the controller, but with the same conditions and parameters. The machining

experiments were carried out at a voltage range of between 50 V and 150 V and duty cycle of between 10 and 90 percent. The machining frequency was maintained at 100 kHz. The experiments were carried out using a tungsten carbide tool and three workpiece materials namely; aluminium, brass and medium carbon steel (0.47% C). The controller works by adjusting the gap voltage via a linear piezo actuator. The data obtained in the experiments is shown in tables B.13 through B.24.

4.3.1 Optimization of gap voltage with respect to surface quality

The investigation into the effect of voltage on surface finish was established by conducting the machining experiments using different machining voltages from a minimum of 50 V to a maximum of 150 V, at increments of 20 V. The surface roughness was checked with the 3D laser scanning microscope. The arithmetic average of absolute roughness values R_a was used as a measure of surface roughness.

Figure 4.17 shows the influence of gap voltage on surface roughness in machining, for the three materials namely; aluminium, brass and steel, machined both controlled and uncontrolled modes. In Figure 4.17 (a), it can be seen that for the uncontrolled mode, the surface roughness for machining aluminium increases linearly with increase in gap voltage, while for the controlled modes, there is no significant change of surface roughness with change of gap voltage. By comparing the values of surface roughness, R_a, there is an improvement of between 19.5% and 65.9% in surface finish from the non controlled to the controlled EDM process. This can be attributed to the regulation of the spark gap which ensures that there is uniform removal of material by application of uniform power density around the machining area which leads to uniform finish. The higher the power density is, the poorer the surface finish according to Dasa *et al.* [64].

For machining of brass, the relationship between surface finish and gap voltage is

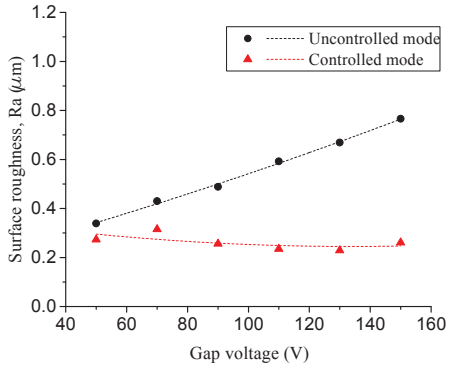

(a) Aluminium

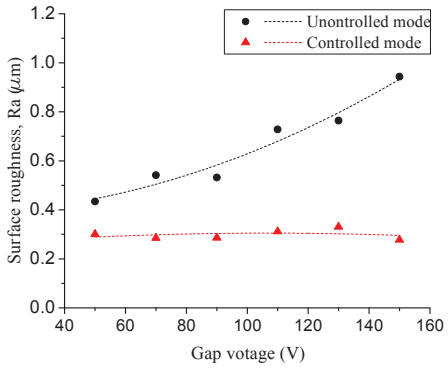

(b) Brass

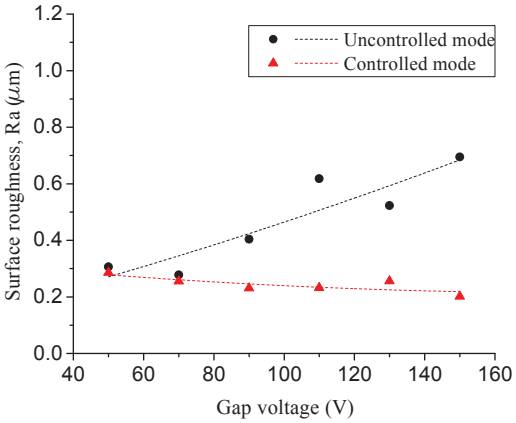

(c) Medium carbon steel (0.47% C)

Figure 4.17: Effect of gap voltage on surface roughness for controlled and uncontrolled machining modes(T_{ON}=50%, f=100 kHz)

shown in Figure 4.17 (b) similar trends are seen as for aluminium. Notable also is the fact that even the highest surface roughness value for the controlled electrical discharge machining of brass, which is 0.3 μm, is much lower than the lowest value of roughness in the uncontrolled process which is 0.45 μm. Comparing the quality of surface finish, it can be seen that there is an improvement of between 30.6% and 70.5% in surface finish. These observations demonstrate the capability of the controller to optimize the gap voltage for achievement of the best surface finish.

The surface finish for machining medium carbon steel is presented in Figure 4.17 (c), and, like in machining of aluminium and brass the surface roughness in the controlled mode remains almost constant even when the gap voltage is changed. However, for the uncontrolled process, any change in the machining voltage is reflected in the surface roughness of the machined surface. As can be seen from the graph in Figure 4.17 (c), the surface roughness values for the controlled process do not show a significant change and remain around 0.3 μm. However, for the uncontrolled mode, surface roughness increases with increase in gap voltage. There is also a significantly large improvement of between 6.5% and 70.9% in surface finish in the controlled machining of steel.

It can thus be concluded that, on controlled machining of the three materials, the values of surface roughness parameter, R_a, measured at different gap voltages remains almost constant regardless of changes in gap voltage.

However, in the uncontrolled mode, this is not the case and the surface roughness increases with increase in gap voltage as in the case of machining aluminium and brass. This difference between the controlled and uncontrolled process demonstrates that the controller was able to adjust the spark gap well enough to maintain the roughness values of the machined surface at minimum, the result of which is improved surface finish for the controlled EDM process. This achievement could be attributed to the fact that the controller's time monitoring unit minimizes the

occurrence of short and open circuits as well as prolonged or non effective discharges, allowing only effective and uniform machining discharges to occur. With uniform discharges, the surface finish is even and smoother as explained in the works done by Teepu *et al.* [63].

4.3.2 Optimization of gap voltage with respect to material removal rate

One of the main challenges of EDM process is the low MRR as compared to other subtractive machining processes. The main purpose of this research was to maximize MRR without compromising on the quality of the surface finish. The fuzzy logic based adaptive controller is tested for its ability to maximize MRR. In EDM process, MRR is governed by duty cycle, gap voltage/current and the workpiece/tool materials properties. This means that for each set of these machining parameters, the controller should be able to adjust the spark gap so that the best possible MRR is achieved. In chapter 3, it was found out that maximum MRR is achieved at a duty cycle of about 50% for all the values of machining voltage, and hence, all experiments aimed at achieving the highest MRR are conducted at this value of duty cycle. The effectiveness of the FLC-based controller in increasing MRR is ascertained by conducting several timed experiments, calculating the amount of material removed per unit time (MRR) and then comparing the controlled and the uncontrolled machining processes. For each machining voltage, three experiments were conducted and the average values of machining time, diameter and depth of the machined profile used to calculate MRR.

Figure 4.18 shows the effect of gap voltage on MRR for aluminium, brass and medium carbon steel. The relationship between material removal rate and applied machining voltage for the machining of Aluminium is shown in Figure 4.18 (a). From this figure, the MRR for the controlled mode is higher than that of the uncontrolled EDM process, for all machining voltages. The MRR increases by between 1.6×10^{-3} mm^3/min (4%) and 2.2×10^{-2} mm^3/min (138%) in the

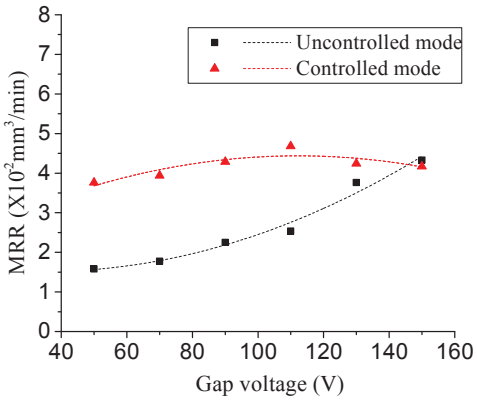

(a) Aluminium

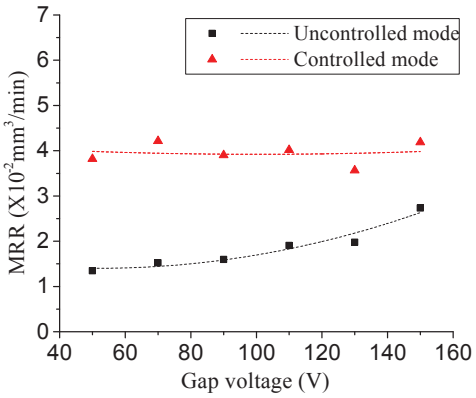

(b) Brass

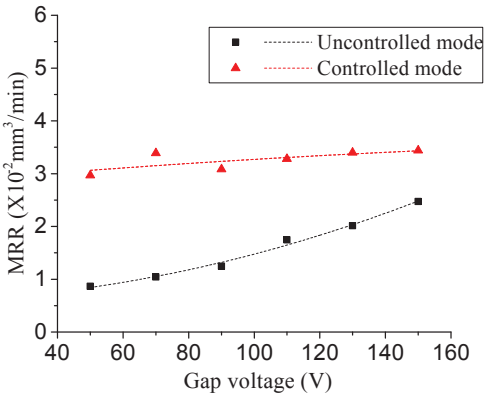

(c) Medium carbon steel (0.47% Carbon)

Figure 4.18: Effect of gap voltage on MRR for controlled and uncontrolled machining (T_{ON}=50%, f=100 kHz)

controlled machining mode. This increase in MRR is achieved through realtime monitoring of the sparking process and control of the spark gap.

The effect of voltage on MRR for brass shown in Figure 4.18 (b) for both the controlled and the uncontrolled modes. It can be seen that machining under FLC control results in increased MRR for the entire range of gap voltages. The MRR for the controlled process increased by between 1.5×10^{-2} mm^3/min (53.2%) and 2.5×10^{-2} mm^3/min (183.5%). This increase in MRR for the controlled mode shows the ability of the adaptive controller in maximizing MRR. Material removal rate for the optimized EDM process for brass was between 3.5×10^{-2} mm^3/min and 4.3×10^{-2} mm^3/min. However, for the uncontrolled EDM process, MRR was between 1.3×10^{-2} mm^3/min and 2.8×10^{-2} mm^3/min. These ranges further illustrate the increased rate of material removal throughout the optimized EDM process as compared to the non optimized one.

As was seen in chapter 3, MRR in machining of steel was the lowest compared to MRR in machining of aluminium and brass. The target machining condition is that the MRR remains high throughout the machining process regardless of the workpiece material composition, value of gap voltage or any changes in machining parameters. The process should also result in good surface finish.

The MRR for machining steel in both controlled and uncontrolled modes is shown in Figure 4.18 (c). From this figure, it can be seen that, MRR for the controlled process is much higher than that of the uncontrolled EDM process. The differences in MRR between the controlled and the uncontrolled processes range between 9.7×10^{-3} mm^3/min (39.1%) and 2.1×10^{-2} mm^3/min (243.1%).

In the uncontrolled mode, it is observed that MRR increases with increase in gap voltage. However, for the controlled mode, MRR does not change with change in voltage, but remains constant and at a higher value than for the uncontrolled mode. The improved MRR is due to the realtime monitoring of the sparking

process and control of the spark gap in the controlled process.

In conclusion, it has been demonstrated that the FLC based adaptive controller increases MRR considerably. It has also been seen that using FLC based controller increases MRR by between 4% and 243%. The increased MRR in the controlled process is achieved by adjustment of spark gap which ensures that the maximum MRR is achieved throughout the machining process.

4.3.3 Optimization of gap voltage with respect to tool wear rate

Tool wear is a major challenge in most machining processes. Tool life has a major impact on productivity and cost of machining. In some processes, the tool life is short and the cost of tooling directly contributes to the costs in machined products. Electrical discharge machining process is by no means an exception from higher tool wear rates and shorter tool life cycles [63]. In view of this, the current research sought to minimize tool wear rate through optimization of the machining process. For the three materials that were machined, tool wear rate for each material in the optimized and the non optimized process were compared. The results are shown in Figure 4.19. This is done in order to test the effectiveness of the FLC based controller in minimizing TWR.

The effect of gap voltage on TWR in machining of aluminium for both the controlled and uncontrolled modes is presented in Figure 4.19 (a). The results in the controlled mode show that, the TWR is kept at the minimum attainable value with the given set of parameters. The TWR for the controlled mode falls between 5.9×10^{-4} mm^3/min and 6.5×10^{-4} mm^3/min, while that in the uncontrolled mode falls between 5.4×10^{-4} mm^3/min and 1.02×10^{-3} mm^3/min. This represents an average drop of 13.3% in TWR in the controlled mode. It is worth noting that, at lower gap voltage, TWR for the both processes is almost the same. However, as the gap voltage increases, the TWR in the uncontrolled mode increases while that in the controlled mode remains almost constant with a standard deviation of

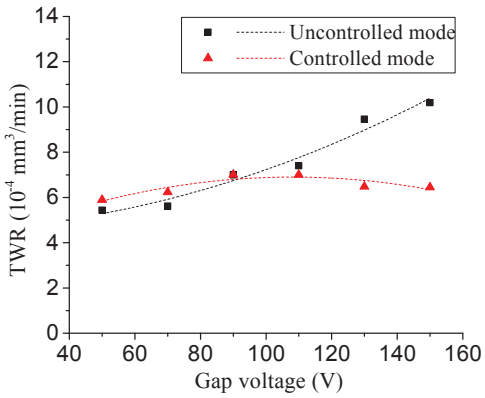

(a) Aluminium

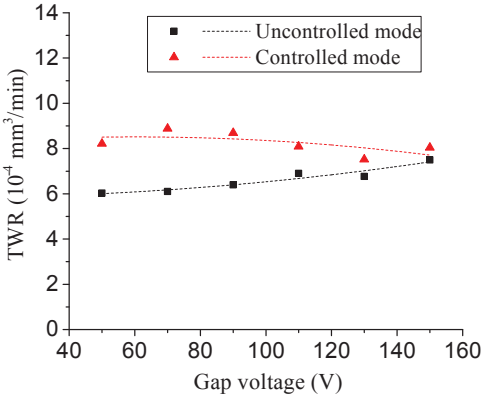

(b) Brass

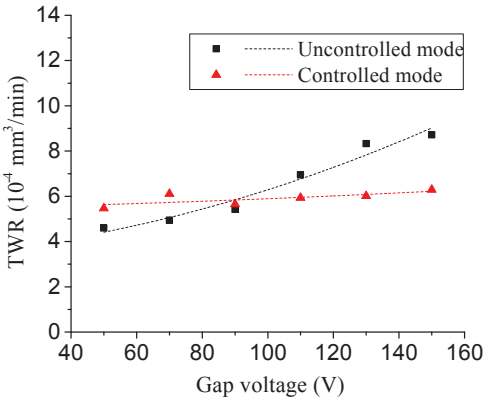

(c) Medium carbon steel (0.47% C)

Figure 4.19: Effect of gap voltage on TWR for controlled and uncontrolled machining (T_{ON}=50%, f=100 kHz)

4.38×10^{-5} mm^3/min. The standard deviation for the uncontrolled EDM process is 1.96×10^{-4} mm^3/min. This high standard deviation in the uncontrolled mode results from the fact that, as machining voltage increases, power density across the spark gap increases. This is because of the absence of rapid and realtime control that is offered by the adaptive controller in the controlled mode.

The results obtained in the machining of brass are shown in Figure 4.19 (b). The TWR for the controlled mode ranges between 8.9×10^{-4} mm^3/min and 8.0×10^{-4} mm^3/min. On the other hand, the TWR in the uncontrolled mode falls between 6.0×10^{-4} mm^3/min and 7.5×10^{-4} mm^3/min. This shows an average increase of 24.6% in tool wear rate for the controlled mode. However, the MRR to TWR ratio shows an increase from 2.79 for the uncontrolled mode to 4.91 for the controlled mode. This ratio is shows that for the optimized process, the tool wear rate per unit MRR is lower for the controlled process. The implication is that the total amount of tool worn out is reduced for each machining case. This is because even if TWR is high, the MRR is much higher and thus the machining time for each product is reduced. Because the total amount of tool wear is directly proportional to machining time, as machining time is reduced, the amount of tool wear also reduces.

The results of tests on the effectiveness of the FLC based controller in minimizing TWR in the machining of steel are shown in Figure 4.19 (c). The TWR for the controlled mode ranges between 5.5×10^{-4} mm^3/min and 6.3×10^{-4} mm^3/min, while that in the uncontrolled mode falls between 4.6×10^{-4} mm^3/min and 8.7×10^{-4} mm^3/min. This shows an average decrease of 9% in TWR in the controlled machining of steel.

For the controlled mode shown in Figure 4.19 (c), the standard deviation of TWR is 3.043×10^{-5} mm^3/min while that of the uncontrolled mode is 1.769×10^{-4} mm^3/min. This shows that TWR remains almost constant even when the gap

voltage changes in the controlled machining mode as opposed to the uncontrolled mode.

4.3.4 Optimization of duty cycle with respect to surface quality

Machining experiments were carried out to test the effectiveness of the FLC based controller in minimizing surface roughness of the machined surface. The machining experiments were done at a voltage of 100 V. The duty cycle was varied between 10% and 90% at intervals of 20%. Results for the relationship between duty cycle and surface roughness are shown in Figure 4.20, for both the controlled and uncontrolled modes. Figure 4.20 (a) shows the relationship between duty cycle and surface roughness in machining of aluminium for controlled and uncontrolled machining modes. From this figure, the surface roughness for the controlled mode is in the range between 0.42 μm and 0.47 μm while that in the uncontrolled mode ranges between 0.42 μm and 0.51 μm. This shows an improvement in surface finish by 5%. The standard deviation for the controlled mode is 0.017 μm, while that in the uncontrolled mode is 0.041 μm. The low value of standard deviation in the controlled mode indicates a more even surface which produces better surface finish.

The values of surface roughness, (R_a) are obtained from surface measurements done by 3D laser scanning microscope which scans the whole surface under investigation hence they give a more accurate picture of the surface finish. This is unlike most other surface roughness measurement techniques such as probe based methods.

Figure 4.20 (b) shows the relationship between duty cycle and surface roughness in machining of brass. In the controlled mode, surface roughness ranges between 0.52 μm and 0.57 μm with a standard deviation of 0.023 μm. In the uncontrolled machining mode, the roughness ranges between 0.47 μm and 0.59 μm with a standard deviation of 0.047 μm. The surface roughness values do not reveal much

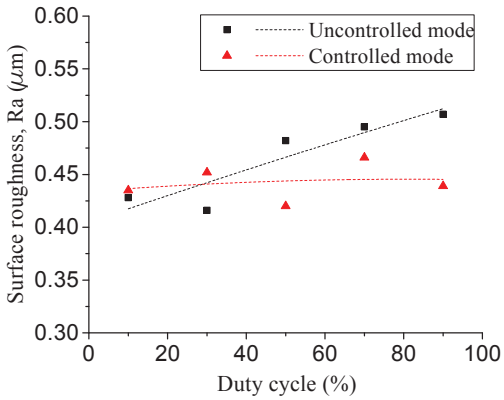

(a) Aluminium

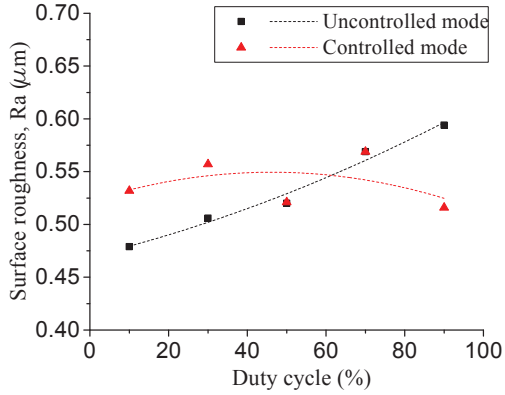

(b) Brass

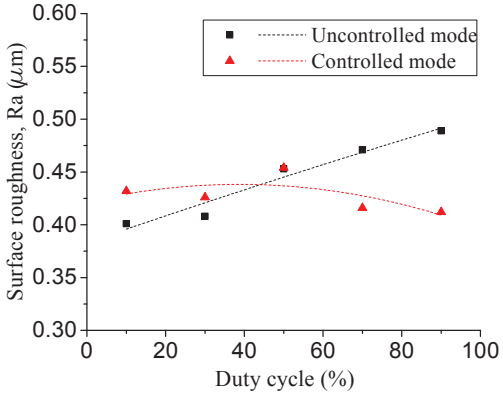

(c) Medium carbon steel (0.47% C)

Figure 4.20: Surface roughness for controlled and uncontrolled electrical discharge machining at different duty cycles (v=100 V, f=100 kHz)

difference, but the standard deviation indicates that for the controlled mode, the surface roughness values are close together, an indicator of a surface finish that is even. The standard deviation for the uncontrolled mode on the other hand indicates a more uneven surface.

The relationship between duty cycle and surface roughness in machining of medium carbon steel is shown in Figure 4.20 (c). From the figure, the surface roughness for the controlled mode ranges between 0.41 μm and 0.45 μm , while that in the uncontrolled mode ranges between 0.40 μm and 0.49 μm. The standard deviations are 0.017 μm and 0.039 μm for the controlled and uncontrolled modes respectively. Like in machining of brass, there is not much difference in surface roughness values, but the standard deviations show some difference in the controlled and uncontrolled modes. For the controlled process, the low standard deviation is an indicator of surface finish that is even, while high standard deviation in the uncontrolled mode indicates an uneven surface finish.

4.3.5 Optimization of duty cycle with respect to material removal rate

Machining experiments were conducted in order to test the effectiveness of the controller in the optimization of duty cycle for maximum MRR. The duty cycle was varied between 10% and 90%. The average diameters and depths of the holes that were machined were used to calculate MRR. Figure 4.21 shows the relationships between MRR and duty cycle for machining the three materials in controlled and uncontrolled modes at different duty cycles. As seen in Figure 4.21 (a), the MRR for the controlled mode remains almost constant whereas that of the uncontrolled process changes with change in duty cycle. The maximum MRR in the uncontrolled mode occurs at a duty cycle of 50%. The standard deviations for machining of aluminium are 8.5×10^{-4} mm^3/min and 2.98×10^{-3} mm^3/min for the controlled and uncontrolled modes respectively. These values show a 3.2% improvement in machining rate for the controlled mode. The low

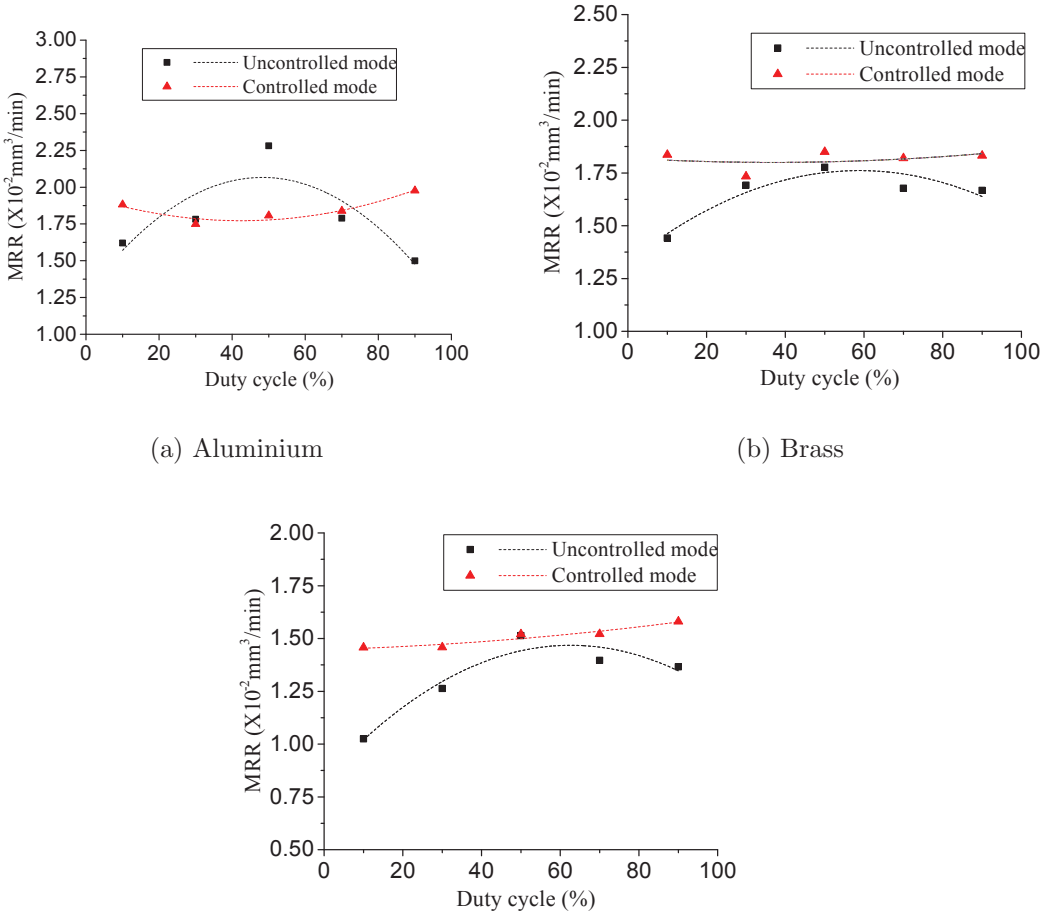

(a) Aluminium

(b) Brass

(c) Medium carbon steel (0.47% C)

Figure 4.21: MRR for controlled and uncontrolled electrical discharge machining at different duty cycles (v=100 V, f=100 kHz)

standard deviation in the controlled mode indicates that the controller is able to ensure that MRR is maintained uniform. Also, high values of MRR indicate fast machining speeds for the controlled mode. Maximum MRR is achieved by ensuring that the gap is adjusted in such a way that the power density at the spark gap is highest, while at the same time avoiding short and open circuits, which could result in poor surface finish.

Figure 4.21 (b) shows the relationship between duty cycle and MRR for machining brass at different duty cycles. From this graph, it can be seen that the MRR for the controlled mode ranges between 1.7×10^{-2} mm^3/min and 1.85×10^{-2} mm^3/min and for the uncontrolled mode ranges between 1.4×10^{-2} mm^3/min and 1.78×10^{-2} mm^3/min. These ranges indicate that the MRR in the controlled mode is higher than that in the uncontrolled mode. More specifically, they show a 9.9% improvement in machining rate in the controlled mode. Also, the standard deviation of the controlled process is 4.6×10^{-4} mm^3/min, while that of the uncontrolled machining is 1.25×10^{-3} mm^3/min. These standard deviations indicate consistent MRR (machining rate) throughout the machining process in the controlled mode, while they show inconsistent machining rate in the uncontrolled mode. As earlier observed, in the uncontrolled mode the MRR changes from minimum at 10% duty cycle, to maximum at 50% duty cycle after which it then decreases.

The results for the tests on effectiveness of the controller in the optimization of MRR for machining steel are shown in Figure 4.21 (c). From this figure, a similar trend to that observed in machining of aluminium and brass is seen where the MRR in the controlled mode is higher than that in the uncontrolled mode. The MRR in the controlled mode ranges between 1.45×10^{-2} mm^3/min and 1.58×10^{-2} mm^3/min while that in the uncontrolled mode ranges between 1.02×10^{-2} mm^3/min and 1.51×10^{-2} mm^3/min. These values of MRR show an average improvement in machining rate by 14.9%. The standard deviations for

the controlled and uncontrolled modes are 0.086 and 0.307 respectively. Like in earlier discussions, the lower standard deviation in the controlled mode indicates uniform material removal rate.

4.3.6 Optimization of duty cycle with respect to tool wear rate

Finally, experimental work was done to establish if and to what extent the FLC based controller is able to reduce tool wear rate in machining of the three materials under consideration. During the machining process, the tool wear length for each profile that was machined was recorded and later used to calculate the tool wear rate which is presented in Figure 4.22. The tool wear rate obtained from machining of aluminium is shown in Figure 4.22 (a). From this figure, the tool wear rate in the controlled mode falls between is 5.7×10^{-4} mm^3/min and 6.7×10^{-4} mm^3/min. In the uncontrolled mode, TWR falls between 6.0×10^{-4} mm^3/min and 6.3×10^{-4} mm^3/min. It can be seen that, TWR for the controlled process increases as the duty cycle is increased in the controlled mode. However, the average TWR for the two modes of machining does not show a significant difference.

In the controlled mode, the ratio of MRR to TWR is 3000 while that in the uncontrolled mode is 2907. These ratios show a 3.2% improvement in the amount of material removed per unit tool wear. This means that, for the same amount of tool wear in both controlled and uncontrolled machining modes, the total amount of material removed in the controlled mode is higher than that removed in the uncontrolled mode, the result of which is longer tool life.

In the experiments for machining brass to test the effectiveness of the adaptive controller in minimizing the TWR the results obtained are shown in Figure 4.22 (b). As seen in this figure, the TWR for controlled mode ranges between 5.8×10^{-4} mm^3/min and 7.2×10^{-4} mm^3/min, while that of the uncontrolled machining ranges between 6.0×10^{-4} mm^3/min and 6.2×10^{-4} mm^3/min. It can

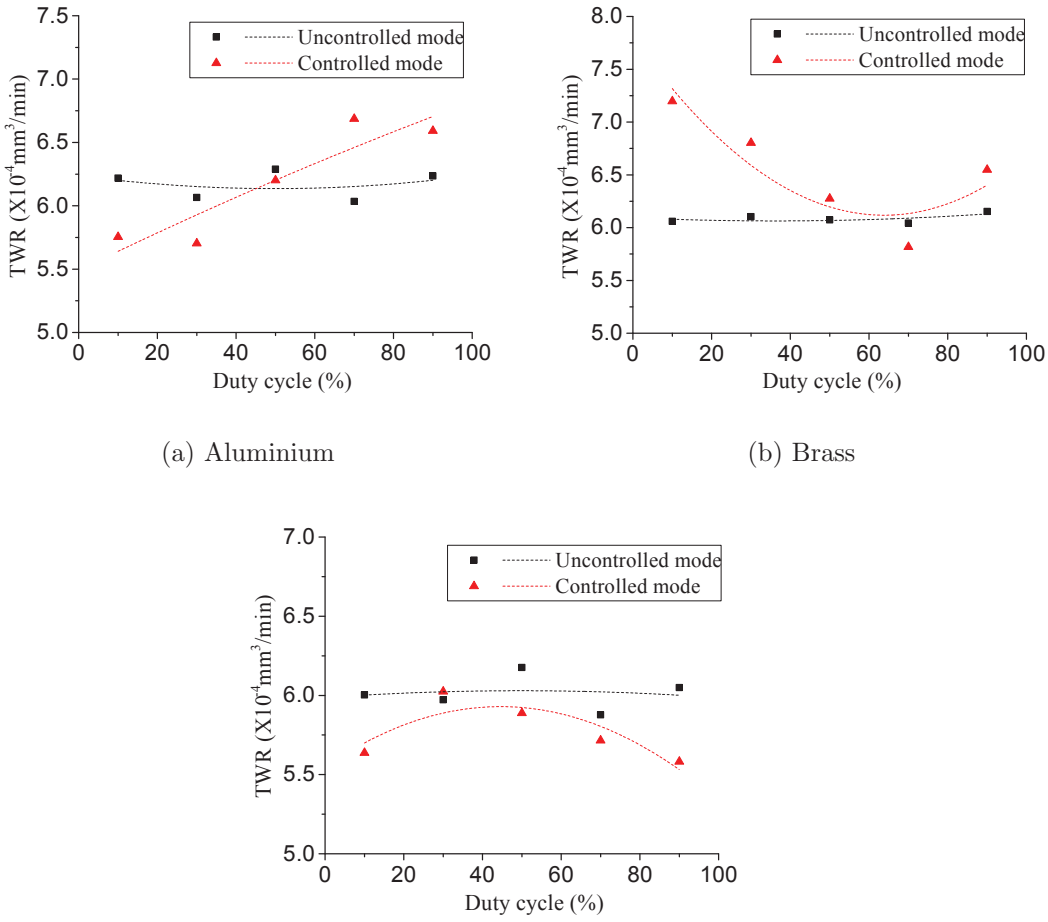

(a) Aluminium

(b) Brass

(c) Medium carbon steel (0.47% C)

Figure 4.22: TWR for controlled and uncontrolled electrical discharge machining at different duty cycles (v=100 V, f=100 kHz)

be seen that the tool wear rate in the controlled mode is higher. This would result in shorter tool life which is undesirable and is thus a subject for further improvement in the controller. This could have resulted from the fact that the controller monitors the EDM process by feedback on frequency and periodic times of discharges, and, gap voltage. However, in machining brass, there was welding of machined particles and arcing as was reported by Shabgard *et al.* [15]. These two processes were not checked and may have been the cause of higher TWR and poor surface finish.

After some investigation was done to establish the reasons behind the high TWR in the controlled machining mode, it was found that there was a mix up of brass workpieces and that the properties of brass for the two workpieces were different. The ideal experimental work would have been to use brass with matching properties. However, due to the mix up, the type of the brass material that was used in the controlled mode was alpha brass (with 65% Cu and 35%Zn), while the one that was used in the uncontrolled mode was beta brass (with 50% Cu and 50% Zn). As has been established in all the results obtained in this research work and in the research done by Shahul *et al.* [65], MRR, TWR and surface finish are affected by the electrodes' materials, i.e., the composition of electrodes materials influences the conduction properties for both the workpiece and tool electrodes and therefore, it was impractical to compare the results for the controlled mode and uncontrolled mode for machining of brass for samples with different physical properties. However, the adaptive controller was able to reduce the TWR for controlled machining of this sample and maintain it at a low value regardless of the mixup. This is a clear indication that the controller is able to monitor the process and adjust parameters to optimize the EDM process regardless of the material of the workpiece.

In machining steel, the TWR in the controlled mode has a range of between 5.58×10^{-4} mm^3/min and 6.02×10^{-4} mm^3/min, while in the uncontrolled mode,

the range of TWR was between 5.88×10^{-4} mm^3/min and 6.17×10^{-4} mm^3/min as can be seen in Figure 4.22 (c). Similar to the case of machining aluminium, the difference in TWR is significantly small for the two modes and not much conclusion can be drawn from it.

However, the ratio of MRR to TWR for the controlled mode is 2616 and 2181 for the uncontrolled mode. These ratios show an improvement of 20% in machining rate for unit amount of tool wear. An important point to note here is that, since the controller that was developed is generic in nature, the output/performance parameters for controlled mode of machining different materials may differ in magnitude, but generally have a trend of improvement in the output parameters and higher efficiency in machining.

4.3.7 Summary of the results

From the experimental work carried out to demonstrate the effectiveness of the FLC based adaptive controller in optimizing the EDM process, the following general observations can be drawn.

- The controller is able to improve the surface quality of the machined product by reducing surface roughness by between 6.5% and 70.9% regardless of the value of gap voltage.
- That the controller is able to improve the machining speed by increasing MRR by between 4% and 243.1% regardless of the gap voltage.
- The TWR is reduced by 9% or more for all values of gap voltage.
- The surface roughness, measured as R_a, is improved when the controller is used. This is indicated by decrease in the R_a values and reduced standard deviation in surface roughness values for the optimized EDM processes.

- Regardless of any changes in duty cycle during machining, the MRR is improved by over 3% in the optimized EDM process, and,
- The TWR does not show any significant changes when duty cycle is changed for both controlled and uncontrolled EDM process. However, the MRR to TWR ratio is high for the optimized electrical discharge machining process indicating a healthy EDM process and better use of the tool.

CHAPTER FIVE

CONCLUSIONS AND RECOMMENDATIONS

5.1 Conclusions

From the current research work, it is concluded that;

1. The transistorized pulse generation circuit has been developed, tested and verified to provide smooth and accurate control and adjustment of duty cycle, pulse frequency and gap voltage.

2. From the investigation conducted to establish the effects of the machining parameters on EDM process outputs;

    i. increase in gap voltage leads to increase in MRR and TWR for the uncontrolled EDM process.

    ii. increasing gap voltage leads to higher roughness of the machined surface in uncontrolled EDM process.

    iii. MRR increases as duty cycle is adjusted from 10% to 50% after which it then starts to decrease.

    iv. as duty cycle is increased, surface roughness increases in an almost linear manner.

    v. duty cycle has no significant affect on TWR.

3. Following tests done to evaluate the effectiveness of the adaptive controller in optimization of the EDM process;

    i. MRR increases by 3% or higher percentage under the control of the FLC based adaptive controller.

    ii. improved surface finish was achieved in the controlled EDM process. This is indicated by low surface roughness values achieved in the controlled process.

iii. tool wear rate reduced in the controlled EDM process for all materials under investigation as compared to the uncontrolled EDM process.

From these three main conclusions, it is evident that the FLC based controller was able to effectively optimize the EDM process by improving the machining rate, reducing tool wear and producing improved surface finish as per the measured output parameters.

5.2 Highlight of the contributions of the study

This study has shed light in the area of electrical discharge machining by investigating the effects of the machining parameters on the EDM process output parameters. The study has also ventured into the area of adaptive control by combining the feedback aspect of conventional control with the heuristic capability of fuzzy logic control. This expands the limits of process control as both approaches compliment each other in real-time monitoring and control, thus equipping the resulting controller with the capability of dealing with uncertainties.

5.3 Recommendations for future work

From the results obtained, it is recommended that;

1. A detailed investigation be carried out on the large heat affected zone resulting especially from machining of brass at high gap voltage to establish the impact on the product quality.

2. The current work be extended to cover other materials that were not investigated under the current research with a view to increasing the knowledge base that would be useful in improvement of efficiency of the controller in optimizing the EDM process by tuning it further.

3. The research be extended to wire electrical discharge machining process with a view to optimize it.

4. In development of EDM machines and for achievement of fast response and speed as desired, more emphasis needs to be put on the design of the spindle motor driver circuits to emphasize on speed of response.

5. A multi-objective optimization technique such as use of Pareto front can be applied to extend the scope of this work further.

REFERENCES

[1] Sandeep K., "Status of recent developments and research issues of electrical discharge machining (EDM)," *International Journal of Latest Trends in Engineering and Technology (IJLTET)*, vol. 2 Issue 3, pp. 242–248, 2013.

[2] Bangalore H. M., *Production technology.* ISBN-10: 0070964432, ISBN-13: 978-0070964433, Tata McGraw-Hill Education, 2001.

[3] Tarng Y. S., Tseng C. M. and Chung L. K., "A fuzzy pulse discriminating system for electrical discharge machining," *International Journal of Machine Tools and Manufacture*, vol. 37, pp. 511–522, 1997.

[4] Byiringiro J. B., Ikua B. W., and Nyakoe G. N., "Design and simulation of a fuzzy logic based servo controller of a micro-electro discharge machining system," Master's thesis, Jomo Kenyatta University of Agriculture and Technology, 2009.

[5] Tarng Y. S. Ma S. C. and Chung L. K., "Determination of optimal cutting parameters in wire electrical discharge machining," *International Journal of Machine Tools and Manufacture*, vol. 35, no 12, pp. 1693–1701, 1995.

[6] Byiringiro J. B., Ikua B. W. and Nyakoe G. N., "Fuzzy logic based controller for micro-electro discharge machining servo systems," in *IEEE Africon*, September 2009.

[7] Huang J.T. and Liao Y.S., "Optimization of machining parameters of wire-EDM based on grey relational and statistical analysis," *International Journal of Production*, vol. 41, no. 8, pp. 1707–1720, 2003.

[8] Zhang Q.H., Du R., Zhang J.H. and Zhang Q.B., "An investigation of ultrasonic-assisted electrical discharge machining in gas," *International Journal of Machine Tools and Manufacture*, vol. 46, pp. 1582–1588, 2006.

[9] Takahisa M., "A quarterly survey of new products, systems, and technology," Tech. Rep. Vol. 81, Mitsubishi Electric Advance, Dec 1997.

[10] Sourabh K. S., "Experimental investigation of the dry electric discharge machining (dry edm) process," Master's thesis, Indian Institute of Technology Kanpur, April 2008.

[11] Donald B. M., "Wire EDM: The fundamentals," tech. rep., EDM network, Sugar Grove, IL, pp. 1- 22, 2013.

[12] Hassan A.-G. E-H., *Fundamentals of machining processes: Conventional and nonconventional processes, 2nd Edition, ISBN 13: 9781466577022*. CRC Press, 2014.

[13] Robert H., Dell K. and Leo A., *Manufacturing processes reference guide*. Industrial Press Inc.,, 1994.

[14] Gokhan K. and Can C., "A new method for machining of electrically nonconductive workpieces using electric discharge machining technique," *Machining Science and Technology*, vol. 14 Isue 2, pp. 189–207, 2010.

[15] Shabgard M. R., Seyedzavvar M. and Nadimi B. O., "Influence of input parameters on characteristics of EDM process," *Journal of Mechanical Engineering*, vol. 2, pp. 123–135, 2006.

[16] Carlo F., Atanas I. and Antoine P., "Electrical measurements in micro-EDM," *Journal of Micromechanics and Microengineering*, vol. 18, pp. 1–13, 2008.

[17] Scott F. M., Albert J. S. and Jun Q., "Investigation of the spark cycle on material removal rate in wire electrical discharge machining of advanced materials," *International Journal of Machine Tools and Manufacture*, vol. 44, pp. 391–400, 2004.

[18] Yongshun Z., Xingquan Z., Xianbing L. and Kazuo Y., "Geometric modeling of the linear motor driven electrical discharge machining (EDM) die-sinking process," *International Journal of Machine Tools and Manufacture*, vol. 44, pp. 1–9, 2004.

[19] Pecas P. and Henriques E., "Influence of silicon powder-mixed dielectric on conventional electrical discharge machining," *International Journal of Machine Tools and Manufacture*, vol. 43, pp. 1465–1471, 2003.

[20] Scott F. M., Chen-C. K., Albert J. S. and Jun Q., "Investigation of wire electrical discharge machining of thin cross-sections and compliant mechanisms," *International Journal of Machine Tools and Manufacture*, vol. 45, pp. 1717–1725, 2005.

[21] Bulent E., Erman T. and Abdulkadir E., "A semi-empirical approach for residual stresses in electric discharge machining (EDM)," *International Journal of Machine Tools and Manufacture*, vol. 46, pp. 858–868, 2006.

[22] Jin W., Fuzhu H., Gang C. and Fuling Z., "Debris and bubble movements during electrical discharge machining," *International Journal of Machine Tools and Manufacture*, vol. 58, pp. 11–18, 2012.

[23] Nizar B. S., Farhat G. and Kais B. A., "Numerical study of thermal aspects of electric discharge machining process," *International Journal of Machine Tools and Manufacture*, vol. 46, pp. 908–911, 2006.

[24] Yih-F. C. and Zhi-H. C., "Electrode wear-compensation of electric discharge scanning process using a robust gap-control," *Mechatronics*, vol. 14, pp. 121–1139, 2004.

[25] Seiji K., Naoki S. and Koichi T., "Combination of capacitance and conductive working fluid to speed up the fabrication of a narrow, deep hole in electrical

discharge machining using a dielectric-encased wire electrode," *International Journal of Machine Tools and Manufacture*, vol. 46, pp. 1536–1546, 2006.

[26] Muniu J. M., Ikua B. W., Nyaanga D. M. and Gicharu S. N., "Investigation on applicability of diatomite powder-mixed dielectric fluid in electrical discharge machining pocesses," in *Sustainable Research and Innovation Conference Proceedings*, vol. 4, pp. 280–288, 2012.

[27] Kun L. W., Biing H. Y., Fuang Y. H. and Shin C. C., "Improvement of surface finish on SKD steel using electro-discharge machining with aluminum and surfactant added dielectric," *International Journal of Machine Tools and Manufacture*, vol. 45, pp. 1195–1201, 2005.

[28] Kao C. C., Jia Tao and Albert J. Shih, "Near dry electrical discharge machining," *International Journal of Machine Tools and Manufacture*, vol. 47, pp. 2273–2281, 2007.

[29] Robert B., "An overview of nonlinear identification and control with fuzzy systems," in *Intelligent control systems using computational intelligence technique*, 2005.

[30] Jang J.S., Sun C.T. and Mizutani E., *Neuro-fuzzy and soft computing A computational approach to learning and machine intelligence*. Prentice-Hall, Inc., Upper Saddle River, New Jersey, 1997.

[31] Jos C. P., Neil R. E. and Curt L. W., *Neural and adaptive systems: Fundamentals through simulations*. Wiley, 1999.

[32] Timothy J. R., *Fuzzy logic with engineering applications*. John Wiley and Sons Ltd, 2004.

[33] Claudio M., "Introduction to fuzzy logic." Facta Universitatis (NIS), 2000.

[34] Zadeh L. A., "Fuzzy sets," *Information and control*, vol. 8, pp. 338–353, 1965.

[35] James F. B., "Fuzzy systems - tutorial." http://www.austinlinks.com/Fuzzy/tutorial.html, 2004.

[36] Guanrong C., *Introduction to fuzzy sets, fuzzy logic, and fuzzzy control systems*. CRC Press, 2001.

[37] Edward T., Tanya L. and Mo J., "Introduction to Fuzzy Logic Control With Application to Mobile Robotics." NASA Center for Autonomous Control Engineering Department of Electrical and Computer Engineering University of New Mexico, 2009.

[38] Xiaolin Z., Hongwei Z., Yiming Q. and Li W., "Grinding Process Fuzzy Control System Design and Application Based on MATLAB," *IEEE*, vol. 1, pp. 311–315, 2008.

[39] Hellmann M., "Fuzzy logic introduction - Tutorial." Universite de Rennes, 2005.

[40] Takagi T. and Sugeno M., "Derivation of fuzzy control rules from human operators control actions," in *In Procedings, IFAC Symposium: Fuzzy Information, Knowledge Representation and Decision Analysis*, vol. 1, 1983.

[41] Lee C. C., "Fuzzy logic in control systems: Fuzzy logic controller-Part I," *IEEE Transactions, System, Man, Cybernetics*, vol. 20, pp. 404–418, 1990.

[42] Takagi T. and Sugeno M., "Fuzzy identification of systems and its applications to modeling and control," *IEEE Trans. on System, Man and Cybernetics*, vol. 4 , No. 9, pp. 116–132, 1985.

[43] Mohammad J., Nader V. and Timothy J., *Fuzzy logic and control*. Prentice Hall, 1993.

[44] Kipkosgei P. C., Kabini S. K. and Ikua B. W., "A technical report on design of a transistor based pulse generation circuit for electrical discharge machine," tech. rep., Proceedings of the Sustainable Research and Innovation (SRI) Conference, May 2017, ISSN 2079-6226.

[45] Massimo B., *Getting started with Arduino.* O'Reilly, 2011.

[46] Looser A., Linares L., Zwyssig C. and Kolar J., "Novel power supply topology for large working gap Dry EDM," *The 2010 International Power Electronics Conference, IEEE*, pp. 306–310, 2010.

[47] Schubert A. and Zeidler H., "A novel approach to efficiency determination in micro electro discharge machining," in *Proceedings of the Euspen International Conference - Zrich*, 2008.

[48] Piero P. B., "Adaptive neural fuzzy inference systems (ANFIS): Analysis and applications." Lecture notes, Schenectady, NY USA, 2000.

[49] Kabini S. K., Bernard W. Ikua, John M. Kihiu, George N. Nyakoe and Patrick C. Kipkosgei, "Evaluation of the performance of a transistorised pulse generation circuit in electrical discharge machining," *Journal of Sustainable Research in Engineering*, vol. 3 (4), pp. 88–93, 2017.

[50] Subrat K. B. and Srinivasa R. P., "Design of pulse circuit of EDM diesinker," *International Research Journal of Engineering and Technology (IRJET)*, vol. 3 Issue 5, pp. 1 – 4, 2016.

[51] Kabini S. K., Bojer S. K., Ikua B. W., Kihiu J. M., Nyakoe G. N. and Mwangi J. W., "The performance of a resistance-capacitance type pulse generation circuit in electrical discharge machining," *Journal of Sustainable Research in Engineering*, vol. 2 (4), pp. 158 – 162, 2015.

[52] Rajesha R. and Anandb M., "The optimization of the electro-discharge machining process using response surface methodology and genetic algo-

rithms," *International Conference on Modelling, Optimization and Computing*, vol. 38, pp. 3941–3950, 2012.

[53] Pragya S., Jainb P. and Jainc N, "Parametric optimization during wire electrical discharge machining using response surface methodology," in *Procedia Engineering*, vol. 38, pp. 2371–2377, 2012.

[54] Sameh S. Habib, "Study of the parameters in electrical discharge machining through response surface methodology approach," *Applied Mathematical Modelling*, vol. 33, pp. 4397–4407, 2009.

[55] Bharat B., *Surface Roughness Analysis and Measurement Techniques*. CRC Press LLC, 2001.

[56] Ravindranadh B., Madhu V. and Gogia A. , "Modelling and analysis of material removal rate and surface roughness in wire-cut edm of armour materials," *Engineering Science and Technology, an International Journal*, vol. 18, pp. 664–668, 2015.

[57] Chang-H. K., "Influence of the Electrical Conductivity of Dielectric Fluid on WEDM Machinability," in *Dept. of Mechanical Engineering, Dong-Eui University, Gaya-2 Dong, Pusanjin-Gu, Korea*, 2010.

[58] Mona A. Y., Mohamed S. A., Mostafa A. G., Fouad H. M. and Sayed A. A., "Effect of electrode material on electrical discharge machining of tool steel surface," *Ain Shams Engineering Journal*, vol. 6, p. 977986, 2015.

[59] Banker K.S., Oza A. D. and Dave R. B., "Performance capabilities of EDM machining using aluminum, brass and copper for AISI 304L material," *International Journal of Application or Innovation in Engineering & Management (IJAIEM)*, vol. 2 Issue 8, pp. 186–191, 2013.

[60] Revaz B., Witz G. and Flukiger R., "Modeling of the discharge-sample intreraction in the Electron Discharge Machining (EDM) process.," tech. rep., Laboratoire de simulation des materiaux, 2009.

[61] Suleiman A., Ahsan A. and Mohamed K., "Reducing electrode wear ratio using cryogenic cooling during electrical discharge machining," *The International Journal of Advanced Manufacturing Technology*, vol. 45, pp. 1146–1151, 2009.

[62] Jaganathan P., Naveenkumar T. and Sivasubramanian R., "Machining parameters optimization of WEDM process using Taguchi method," *International Journal of Scientific and Research Publications*, vol. 2 Issue 2, pp. 1–4, 2012.

[63] Teepu S., Anish K., and R. Dev G., "Material removal rate, electrode wear rate, and surface roughness evaluation in die sinking EDM with hollow tool through response surface methodology," *International Journal of Manufacturing Engineering*, vol. 1, pp. 1–16, 2014.

[64] Dasa K., Kumarb K., Barmana T. and Sahoo P., "Optimization of surface roughness and MRR in EDM using WPCA," *International Conference on Design and Manufacturing (IConDM2013)*, vol. 64, pp. 446–455, 2013.

[65] Shahul B., Cijo M. and Sunny K. G., "Optimization of MRR and TWR on EDM by using Taguchi method and ANOVA," *International Journal of Innovative Research in Advanced Engineering (IJIRAE)*, vol. 1 Issue 8, pp. 106–112, 2014.

Appendix A

A. INITIAL DESIGN OF THE TRANSISTORIZED PULSE GENERATION CIRCUIT

A.1 555 Timer based pulse generation circuit

The 3D representation of the first design of the pulse generator circuit which is based on a 555 timer is shown in Figure A.1 and the schematic diagram for the circuit is shown in Figure A.2.

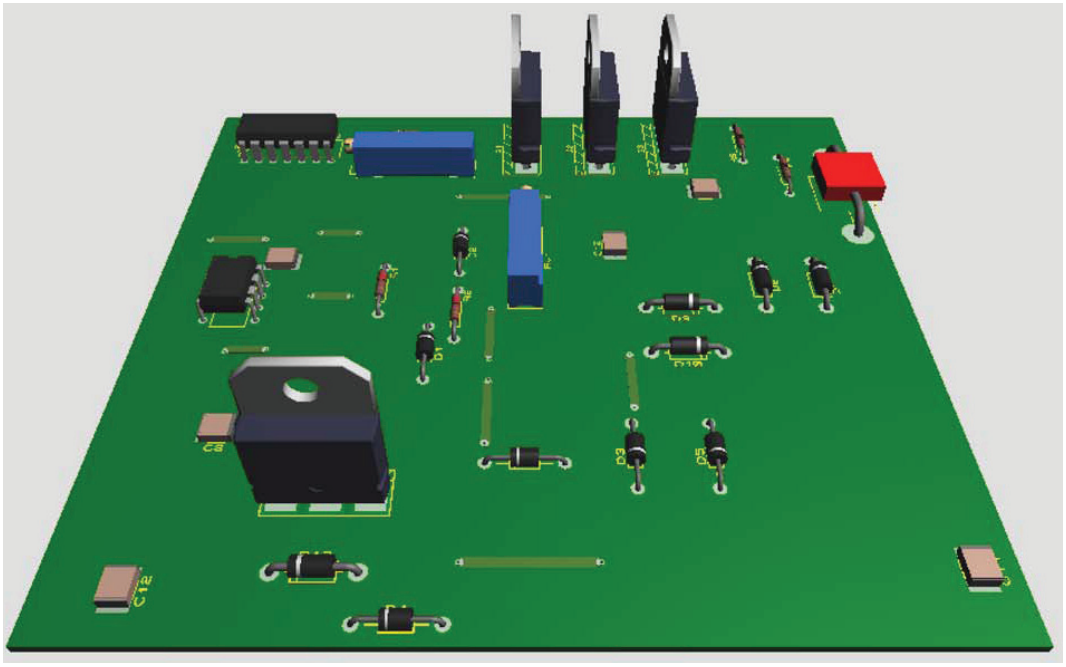

Figure A.1: 3D representation of the 555 timer based pulse generation circuit

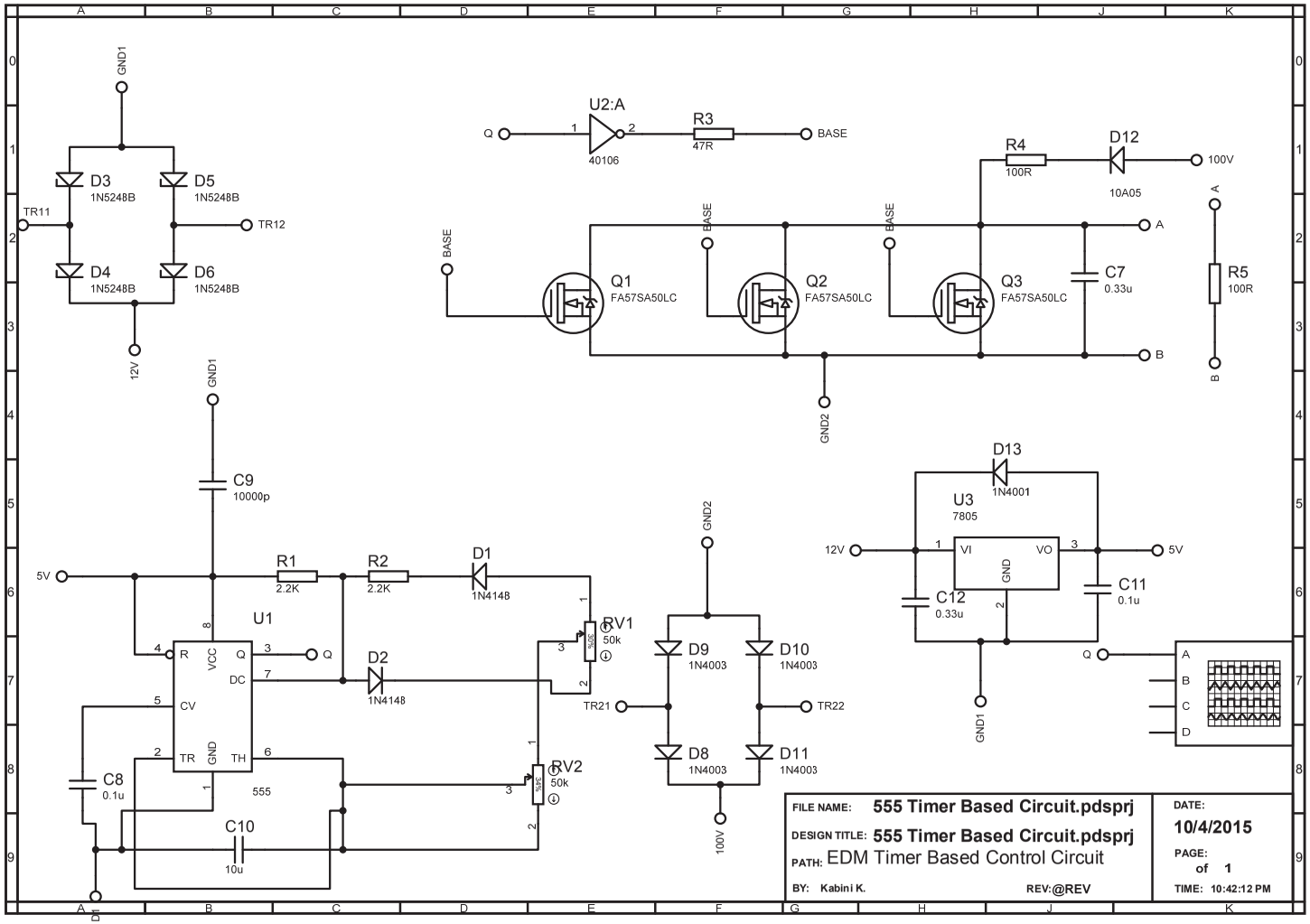

Figure A.2: Schematic of the 555 timer based pulse generation circuit

Appendix B

B. RAW DATA FROM MACHINING EXPERIMENTS

B.1 Calculation of MRR at different gap voltages

Tables B.1 through B.3 show the calculated MRR at the indicated values of gap voltage for uncontrolled EDM process.

Table B.1: MRR for uncontrolled machining of aluminium at different gap voltages

Applied gap voltage (v)	Machining time (s)	Average machining time (s)	Diameter of the machined hole (μm)	Mean diameter of the machined hole (μm)	Depth of the machined hole (μm)	Mean depth of the machined hole (μm)	MRR (mm3/min) (xE-2)
50	18.3	18.2	113.012	112.9	472.53	479.7	1.58104923
	18		112.135		484.265		
	18.4		113.612		482.322		
70	18.7	18.2	120.589	119.2	480.582	482.1	1.7734648
	18.1		115.341		482.565		
	17.8		121.624		483.215		
90	15.2	15.6	123.135	123.6	493.531	486.8	2.25094146
	15.6		121.875		473.215		
	15.9		125.739		493.635		
110	15	15.0	124.775	128.3	484.253	489.7	2.53364725
	15.1		131.323		490.562		
	14.9		128.874		494.265		
130	12	12.3	148.861	141.9	491.551	486.4	3.76384569
	12.5		134.348		485.523		
	12.3		142.521		482.265		
150	11.8	11.1	142.012	143.3	495.864	496.2	4.32912708
	11.2		137.205		496.566		
	10.3		150.808		496.253		

Table B.2: MRR for uncontrolled electrical discharge machining of brass at different gap voltages

Applied gap voltage (v)	Machining time (s)	Average machining time (s)	Diameter of the machined hole (μm)	Mean diameter of the machined hole (μm)	Depth of the machined hole (μm)	Mean depth of the machined hole (μm)	MRR (mm3/min) (xE-2)
50	19.5	19.1	105.254	106.7	476.485	478.3	1.3469125
	18.3		104.804		482.418		
	19.4		110.156		475.925		
70	18.2	18.3	112.752	111.3	478.263	477.1	1.5202086
	18.8		109.45		475.615		
	18		111.781		477.526		
90	18.3	18.1	109.301	113.6	479.256	476.3	1.5972234
	18		117.369		477		
	18.1		114.105		472.553		
110	17.5	17.2	110	120.2	479.55	480.5	1.9058517
	17.3		128.569		481.029		
	16.7		122.023		480.903		
130	16.9	16.6	121.873	120.0	483.156	484.0	1.9780545
	16.1		116.108		484.256		
	16.8		121.953		484.589		
150	15	15.3	138.016	135.0	485.262	485.9	2.7318846
	15.3		125.199		486.301		
	15.5		141.661		486.005		

Table B.3: MRR for uncontrolled machining of medium carbon steel at different gap voltages

Applied gap voltage (v)	Machining time (s)	Average machining time (s)	Diameter of the machined hole (μm)	Mean diameter of the machined hole (μm)	Depth of the machined hole (μm)	Mean depth of the machined hole (μm)	MRR (mm3/min) (xE-2)
50	24.3	23.5	95.882	96.6	462.206	462.5	0.8649082
	25.3		98.71		463.201		
	21		95.305		462.091		
70	23.7	22.2	99.561	102.6	465.025	466.8	1.0422663
	21		102.12		468		
	22		106.223		467.268		
90	21	19.2	103.214	104.1	468.964	468.8	1.2451683
	20.5		103.475		469.265		
	16.2		105.662		468.023		
110	14.2	15.0	107.285	108.5	470.031	470.4	1.7443964
	15		108.32		469.803		
	15.7		109.951		471.355		
130	13	13.5	109.296	110.4	472.952	474.5	2.0136102
	14.1		110.572		475.801		
	13.5		111.313		474.61		
150	11	11.6	112.693	113.1	475.997	477.4	2.4734147
	12.4		112.807		478.256		
	11.5		113.753		478.001		

B.2 Calculation of TWR at different gap voltages

Tables B.4 through B.6 show the tool wear rate for each of the indicated voltages for machining of the three metals for the uncontrolled EDM process.

Table B.4: TWR for uncontrolled machining aluminium at different gap voltages

Applied gap voltage (v)	Machining time (s)	Average machining time (s)	Recorded tool wear (μm)	Average tool wear (μm)	TWR (mm3/min) (xE-4)
50	18.3	18.2	30.256	32.8	5.432464
	18		36.135		
	18.4		32.125		
70	18.7	18.2	36.123	33.9	5.615714
	18.1		35.272		
	17.8		30.258		
90	15.2	15.6	36.216	36.1	6.998831
	15.6		40.12		
	15.9		32.023		
110	15	15.0	36.251	36.8	7.399971
	15.1		35.893		
	14.9		38.255		
130	12	12.3	38.369	38.5	9.457065
	12.5		38.009		
	12.3		39.001		
150	11.8	11.1	38.881	37.5	10.186738
	11.2		35.673		
	10.3		37.907		

B.3 Calculation of MRR for machining at different values of duty cycle

The data that is used to establish the relationship between MRR and duty cycle for aluminium, brass and steel is tabulated as shown in Tables B.7, B.8 and B.9, respectively.

B.4 Calculation of TWR at different duty cycle values

Tables B.10, B.11 and B.12 show the TWR that results from machining with different duty cycles.

Table B.5: TWR for uncontrolled machining of brass at different gap voltages

Applied gap voltage (v)	Machining time (s)	Average machining time (s)	Recorded tool wear (μm)	Average tool wear (μm)	TWR (mm3/min) (xE-4)
50	19.5	19.1	38.099	38.1	6.028896
	18.3		39.105		
	19.4		37.125		
70	18.2	18.3	39.023	37.1	6.1037703
	18.8		36.912		
	18		35.362		
90	18.3	18.1	37.191	38.4	6.3941548
	18		40.107		
	18.1		38.022		
110	17.5	17.2	39.052	39.3	6.9021016
	17.3		40.936		
	16.7		37.857		
130	16.9	16.6	35.236	37.2	6.7629165
	16.1		39.255		
	16.8		37.166		
150	15	15.3	35.139	37.9	7.4977944
	15.3		38.807		
	15.5		39.901		

Table B.6: TWR for uncontrolled machining of medium carbon steel at different gap voltages

Applied gap voltage (v)	Machining time (s)	Average machining time (s)	Recorded tool wear (μm)	Average tool wear (μm)	TWR (mm3/min) (xE-4)
50	24.3	23.5	35.027	35.9	4.5980936
	25.3		34.911		
	21		37.685		
70	23.7	22.2	35.125	36.4	4.9421521
	21		37.155		
	22		37.006		
90	21	19.2	31.82	34.6	5.4203845
	20.5		39.132		
	16.2		32.736		
110	14.2	15.0	33.802	34.4	6.9414324
	15		34.172		
	15.7		35.354		
130	13	13.5	38.261	37.4	8.3282378
	14.1		37.642		
	13.5		36.196		
150	11	11.6	33.232	33.6	8.7155227
	12.4		35.903		
	11.5		31.707		

Table B.7: MRR for uncontrolled machining of aluminium at different values of duty cycle

Duty cycle (%)	Machining time (s)	Average machining time (s)	Diameter of the machined hole (μm)	Mean diameter of the machined hole (μm)	Depth of the machined hole (μm)	Mean depth of the machined hole (μm)	MRR (mm3/min) (xE-2)
10	19.1	18.8	115.203	116.2	481.02	479.3	1.6199637
	18.5		118.791		476.237		
	18.9		114.65		480.662		
30	18.2	18.0	118.254	118.5	485.691	484.6	1.7826577
	17.3		119.635		481.723		
	18.5		117.708		486.339		
50	15.2	15.6	125.261	123.7	495.261	492.6	2.2808194
	15.6		124.005		490.355		
	15.9		121.739		492.108		
70	17.5	18.0	121.527	119.2	483.256	480.8	1.7893259
	18.6		118.202		482.991		
	17.9		117.916		476.28		
90	18.7	19.1	113.253	113.0	480.312	476.8	1.4986368
	19.5		111.608		471.266		
	19.2		114.008		478.928		

Table B.8: MRR for uncontrolled machining of brass at different values of duty cycle

Duty cycle (%)	Machining time (s)	Average machining time (s)	Diameter of the machined hole (μm)	Mean diameter of the machined hole (μm)	Depth of the machined hole (μm)	Mean depth of the machined hole (μm)	MRR (mm3/min) (xE-2)
10	18.2	18.0	108.327	107.2	481.661	479.9	1.4410461
	18.7		105.681		475.989		
	17.2		107.549		482.157		
30	18.5	17.5	115.62	114.2	489.284	480.7	1.6918475
	17.1		112.609		474.711		
	16.8		114.395		478.127		
50	18	17.8	117.505	118.0	482.709	480.7	1.7763341
	17.5		115.631		485.916		
	17.8		120.957		473.365		
70	18.3	18.2	118.685	116.0	490.652	481.1	1.677542
	17.9		115.307		476.264		
	18.4		114.13		476.356		
90	19.3	17.1	109.306	112.2	483.956	481.0	1.667646
	16.1		112.325		477.623		
	15.9		114.841		481.428		

B.5 Calculation of MRR for controlled EDM process at different of gap voltages

Table B.13 through B.15show the material removal rates for controlled machining of aluminium, brass and steel respectively.

Table B.9: MRR for uncontrolled machining of medium carbon steel at different values of duty cycle

Duty cycle (%)	Machining time (s)	Average machining time (s)	Diameter of the machined hole (μm)	Mean diameter of the machined hole (μm)	Depth of the machined hole (μm)	Mean depth of the machined hole (μm)	MRR (mm3/min) (xE-2)
10	21.1	20.3	98.349	97.6	462.206	462.5	1.0245678
	19.6		99.355		463.201		
	20.1		95.101		462.091		
30	20.8	19.6	103.448	106.1	465.025	466.8	1.2630634
	19.3		108.396		468		
	18.7		106.403		467.268		
50	16.2	16.7	109.36	108.2	461.964	459.1	1.5137482
	17.5		104.978		451.265		
	16.5		110.259		464.023		
70	18.7	18.0	106.951	106.5	470.031	470.4	1.3962999
	17		103.664		469.803		
	18.3		108.808		471.355		
90	19.6	18.4	115.356	106.1	472.952	474.5	1.3661085
	18.3		102.902		475.801		
	17.4		100.103		474.61		

Table B.10: TWR for uncontrolled machining of aluminium at different values of duty cycle

Duty cycle (%)	Machining time (s)	Average machining time (s)	Recorded tool wear (μm)	Average tool wear (μm)	TWR (mm3/min) (xE-4)
10	17.1	18.2	37.152	37.5	6.218490
	18.5		39.025		
	18.9		36.181		
30	18.2	18.0	38.237	36.2	6.065038
	17.3		34.337		
	18.5		36.006		
50	19.2	17.2	35.425	35.9	6.288998
	16.6		34.236		
	15.9		38.133		
70	17.5	18.0	38.212	36.0	6.034260
	18.6		33.21		
	17.9		36.607		
90	18.7	18.5	41.068	38.2	6.235289
	17.5		37.583		
	19.2		35.871		

Table B.11: TWR for uncontrolled machining of brass at different values of duty cycle

Duty cycle (%)	Machining time (s)	Average machining time (s)	Recorded tool wear (μm)	Average tool wear (μm)	TWR (mm3/min) (xE-4)
10	18.2	18.0	37.265	36.2	6.0588446
	18.7		33.249		
	17.2		38.156		
30	17.5	17.1	35.404	34.7	6.1031773
	17.1		34.391		
	16.8		34.207		
50	18	17.8	36.205	35.8	6.073499
	17.5		33.109		
	17.8		38.008		
70	18.3	18.2	38.263	36.5	6.0432468
	17.9		34.901		
	18.4		36.228		
90	19.3	17.4	35.023	35.6	6.1520817
	16.1		33.987		
	16.9		37.661		

Table B.12: TWR for uncontrolled machining of steel at different values of duty cycle

Duty cycle (%)	Machining time (s)	Average machining time (s)	Recorded tool wear (μm)	Average tool wear (μm)	TWR (mm3/min) (xE-4)
10	20.1	18.9	39.263	37.7	6.00279543
	18.6		37.02		
	18.1		36.755		
30	18.8	18.9	35.152	37.5	5.9723667
	19.3		38.309		
	18.7		39.004		
50	16.2	17.4	35.608	35.6	6.17594409
	19.5		37.831		
	16.5		33.441		
70	18.7	18.0	33.205	35.1	5.87763467
	17		35.902		
	18.3		36.118		
90	19.6	18.4	38.027	37.0	6.04905794
	18.3		37.001		
	17.4		35.873		

Table B.13: MRR for controlled machining of aluminium

Applied gap voltage (v)	Machining time (s)	Average machining time (s)	Diameter of the machined hole (μm)	Mean diameter of the machined hole (μm)	Depth of the machined hole (μm)	Mean depth of the machined hole (μm)	MRR (mm3/min) (xE-2)
50	9.4	9.6	126.899	125.1	492.546	491.3	3.7620195
	10.1		124.921		483.712		
	9.4		123.580		497.503		
70	10.5	9.8	123.108	128.5	497.660	494.4	3.937444
	9.6		128.304		494.763		
	9.2		134.100		490.686		
90	9.1	8.9	131.627	128.2	492.326	491.5	4.2868321
	8.3		123.809		496.548		
	9.2		129.264		485.615		
110	8.5	8.9	134.663	133.5	488.804	493.2	4.6806154
	8.7		138.338		494.521		
	9.4		127.540		496.389		
130	9.7	9.7	132.625	133.2	497.424	491.0	4.2408399
	9.2		131.089		486.757		
	10.2		136.001		488.715		
150	9.5	9.7	133.421	131.9	482.624	492.1	4.1690755
	8.9		124.423		497.124		
	10.5		137.918		496.466		

Table B.14: Computation of MRR for brass at different gap voltages

Applied gap voltage (v)	Machining time (s)	Average machining time (s)	Diameter of the machined hole (μm)	Mean diameter of the machined hole (μm)	Depth of the machined hole (μm)	Mean depth of the machined hole (μm)	MRR (mm3/min) (xE-2)
50	8.0	9.0	128.227	123.1	481.927	480.2	3.8183813
	9.3		119.962		480.806		
	9.6		121.060		477.847		
70	10.0	8.6	132.088	126.0	491.665	485.7	4.2169072
	7.8		123.387		486.068		
	8.1		122.587		479.344		
90	8.8	9.1	120.947	123.9	487.789	489.6	3.9027918
	10.5		131.733		495.739		
	8.0		118.983		485.401		
110	9.9	9.7	134.582	129.7	481.745	489.4	4.0154577
	9.4		135.130		497.918		
	9.7		119.520		488.496		
130	10.5	10.3	118.245	126.4	489.325	488.9	3.5636105
	9.7		134.890		485.527		
	10.8		125.995		491.813		
150	9.7	9.1	129.615	128.4	494.073	491.2	4.185421
	8.4		128.870		489.831		
	9.3		126.758		489.820		

Table B.15: Parameters and MRR for controlled machining of steel at different gap voltages

Applied gap voltage (v)	Machining time (s)	Average machining time (s)	Diameter of the machined hole (μm)	Mean diameter of the machined hole (μm)	Depth of the machined hole (μm)	Mean depth of the machined hole (μm)	MRR (mm3/min) (xE-2)
50	9.7	12.1	119.977	124.8	488.407	490.0	2.9674301
	13.3		129.547		486.270		
	13.4		124.962		495.242		
70	9.4	10.5	131.110	124.2	489.043	490.2	3.3889574
	10.6		121.950		491.780		
	11.5		119.526		489.732		
90	10.7	11.3	124.278	122.5	486.775	491.0	3.083929
	13.5		118.965		494.998		
	9.5		124.304		491.203		
110	10.7	11.1	124.584	126.3	485.946	486.1	3.2799273
	9.3		123.548		485.134		
	13.4		130.635		487.345		
130	11.9	11.2	129.005	128.5	493.984	489.3	3.39784
	11.6		125.892		489.085		
	10.1		130.745		484.905		
150	12.3	10.4	125.333	124.5	486.811	491.2	3.4404232
	9.5		125.469		495.503		
	9.5		122.616		491.256		

B.6 Calculation of TWR for controlled EDM process with respect to gap voltage

Table B.16 shows the tool wear rates for machining of aluminium at different machining voltages. From the table, it can be seen that the average machining time for the optimized EDM process is about 8.4 seconds, which is a lesser machining time as compared to that of uncontrolled machining process which is 15.1 seconds. This means that the amount of tool wear rate may be higher but the ratio of MRR to TWR is higher for the optimized process than for the non controlled process.

The data used for experimental work on controlled machining of brass and the calculated tool wear rate for each set of experiments is shown in Table B.17. Tool wear rate for optimized machining process for steel for different values of machining voltage is worked out as shown in Table B.18. From this table, aver-

Table B.16: TWR for controlled machining of aluminium at different gap voltages

Applied gap voltage (v)	Machining time (s)	Average machining time (s)	Recorded tool wear (μm)	Average tool wear (μm)	TWR (mm3/s) (xE-5)
50	9.4	9.6	18.274	18.8	0.981876
	10.1		18.169		
	9.4		20.021		
70	10.5	9.8	20.285	20.2	1.039726
	9.6		22.086		
	9.2		18.258		
90	9.1	8.9	19.009	20.7	1.169081
	8.3		20.174		
	9.2		22.808		
110	8.5	8.9	19.705	20.6	1.167572
	8.7		19.484		
	9.4		22.497		
130	9.7	9.7	21.441	20.8	1.079992
	9.2		18.357		
	10.2		22.628		
150	9.5	9.7	21.847	20.7	1.075522
	8.9		18.852		
	10.5		21.434		

age machining time for the optimized electrical discharge machining of steel was 11.1 seconds. This average machining time was higher than the time spent in machining of brass and aluminium. This means that the machining process for steel was much slower as compared to machining of the other two metals. This was also evident in the analysis of MRR for steel. On the other hand, the average machining time for the non optimized process was 17.5 seconds. The difference in average machining time for the optimized and non optimized machining of steel illustrates a significant improvement in terms of speed of machining.

Table B.17: TWR for controlled machining of brass at different gap voltages

Applied gap voltage (v)	Machining time (s)	Average machining time (s)	Recorded tool wear (μm)	Average tool wear (μm)	TWR (mm3/s) (xE-5)
50	8.0	9.0	23.885	24.5	1.369346
	9.3		25.830		
	9.6		23.658		
70	10.0	8.6	23.961	25.4	1.480518
	7.8		26.530		
	8.1		25.674		
90	8.8	9.1	25.738	26.1	1.447983
	10.5		26.180		
	8.0		26.501		
110	9.9	9.7	27.972	25.9	1.348851
	9.4		24.004		
	9.7		25.855		
130	10.5	10.3	22.958	25.7	1.25265
	9.7		27.962		
	10.8		26.272		
150	9.7	9.1	23.432	24.3	1.340301
	8.4		26.113		
	9.3		23.413		

B.7 Calculation of material removal rates for controlled EDM process at different duty cycles

Table B.19 shows the parameters that are used to calculate material removal rate for controlled machining of aluminium with different duty cycles.

Table B.20 shows the MRR values that are achieved in the electro-discharge machining of brass under the control of the FLC based robust controller. The average values of the diameters and depths of the machined holes are used to calculate MRR in each case.

In total, fifteen experiments were carried out under identical conditions as those of the non optimized process and the results tabulated in Table B.20. The only difference here being that the EDM process is under optimization of by the FLC

Table B.18: TWR for controlled machining of steel

Applied gap voltage (v)	Machining time (s)	Average machining time (s)	Recorded tool wear (μm)	Average tool wear (μm)	TWR (mm3/s) (xE-5)
50	9.7	12.1	23.508	22.0	0.910807
	13.3		22.683		
	13.4		19.717		
70	9.4	10.5	20.414	21.3	1.018435
	10.6		23.468		
	11.5		20.022		
90	10.7	11.3	19.157	21.1	0.940885
	13.5		20.633		
	9.5		23.449		
110	10.7	11.1	19.959	21.9	0.9888
	9.3		21.911		
	13.4		23.835		
130	11.9	11.2	22.111	22.4	1.00285
	11.6		20.721		
	10.1		24.288		
150	12.3	10.4	23.784	21.7	1.047933
	9.5		21.380		
	9.5		20.031		

based robust controller. For machining of steel, MRR that is obtained for each set of three experiments as shown in Table B.21. Similar experiments had been done earlier in chapter 3 for the non controlled EDM process.

B.8 Calculation of tool wear rate for controlled EDM process at different duty cycles

Parameters that are measured for the EDM machining of aluminium are shown in Table B.22 against the duty cycle used for machining. The TWR is calculated from the average values of tool wear length from three machining experiments as shown in the table. Also, the average machining time is calculated from the three machining experiments. The data for experimental work of investigation of the effectiveness of the robust controller in minimizing TWR in machining of brass is shown in Table B.23. Table B.24 shows the applied and measured parameters

Table B.19: Parameters and MRR for optimized electro-discharge machining of aluminium

Duty cycle (%)	Machining time (s)	Average machining time (s)	Diameter of the machined hole (μm)	Mean diameter of the machined hole (μm)	Depth of the machined hole (μm)	Mean depth of the machined hole (μm)	MRR (mm3/min) (xE-2)
10	13.3	12.0	97.929	100.3	476.832	475.4	1.882
	11.4		100.601		475.359		
	11.2		102.486		473.981		
30	12.9	13.2	105.050	101.7	475.923	474.9	1.750
	13.1		103.517		475.171		
	13.7		96.600		473.619		
50	12.3	12.3	98.560	99.7	474.392	473.6	1.807
	11.5		99.352		472.311		
	12.9		101.124		473.957		
70	13.9	12.7	103.038	102.0	477.338	476.3	1.839
	13.8		98.617		474.150		
	10.4		104.366		477.293		
90	11.4	11.9	102.528	102.6	476.197	474.1	1.977
	12.6		100.883		470.494		
	11.7		104.522		475.609		

Table B.20: Parameters and MRR for optimized electro-discharge machining of brass

Duty cycle (%)	Machining time (s)	Average machining time (s)	Diameter of the machined hole (μm)	Mean diameter of the machined hole (μm)	Depth of the machined hole (μm)	Mean depth of the machined hole (μm)	MRR (mm3/min) (xE-2)
10	14.9	12.6	99.526	102.1	471.307	472.6	1.8360653
	14.6		103.560		472.620		
	8.4		103.102		473.725		
30	10.8	13.0	101.308	100.7	473.964	471.2	1.7336359
	14.3		99.550		469.588		
	13.8		101.193		470.033		
50	11.5	12.4	102.779	101.4	471.307	471.7	1.8498537
	12.1		98.873		473.910		
	13.5		102.632		469.977		
70	11.3	12.8	103.551	102.4	472.104	471.0	1.819992
	12.3		99.507		470.359		
	14.7		104.033		470.450		
90	12.7	12.1	100.021	99.7	471.286	472.1	1.8318622
	10.5		98.962		472.388		
	13.0		100.104		472.643		

in the optimized machining of steel and the resultant tool wear rate for each set of parameters.

Table B.21: Parameters and MRR for optimized electro-discharge machining of steel

Duty cycle (%)	Machining time (s)	Average machining time (s)	Diameter of the machined hole (μm)	Mean diameter of the machined hole (μm)	Depth of the machined hole (μm)	Mean depth of the machined hole (μm)	MRR (mm3/min) (xE-2)
10	14.5	13.3	91.260	94.2	466.232	465.1	1.4575737
	14.0		95.211		465.044		
	11.6		96.106		464.100		
30	12.0	13.9	93.776	96.1	463.968	466.4	1.4584427
	15.3		97.431		471.937		
	14.5		97.054		463.157		
50	14.8	13.5	93.848	95.7	477.304	474.1	1.520242
	13.6		95.276		470.211		
	12.0		98.041		474.759		
70	13.5	13.0	91.876	94.1	474.676	475.5	1.5215867
	12.3		96.290		475.665		
	13.3		94.039		476.217		
90	12.0	12.3	97.658	94.0	473.408	468.8	1.5810132
	10.4		91.705		465.620		
	14.7		92.647		467.291		

Table B.22: Parameters and TWR for optimized electro-discharge machining of aluminium

Duty cycle (%)	Machining time (s)	Average machining time (s)	Recorded tool wear (μm)	Average tool wear (μm)	TWR (mm3/min) (xE-4)
10	10.6	9.4	16.336	18.0	5.753444
	8.7		16.360		
	8.9		21.216		
30	9.1	10.1	17.070	19.0	5.703233
	10.6		21.652		
	10.5		18.315		
50	10.2	9.8	20.952	20.2	6.201233
	8.8		22.796		
	10.5		16.755		
70	8.4	8.7	18.779	19.2	6.686964
	9.2		18.040		
	8.4		20.901		
90	9.9	9.5	20.477	20.8	6.591551
	9.2		22.592		
	9.4		19.420		

Table B.23: Parameters and TWR for optimized electro-discharge machining of brass

Duty cycle (%)	Machining time (s)	Average machining time (s)	Recorded tool wear (μm)	Average tool wear (μm)	TWR (mm3/min) (xE-4)
10	7.4	8.3	20.493	19.7	7.1972343
	8.1		18.122		
	9.3		20.528		
30	7.4	8.8	21.046	19.7	6.8035027
	8.4		19.262		
	10.4		18.904		
50	9.9	9.3	19.500	19.4	6.2746229
	9.3		17.212		
	8.8		21.587		
70	10.9	10.2	17.552	19.6	5.8163732
	8.4		19.471		
	11.2		21.728		
90	7.6	9.6	20.485	20.9	6.5486486
	11.5		20.464		
	9.8		21.784		

Table B.24: Parameters and TWR for optimized electro-discharge machining of steel

Duty cycle (%)	Machining time (s)	Average machining time (s)	Recorded tool wear (μm)	Average tool wear (μm)	TWR (mm3/min) (xE-4)
10	10.1	11.4	23.71336	21.3	5.6373451
	12.2		18.14855		
	11.9		21.96189		
30	9.9	11.2	19.92655	22.3	6.0248812
	11.3		23.75118		
	12.3		23.17606		
50	11.2	10.7	19.06247	21.0	5.8882413
	10.9		21.43451		
	10.2		22.42697		
70	11.8	11.6	21.58418	22.0	5.7149865
	12.4		21.85311		
	10.5		22.49509		
90	11.3	11.2	20.2627	20.7	5.581936
	10.1		19.22176		
	12.2		22.70491		